Power Systems Model Developments for Power Qality Monitoring : Application to Fundamental Frequency and Unbalance Estimation

Anh Tuan Phan

Université de Haute Alsace

École Doctorale Mathématiques, Sciences de l'Information et de l'Ingénieur (MSII, ED 269)
Laboratoire Modélisation, Intelligence, Processus et Systèmes (MIPS, EA 2332)

Power Systems Model Developments for Power Quality Monitoring: Application to Fundamental Frequency and Unbalance Estimation

Contribution à la modélisation des systèmes électriques pour la surveillance de la qualité de l'énergie électrique : application à l'estimation de la fréquence fondamentale et du déséquilibre

Thèse

préparée par

Anh Tuan PHAN

présentée pour obtenir le grade de
Docteur de l'Université de Haute Alsace
Discipline : Électronique, Électrotechnique et Automatique

soutenue publiquement le 16 septembre 2016 devant le jury composé de :

M. Moamar Sayed-Mouchaweh, Professeur des Universités, Mines de Douai (rapporteur)
M. Laurent Rambault, Maître de Conférences HDR, Université de Poitiers (rapporteur)
M. Malek Ghanes, Professeur des Universités, Ecole Centrale de Nantes (examinateur)
M. Edouard Laroche, Professeur des Universités, Université de Strasbourg (Président)
M. Gilles Hermann, Maître de Conférences, Université de Haute Alsace (co-encadrant)
M. Patrice Wira, Professeur des Universités, Université de Haute Alsace (directeur de thèse)

Acknowledgements

I started my PhD research signal processing with some lacking skills and knowledge in this field. Fortunately, I had two wonderful supervisors: Prof. Patrice Wira and Dr. Gilles Hermann who were so patient and showed me how to do things effectively and professionally step by step. They suggested me many ideas for my research and I had never felt stressed when working with them. Thanks to their help, I could complete my research activities.

I would like to express a deep thank to my parents who always support me at any time in my life. Their encouragement is my great motivation to move further in a research career.

I am grateful to my colleagues in MIPS laboratory who have shared with me stories of the life in France even when my French was limited.

Abstract

Renewable energy, electricity and smart grids are core subjects as they have great environmental and societal impacts. Thus, generating, transporting and managing electric energy, i.e., power, still continue to drive a growing interest. In order to properly achieve these goals, several locks must be removed. Beyond issues related to the distribution architecture, the formalization of models, sizing tools, features and indicators, constraints and criteria, decentralized generation and energy management, power quality is central for the whole grid's reliability. Disturbances affect the power quality and can cause serious impact on other equipment connected to the grid. The work of this thesis is part of this context and focuses on the development of models, indicators, and signal processing methods for power quality monitoring in time-varying power distribution systems.

This thesis analyzes the power quality including several well-known features and their relevance. Power system models and signal processing methods for estimating their parameters are investigated for the purpose of real-time monitoring, diagnostic and control tasks under various operating conditions. Among all, the fundamental frequency is one of the most important parameters of a power distribution system. Indeed, its value which is supposed to be a constant varies continuously and reflects the dynamic availability of electric power. The fundamental frequency can also be affected by renewable energy generation and by nasty synchronization of some devices. Moreover, the power absorbed by loads or produced by sources is generally different from one phase to the other one. Obviously, most of the existing residential and industrial electrical installations with several phases work under unbalanced conditions. Identifying the symmetrical components is therefore an efficient way to quantify the imbalance between the phases of a grid.

New state-space representations of power systems are proposed for estimating the fundamental frequency and for identifying the voltage symmetrical components of unbalanced three-phase power systems. A first state-space representation is developed by supposing the fundamental frequency to be known or to be calculated by another estimator. In return, it provides other parameters and characteristics from the power system. Another original state-space model is introduced which does not require the fundamental frequency. Here, one state variable is a function of the frequency which can thus be deduced. Furthermore this new state-space model is perfectly are able to represent a three-phase power system in both balanced and unbalanced conditions. This not the case of lots of existing models. The advantage of the proposed state-space representation is that it gives directly access to physical parameters of the system, like the frequency and the amplitude and phase values of the voltage symmetrical

components. Power systems parameters can thus be estimated in real-time by using the new state-space with an online estimation process like an Extended Kalman Filter (EKF). The digital implementation of the proposed methods presents small computational requirement, elegant recursive properties, and optimal estimations with Gaussian error statistics.
The methods have been implemented and validated through various tests respecting real technical constraints and operating conditions. The methods can be integrated in active power filtering schemes or load-frequency control strategies to monitor power systems and to compensate for electrical disturbances.

Key words: electrical disturbances; power quality; power system model; power distribution; unbalanced power systems; voltage symmetrical components; fundamental frequency estimation; state space; Kalman filter; online estimation

Résumé

Les énergies renouvelables, l'énergie sous la forme électrique et son transport à l'aide de réseaux électriques intelligents représentent aujourd'hui des enjeux majeurs car ils ont de grands impacts environnementaux et sociétaux. Ainsi, la production, le transport et la gestion de l'énergie électrique, continuent toujours à susciter un intérêt croissant. Pour atteindre ces objectifs, plusieurs verrous technologiques doivent être levés. Au-delà des questions liées aux architectures des réseaux électriques, aux modèles, aux outils de dimensionnement, à la formalisation de caractéristiques et d'indicateurs, aux contraintes et aux critères, à la gestion et à la production décentralisée, la qualité de la puissance électrique est centrale pour la fiabilité de l'ensemble du système de distribution. Les perturbations affectent la qualité des signaux électriques et peuvent provoquer des conséquences graves sur les autres équipements connectés au réseau. Les travaux de cette thèse s'inscrivent dans ce contexte et de fait ils sont orientés vers le développement de modèles, d'indicateurs et de méthodes de traitement des signaux dédiés à la surveillance en temps-réel des performances des réseaux de distribution électrique.

Cette thèse analyse la qualité de la puissance électrique, en prenant en compte plusieurs caractéristiques bien connues ainsi que leur pertinence. Les modèles des systèmes électriques et les méthodes de traitement du signal pour estimer leurs paramètres sont étudiés pour des applications en temps-réel de surveillance, de diagnostic et de contrôle sous diverses conditions. Parmi tous, la fréquence fondamentale est l'un des paramètres les plus importants pour caractériser un système de distribution électrique. En effet, sa valeur qui est censée être une constante, varie en permanence et reflète la dynamique de l'énergie électrique disponible. La fréquence peut également être affectée par certaines productions d'énergie renouvelable et peut être influencée par des mauvaises synchronisations de certains équipements. En outre, la puissance absorbée par les charges ou produite par des sources est généralement différente d'une phase à l'autre. Évidemment, la plupart des installations électriques existantes avec plusieurs phases, qu'elles soient résidentielles ou industrielles, travaillent dans des conditions déséquilibrées. Identifier les composantes symétriques de tension est dans ce cas un moyen pertinent pour quantifier le déséquilibre entre les phases d'un système électrique.

De nouvelles représentations de type espace d'état et modélisant des systèmes électriques sont proposées pour estimer la fréquence fondamentale et pour identifier les composantes symétriques de tension des systèmes électriques triphasés et déséquilibrés. Le premier modèle d'espace d'état proposé considère la fréquence fondamentale comme connue ou obtenue par un autre estimateur. En contrepartie, il fournit les autres paramètres caractérisant le système électrique. Un second modèle d'état-espace est introduit. Il est original dans le sens où il ne

nécessite aucune connaissance de la fréquence fondamentale. Une de ses variables d'état est directement reliée à la fréquence et permet donc de la déduire. En outre, ce nouvel espace d'état est parfaitement capable de représenter des systèmes électriques à trois phases équilibrés et non équilibrés. Ceci n'est pas le cas de la majorité des modèles déjà existants. L'avantage de l'espace d'état proposé réside dans le fait qu'il permet d'estimer directement les paramètres physiques du système électrique, tels que la fréquence, l'amplitude et la phase des composantes symétriques en tension. Les paramètres des systèmes électriques peuvent donc être estimés en temps réel en utilisant le nouvel espace d'état avec un processus d'estimation en ligne comme un Filtre de Kalman Etendu (EKF). L'implémentation numérique de la méthode proposée présente des exigences calculatoires modestes, des caractéristiques récursives avantageuses et des estimations optimales avec des statistiques d'erreur de type gaussienne.
Les méthodes ont été mises en œuvre et validées par le biais de différents tests proches des contraintes techniques et des conditions d'utilisation réelles. Les méthodes peuvent être intégrées aisément dans des filtres actifs de puissance ou dans des schémas de contrôle de la fréquence côté charge, et ceci afin de réaliser des stratégies de surveillance ou de compensation des perturbations présentes dans les systèmes électriques.

Mots clefs : Perturbation électrique ; qualité de l'énergie électrique ; modèle de système électrique ; distribution de l'énergie électrique ; système électrique déséquilibré ; composantes symétriques de tension ; estimation de la fréquence fondamentale ; estimation en ligne ; espace d'état ; filtre de Kalman

Contents

Acknowledgements i

Abstract (English/Français) iii

List of figures xi

List of tables xv

Introduction 1

0.1 Publications and Authors' Contribution . . . 5
0.2 Organization of this thesis . . . 6

1 Power quality disturbances in power systems 7

1.1 Introduction . . . 7
1.2 Definition of power quality . . . 10
1.3 Power quality disturbances . . . 11
1.3.1 Reactive power . . . 12
1.3.2 Unbalance in three phase power systems . . . 14
1.3.3 Harmonics . . . 16
1.3.4 Fundamental frequency variations . . . 19
1.3.5 Short-duration voltage variations . . . 22
1.3.6 Long-duration voltage variations . . . 23
1.3.7 Other power quality problems . . . 24
1.4 Power quality monitoring and control . . . 24
1.4.1 Frequency Control . . . 24
1.4.2 Compensation . . . 25
1.4.3 Power system protection . . . 29
1.5 Conclusion . . . 30

2 Advanced signal processing methods for power quality improvement 31

2.1 Adaptive signal processing methods to estimate the fundamental frequency of a power system . . . 32
2.1.1 Phase-locked Loop (PLL) . . . 33

2.1.2 Extended Kalman Filter for fundamental frequency estimation of balanced three phase power systems (3P EKF) . . . 34
2.1.3 Extended Kalman Filter for fundamental frequency estimation of single phase power systems (1P EKF) . . . 39
2.1.4 Adaptive Notch Filter . . . 40
2.1.5 Adaptive Prony's method . . . 42
2.1.6 Performances and comparison of well-known methods . . . 44
2.1.7 Discussion . . . 48
2.2 Adaptive signal processing methods to identify symmetrical components of a power system . . . 51
2.2.1 Signal modeling . . . 51
2.2.2 Multi-output Adaline (MO-Adaline) for tracking symmetrical components 52
2.2.3 Discussion . . . 53
2.3 Conclusion . . . 53

3 New state-space representations 55
3.1 Introduction . . . 55
3.2 New state-space models of unbalanced three phase signals . . . 56
3.2.1 A new state-space model of unbalanced three phase signals of which the fundamental frequency is an unknown parameter . . . 56
3.2.2 A new state-space model of unbalanced three phase signals of which the fundamental frequency is a known variable . . . 59
3.3 Algorithms for online estimation of a three phase power system's parameters and states . . . 60
3.4 Discussion about the two proposed methods . . . 60
3.4.1 Discussion of the proposed linear method . . . 60
3.4.2 Discussion of the proposed nonlinear method . . . 61
3.5 A solution to the initialization problem of the proposed nonlinear method . . . 62
3.6 Applications of the proposed methods for estimating power system's parameters in real-time . . . 63
3.6.1 Fundamental frequency estimation . . . 63
3.6.2 Symmetrical component identification . . . 63
3.6.3 Discussion . . . 65
3.7 Applications of the ability of estimating power systems' parameters of the proposed methods in improving power quality of power systems . . . 66
3.8 Conclusion . . . 67

4 Simulations and Results 69
4.1 Introduction . . . 69
4.2 Tests with the proposed linear method . . . 69
4.2.1 Test with an unbalanced system . . . 70
4.2.2 Robustness against load changes . . . 71

4.2.3 Tracking symmetrical components when the fundamental frequency constantly varies in time . . . 72
4.3 Test with the proposed nonlinear method . . . 74
4.3.1 Fundamental frequency estimation . . . 74
4.3.2 Symmetrical component estimation . . . 84
4.4 Test the proposed initialization of the proposed nonlinear method . . . 92
4.4.1 Robustness against noises . . . 92
4.4.2 Robustness against load changes . . . 96
4.4.3 Frequency tracking . . . 100
4.5 Conclusion . . . 100

Conclusion **103**

A Appendixes **107**
A.1 List of Acronyms . . . 108
A.2 The $\alpha - \beta$ transform and the complex form of three phase signals . . . 109

Bibliography **120**

List of Figures

1 A classic power distribution system 2

2 A modern, smart, and distributed power system including local renewable generation 3

1.1 IEEE Standards for Information applied to energy management and Communication Technology [85] 8

1.2 Standards for Smart Homes [84] 9

1.3 Power system facilities for energy management with transportation, distribution, renewable production and storage 10

1.4 Example the signals of an unbalanced three phase power system 14

1.5 Harmonic components caused by a) TV receiver, b) PC and printer, c) microwave oven 17

1.6 Frequency deviations of power systems of different countries: a) Sweden, b) Central Europe, c) Greate Britain, d) Singapore, e) China (East), recording during two days 20

1.7 Estimation of a fluctuating frequency during 500 s [75] 20

1.8 Short duration voltage variations: a) Interruption, b) Sag, c) Swell 23

1.9 Principle of a passive power filter [71] 25

1.10 Main parts of an active power filter with associated scientific skills 26

1.11 A typical architecture of a Voltage Source Inverter (VSI) 27

1.12 Basic series active filter [5] 28

2.1 Basic principle of a Digital PLL [6] 34

2.2 Performance of the four considered methods in estimating the fundamental frequency of a power system under different conditions, a) signals (2.52), b) signals (2.52) with a 40 dB noise, c) signals (2.52) disturbed by harmonics, d) unbalanced three phase signals 46

3.1 Principles of the proposed nonlinear method 65

3.2 Applications of the new methods in an APF 66

3.3 Processes for estimating the symmetrical components of a power system in a digital protective relay 67

4.1 Estimation of symmetrical components by the proposed linear method and MO-Adaline a) the unbalanced three-phase signals, b) estimated amplitudes of the positive and negative components, and c) phase angles of the positive and negative components 70
4.2 Estimation of the symmetrical components of the power system in load changes by the proposed method and MO-Adaline a) the unbalanced three-phase signals, b) estimated amplitudes of the positive and negative components 72
4.3 Reconstruction of the positive components of the power system in load changes by the proposed method and MO-Adaline a) positive component in phase a b) positive component in phase b c) positive component in phase c 73
4.4 Reconstruction of the negative components of the power system in load changes by the proposed method and MO-Adaline a) positive component in phase a b) positive component in phase b c) positive component in phase c 74
4.5 varying fundamental frequency 74
4.6 The estimated amplitudes of the positive and negative components of the proposed method and MO-Adaline 75
4.7 The errors of the estimation of the positive and negative components of the signals (4.1) with the frequency varies as in Fig. 4.5 by MO-Adaline compared to the real ones: a) phase a, b) phase b, c) phase c 76
4.8 The errors of the estimation of the positive and negative components of the signals (4.1) with the frequency varies as in Fig. 4.5 by the proposed method compared to the real ones: a) phase a, b) phase b, c) phase c 77
4.9 The signals of the unbalanced three-phase system defined by (4.6), a) without noise, b) with a 30 dB noise, c) with higher-order harmonics of rank 5 and 7, d) histogram corresponding to the signal with higher-order harmonics of rank 3 and 5 79
4.10 Estimated frequencies by the three methods, a) without noise and harmonics, b) with a 30 dB noise, c) with harmonics of rank 3 and 5 80
4.11 Fundamental frequency estimation when steps appear with different amplidutes and respectively, a) of 0.00001 Hz, b) of 0.0001 Hz and c) of 0.001 Hz 80
4.12 Performance in estimating the frequency with a changing fundamental frequency, a) real and estimated frequency (Hz), b) frequency error (Hz) 83
4.13 Identification of the symmetrical components, a) the unbalanced three-phase signals, b) estimated amplitudes of the positive and negative components 85
4.14 Identified currents compared to the real ones, a) i_{α}^{+}, b) i_{β}^{+}, c) i_{α}^{-} and d) i_{β}^{-} 86
4.15 Identification of the symmetrical components, a) the unbalanced three-phase signals, b) estimated amplitudes of the positive and negative components, and c) phase angles of the positive and negative components 87
4.16 Reconstruction of the system's symmetrical components, a) recovered positive components, b) recovered negative component, and c) recovered zero component 87
4.17 Identified currents compared to the real ones, a) i_{α}^{+}, b) i_{β}^{+}, c) i_{α}^{-} and d) i_{β}^{-} . . . 89

4.18 The estimated amplitudes of the positive and negative components of the proposed nonlinear method: a) the positive, b) the negative 90
4.19 the errors of the estimated phases of the symmetrical components: a) the phase error of the positive components b) the phase error of the negative components 90
4.20 The error of the estimated three phase signals of the positive and negative components compared to the real signals, a) phase a, b) phase b, c) phase c . . . 91
4.21 The estimated frequency of the proposed nonlinear method combined with the initialization scheme in disturbance of 30 dB noise a) Initialization with Case 1, b) Initialization with Case 2 93
4.22 The estimation of the three phases of the positive components of the proposed nonlinear method combined with the initialization scheme: a) phase a, b) phase b, c) phase c 94
4.23 The estimation of the three phases of the negative components of the proposed nonlinear method combined with the initialization scheme: a) phase a, b) phase b, c) phase c 95
4.24 The three phase signals with load change at time 0.1s 97
4.25 The estimated frequency of the proposed nonlinear method combined with the initialization scheme in case of unbalanced system and load changes a) Initialization with Case 1, b) Initialization with Case 2 97
4.26 The estimation of the three phases of an unbalanced system in load changes of the positive components of the proposed nonlinear method combined with the initialization scheme: a) phase a, b) phase b, c) phase c 98
4.27 The estimation of the three phases of the negative components of an unbalanced system in load changes of the proposed nonlinear method combined with the initialization scheme: a) phase a, b) phase b, c) phase c 99
4.28 the estimated fundamental frequency of the proposed nonlinear method combined with the initialization scheme: a) the estimated frequency and the real one, b) the estimation error 100

List of Tables

1.1 Several types and Sources of Power System Harmonics [34] 18
1.2 Selection of APF for specific application considerations [99] (a higher number of '•' is preferred) 29

2.1 Summary of Kalman variables 37
2.2 Performance of the four methods in estimating the frequency of three phase sinusoidal signals 48
2.3 Performance of the four methods in estimating the frequency of three phase sinusoidal signals disturbed by a noise of 40 dB 48
2.4 Performance of the four methods in estimating the frequency of three phase sinusoidal signals disturbed by higher-order harmonics 48
2.5 Performance of the four methods in estimating the frequency of unbalanced three phase sinusoidal signals 48
2.6 The characteristics of the four methods APM, ANF, 3P EKF and 1P EKF 49

3.1 Comparison of the proposed method and the EKFs in Chapter 2 61

4.1 Performance of the new method for estimating the amplitudes of the positive components of three phase signals 71
4.2 Performance of the new method for estimating the amplitudes of the negative components of three phase signals 71
4.3 Performance of the proposed nonlinear method compared to the 3P EKF and the 1P EKF in estimating the frequency of a balanced system 78
4.4 Performance of the proposed nonlinear method compared to the 3P EKF and the 1P EKF in estimating the frequency of an unbalanced system 78
4.5 Performance of the proposed nonlinear method compared to the 3P EKF and the 1P EKF in estimating the frequency of an unbalanced system with an additional 30 dB noise 78
4.6 Performance of the proposed nonlinear method compared to the 3P EKF and the 1P EKF in estimating the frequency of an unbalanced system disturbed by harmonics 78
4.7 Performance of the proposed state-space method in tracking fundamental frequency steps 81

4.8 Performance of the new method for estimating the amplitudes of the positive and negative components of three phase signals disturbed by noise of 30 dB . . 88
4.9 Performance of the new method for estimating the amplitudes of positive and negative components of three phase signals disturbed by harmonics of rank 5 and 7 88
4.10 The estimated frequencies of an unbalanced system disturbed by a noise of 30 dB of the proposed method combined with the initialization scheme corresponding to the two case of initialization 93
4.11 The estimated frequencies of an unbalanced system in load changes of the proposed method combined with the initialization scheme corresponding to the two case of initialization 96

Introduction

Electricity is one of the most important energy. Indeed, energy can be found in a number of different forms. It can be chemical energy, electrical energy, heat (thermal energy), light (radiant energy), mechanical energy, and nuclear energy. Obviously, compared to the other forms, electrical energy is very useful and presents one main advantage: Electricity can be very easily transported and thus distributed very quickly from one location to another one. Another advantage is that it is possible to store it for a while but under a different form of energy. For being stored, the electrical energy must be converted in another form of energy, and then this energy must be converted back to electricity in other to be used.

Nowadays, the need of electrical energy is everywhere and permanent, i.e., at all-time by everyone. Electricity is used by various equipment presents in resident houses and industrial installations. Fossil sources such as coal and oil are traditional sources used to generate electricity energy. The system responsible for generation, transmission and distribution of electricity energy is called a power system. Fig. 1 illustrates a traditional power system where the generation of the electrical energy from other forms of energy is concentrated in one point of a grid [40]. The electrical energy must thus be transported and distributed from the source – where is has been generated - to large amounts of loads - where it is consumed - connected to the grid and sometime very far away. It is a kind of a hierarchical organization [40].

Electric power systems are complex and composed of various types of sources and of non-homogeneous loads. A power system can be considered as a non-stationary system because of all its parts which can show random behaviors. Indeed, loads can be switched on and off according to users' unpredictable needs and sources generate electricity in a fluctuating and discontinuous manner. This is of course the case of the renewable energy production which is absolutely not constant. All these effects make the whole system to evolve continuously from one state to another state. Additionally, the concern of power system reliability is increasing with the wide development of electronic devices. One the other side, electronic devices are sensitive to electrical disturbances, and the harmonic currents generated by their nonlinear characteristic are considered as major disturbances that have a serious impact to other equipment connected to the grid. Disturbances such as current harmonics, reactive power, fluctuating fundamental frequency and unbalance once generated are propagated at long distances in the branches of the grid [11, 13].

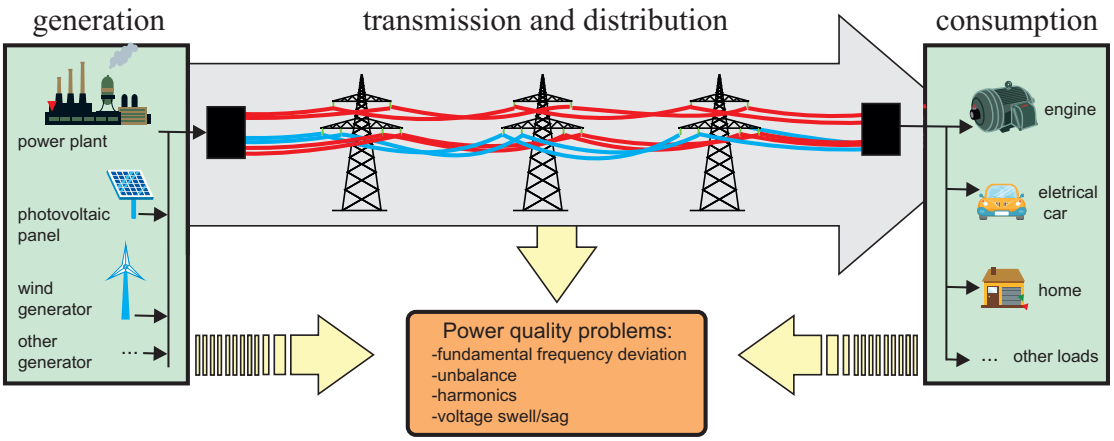

Figure 1 – A classic power distribution system

In addition and due to the fear for fossil energy decline and its corresponding increasing cost, there is a need of a new concept of electricity distribution. Now, there is a need of power systems that are able to generate electricity from various other forms of energy and more specifically from renewable energy such as solar energy and wind energy. All these distributed energy generation processes have to be fully integrated in a unique power system. Obviously, this leads to new consequences and new problems [40]. Therefore, the power system's reliability and stability must be monitored and enhanced continuously and in real-time . This is the basis that leads to the development of new power distribution system which should demonstrate the following capabilities [63, 118]:

- Real-time monitoring of grid conditions;
- Improved automated diagnosis of grid disturbances;
- Automated responses to grid failures that will isolate disturbed zones and prevent or limit cascading blackouts that can spread over wide areas;
- Enhanced ability to manage large amounts of renewable energy power which are rapidly changing power systems;
- "Plug and play" ability to connect new generating plants to the grid, reducing the need for time consuming interconnection studies and physical upgrades to the grid;
- Load balancing and frequency adjustments;
- Compensation of harmonic currents generated by highly nonlinear loads.

A power distribution system with the previous properties can be referred to as a 'smart grid' [103]. Such a communicating, smart, and distributed power system is represented by Fig. 2. It can be seen that it is an unique grid that integrates lots of various sources and loads non homogeneously

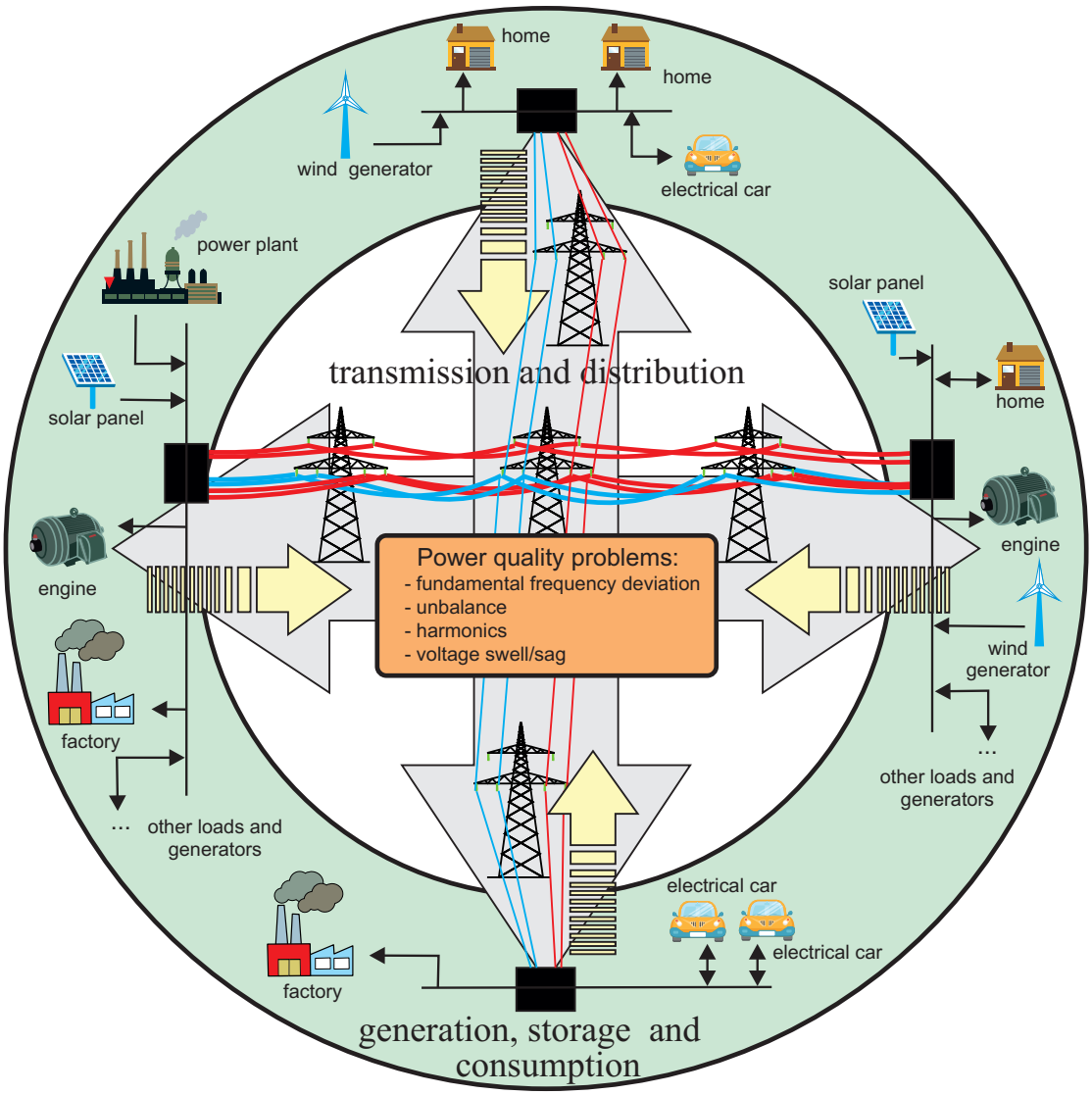

Figure 2 – A modern, smart, and distributed power system including local renewable generation

repartitioned. It is thus a flat organization – in opposition to the hierarchical organization of Fig. 1. As a result, the transportation of the electrical energy is limited; it means that the energy produced by a source can be locally and instantaneously consumed by loads which are in the same area. On the other side, this distributed power system is more complex and therefore requires new capabilities (at least communication and automation capabilities) but also additional intelligent features (distributed computational intelligence) [112, 14]. Advantages and drawbacks of these power distribution systems are further detailed in [23, 61]. The work of this thesis is part of the context of electrical energy transportation and focuses on the development of models, indicators, and signal processing methods for power quality monitoring in time-varying power distribution systems.

Power quality is a central issue for the whole grid's reliability. Power quality refers to the quality of the electrical signals used to transport the power into the grid [38]. Several physical parameters can thus be considered as representative of the quality of the signals. In order to be able to effectively monitor and diagnose, to detect grid failures, to compensate for disturbances, the value of some important parameters are required. For example, the frequencies, the amplitudes, and the phase angles of the voltages and/or currents must be continuously measured or estimated in real-time. If measuring the grid voltages and currents is not a difficult task, some other parameters are not available nor easily measured. Signal processing then allows extracting and deducing quantities from the measured voltages and currents.

This study will develop digital signal processing methods that are able to estimate online relevant parameters and states from power systems under various conditions in order to lead to pertinent diagnoses and control tasks. Of course, a power system is an electrical distribution system, but a very general case can be considered: So, this study considers a power system as any system including electrical aspects, i.e., handling electrical energy within at least one of its part. Among the parameters of a power system, the fundamental frequency is one of the most important parameters that can affect the stability and reliability of the whole system. Although, several methods for estimating the fundamental frequency still exist. Most of them are sensitive to perturbations and disturbances, most of them are not able to take into account several different behaviors (like unbalance).

In this context, several contributions have been developed by the MIPS laboratory through PhD thesis in identifying the harmonic content of signals and in controlling shunt APF [74, 71], in power quality enhancement with renewable energy control [17], in dis-aggregating loads with non-intrusive monitoring strategies [15], in non-intrusive activity analysis, i.e., smart metering [55]. The goal of this PhD thesis is to use parametric modeling techniques for estimating parameters from sinusoidal signals from multi-phase power distribution systems.

This thesis proposes several new state-space models of three phase power systems. If their state-space is new, their design is based on existing power system modeling techniques. Unlike existing models which represent either one phase signal of a power system or balanced three phase signals of a three phase power system, the new state-space models are able to represent a three phase power system in both balanced and unbalanced conditions. For this, the theory of the symmetrical components has been used for their design. One important advantage of these original state-spaces is that their structure gives a direct access to some physical parameters representing the changing behavior of a power system. As for other state-spaces, an iterative estimation algorithm can be associated to them in order to deduce the systems states and parameter continuously and in real-time. Here, Kalman and Extended Kalman filters, which are well-known system identification algorithms, are chosen to be associated with the proposed models. This strategy allows thus to estimate parameters and states of any power system. More specifically, the proposed methods are used for estimating the fundamental frequency and for identifying the symmetrical component of power systems. Different simulation tests have been implemented to evaluate the performance and to demonstrate the efficiency of the

proposed methods over other methods in estimating the fundamental frequency and identifying the symmetrical component of three phase power systems under various and time-changing conditions. The methods can be used for monitoring a power distribution system, for evaluating the power quality and they can be integrated in an Active Power Filter (APF) to compensate for disturbances.

0.1 Publications and Authors' Contribution

The research activities presented in this thesis has been presented in the following publications.

Poster presented in a scientific meeting

- Anh Tuan Phan, Gilles Hermann, and Patrice Wira. Advanced techniques in power transmission system enhancement and smart grid development. In Journée des Ecoles Doctorales à l'Université de Haute Alsace, Poster, 2 juillet, Mulhouse, 2015 [79],

Conference papers published in international conferences with review and proceedings

1. Anh Tuan Phan, Gilles Hermann, and Patrice Wira. "Online Frequency Estimation in Power Systems: A Comparative Study of Adaptive Methods". In: 40th Annual Conference of the IEEE Industrial Electronics Society (IECON 2014), Dallas, TX - USA, pages 4352–4357, 2014 [78]
2. Anh Tuan Phan, Gilles Hermann, and Patrice Wira. Kalman filtering with a new state-space model for three-phase systems: Application to the identification of symmetrical components. In IEEE Conference on Evolving and Adaptive Intelligent Systems (EAIS 2015), Douai-France, pages 216–221, 2015 [80]
3. Anh Tuan Phan, Duc Du Ho, Gilles Hermann, and Patrice Wira. A new state-space model for three-phase systems for kalman filtering with application to power quality estimation. In 11th International Conference of Computational Methods in Sciences and Engineering (ICCMSE 2015), Athens-Greece, 2015 [82]
4. Anh Tuan Phan, Gilles Hermann, and Patrice Wira. A new state-space for unbalanced three-phase systems: Application to fundamental frequency tracking with kalman filtering. In 18th IEEE Mediterranean Electrotechnical Conference (MELECON 2016), Limassol-Cyprus, 2016 [81]

Article submitted in international journals

- Anh Tuan Phan, Patrice Wira, and Gilles Hermann. A Dedicated State Space for Power System Modeling and Frequency and Unbalance Estimation, Evolving Systems, accepted, to appear 2016 [83]

0.2 Organization of this thesis

The thesis contains the following chapters:

- **Chapter 1** introduces power quality issues which directly impact to the reliability and stability of a power system. After defining the concept 'power quality', the chapter analyzes typical power quality disturbances such as fundamental frequency deviation, harmonics, and unbalance, by explaining the phenomenon, sources, effects to the system, and the indices of the disturbances. Active power filter, which takes the advantages of signal processing methods, is mentioned as an effective solution to monitor and compensate the problems.
- **Chapter 2** presents a state of the art of signal processing methods for improving power quality, focusing on the estimation of the fundamental frequency and the symmetrical components of a power system. The advantages and disadvantages of the methods are discussed and the performance of several of them is evaluated via various simulation tests.
- **Chapter 3**, with the aim to overcome the shortcomings of the methods presented in chapter 2, develops new state-space modeling of power signals and proposes two new signal processing methods for estimating parameters of a power system. Possible applications of the two new methods and the conditions for the applications are pointed out.
- **Chapter 4** shows the performance of the new methods to estimate the fundamental frequency and the symmetrical components of a power system with different simulation tests. The simulation results are compared to the results of some methods in chapter 2 of the same simulation tests.
- **Conclusion** chapter that provides an overall summary and some perspectives.

The thesis ends up with an Appendix section that provides a list of the acronyms used in this document in Annex A.1, and useful mathematical transformations used in power systems are recapitulated in Annex A.2.

1 Power quality disturbances in power systems

1.1 Introduction

Power quality can be described in terms of voltage and current waveform deviations from the ideal sinusoidal waveform. This is a very general description of one key issue of electricity transportation and power supply. Furthermore, power quality covers the entire power system, from the generation, transmission, distribution to end-users. Since many years, power quality also means reliability. The major changes in the structure of the grids come from the liberalization of electricity supply, deregulation, integration of renewable energy generation, increase of the power demand, etc. So, power distribution systems are in a period of transformation set in motion by significant changes in their concepts and in their structures. The main developments which are needed on power distribution systems are on high-speed communication, intelligent control of substations and protection devices, integrated power distribution management, monitoring, and high performance automation capabilities [1].

Historically, power grids where designed with the production process that is centralized [30]. This is represented by Fig. 1, it can be seen that there are different steps in the life-cycle of the electrical energy: The generation (or production), transmission and distribution, and its consumption (i.e., conversion in another form of energy in order to produce something). In this figure, the big gray arrow shows the power flow, from the power plant to the users; the direction of the arrow shows the direction of the power flow. This architecture is not compliant to the distributed renewable energy production which is by definition distributed.

Since several years, the key idea is to try to produce the energy, if possible renewable, where it will be consumed. And for costs reasons, the losses related to the energy transportation should be reduced. This is the motivation to develop new architectures of power distribution systems. They have to be distributed, communicating, and smart. Therefore, they are decentralized [38]. This new type of architectures is represented by Fig. 2. Energy can be produced anywhere, it

[1] NREL is the national laboratory of the U.S. Department of Energy, it provides some interesting studies and reports on the future of electricity transportation, as an example: http://www.nrel.gov/docs/fy12osti/52409-1.pdf

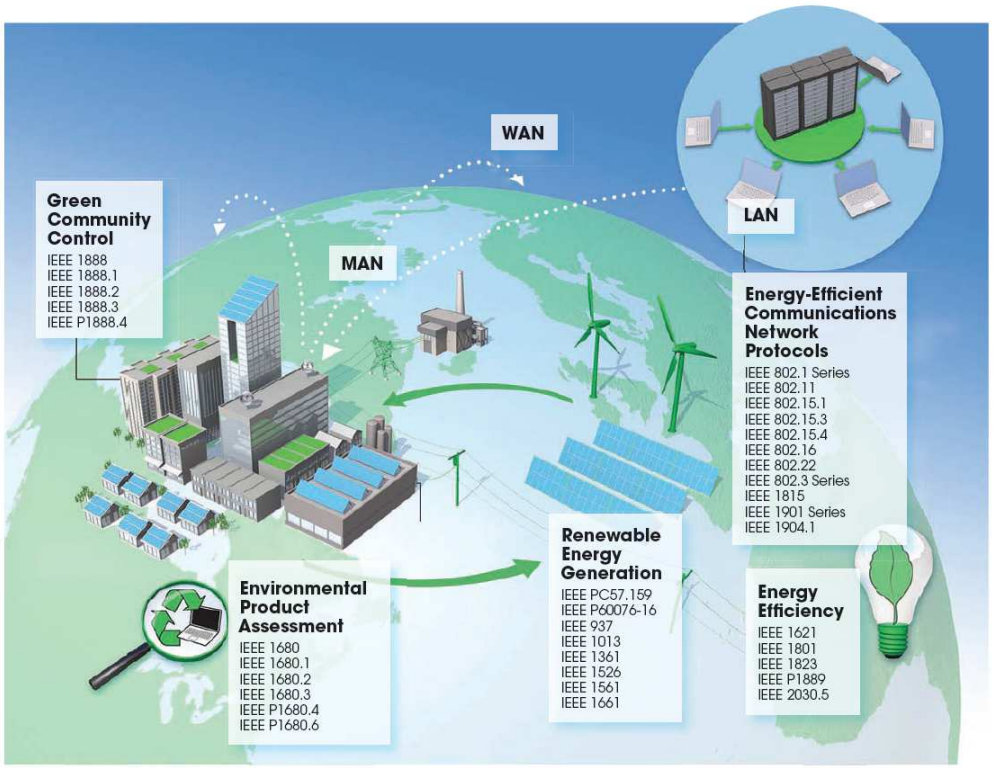

Figure 1.1 – IEEE Standards for Information applied to energy management and Communication Technology [85]

can also be consumed anywhere. As it can be seen, some devices can take power from the grid for one moment, and inject power into the grid on other instants (the big grey arrows and the small black ones show the direction of the power flow). The transportation of the power is thus reduced. On the other side, compared to the first architecture, this architecture is more complex. In addition, each device connected to the grid, loads or sources, are likely to change. Such a power system is thus more sensitive and power quality problems occur more frequently. It must thus be monitored in order to prevent against stability problems. What is not represented on this diagram is the communication network, we can imagine that it can be the Internet, i.e., each device absorbing or producing energy is a connected object able to communicate. Data can be transmitted and received at all moment. New standards [2] for Information and Communication Technology (ICT) have been specially developed for energy-efficiency applications. Some are represented on Fig. 1.1. At the same time, standards for smart homes [53] follows the same objective: Managing alternative energy sources and smart grids into home devices, via smart meters. The whole system can thus lead to an adaptive and intelligent management of the energy and of his quality. This can be illustrated by Fig. 1.2 where the relation between the smart grid and the home devices is very tight.

On both figures, i.e., Fig. 1 and Fig. 2, the yellow arrows shows/locates how failures, faults

[2] For more information about standards: http://standards.ieee.org

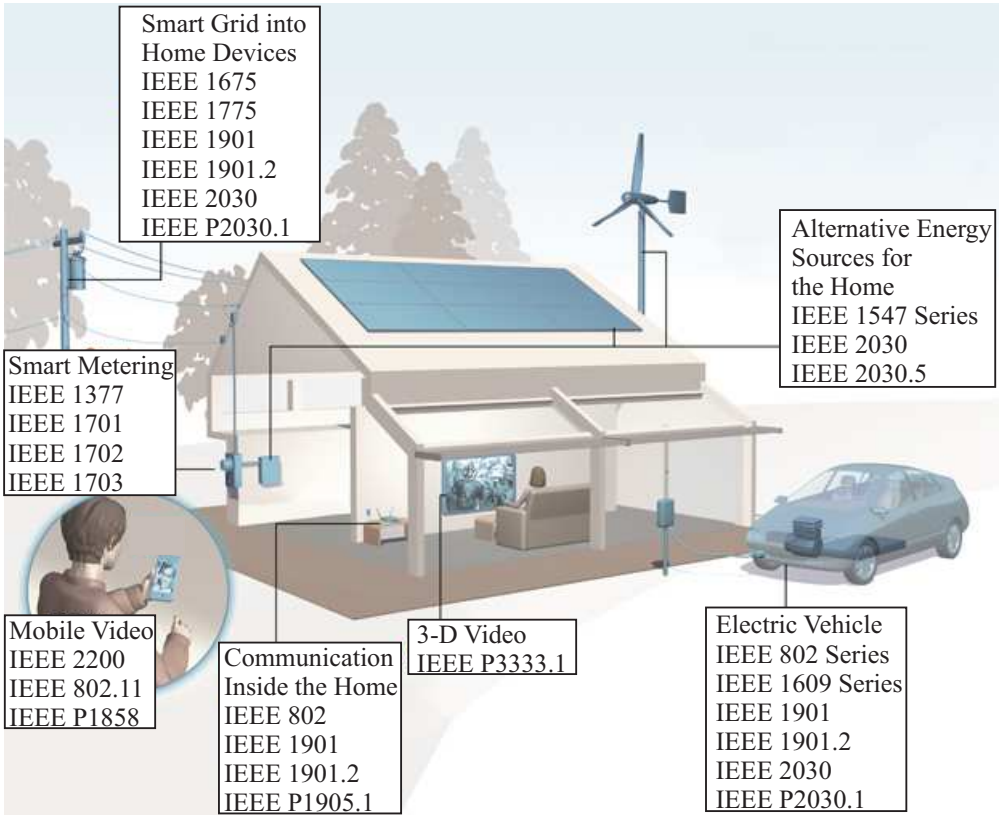

Figure 1.2 – Standards for Smart Homes [84]

troubles, dysfunctions and any malfunctioning can influence the power quality and the stability of the power distribution system. Thus, important parameters related to the quality of the power have to be measured and monitored. Technically, a Point of Common Coupling (PCC), sometimes called Point of Common Connection (PCC) is a point in the electrical system where multiple customers or multiple electrical loads may be connected. According to IEEE-519 [48], this should be a point which is accessible to both the utility and the customer for direct measurement.

Data measured from the power grid can be locally measured but can be transmitted to the transmission grid operator. They can be shared to other legal entities (municipality or local government area, etc.) or companies with other data: Air quality, waste management, parking and lightning information... This can even lead to the concept of smart cities [118]. The energy consumption and mainly electricity consumption can also be an input for a global cyberphysical system that works as of a Building Energy Management System (BEMS). BEMSs control heating, ventilation, and air conditioning and lighting systems in buildings, etc. BEMSs will be essential components of modern buildings and houses [63]. They have to find solutions which represent a tradeoff between contradicting requirements: Maintaining the occupants' comfort while minimizing energy consumption in order to reduce the global impact of the house.

Modern power distribution systems are not only complex because of their architectures, they are

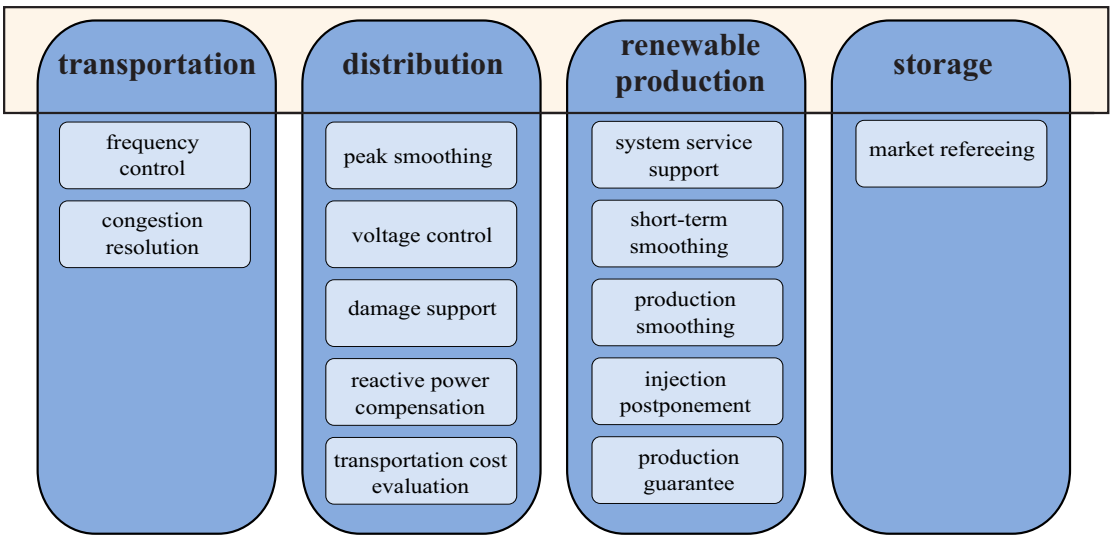

Figure 1.3 – Power system facilities for energy management with transportation, distribution, renewable production and storage

also complex due to their management. Indeed, nowadays in most of the countries, there is not only one legal entity that is responsible of the power distribution system, but there are several legal institutions or companies. This the consequence of the liberalization of the electricity market in these countries. Fig. 1.3 for example shows a general division between the transmission grid operator (transmission), the distribution operator, the actor responsible of renewable production and eventually the actor managing the storage. The tasks and responsibilities of each of them are listed by this figure. Generally, the transmission system operator is responsible not only for the operation of the transmission grid but also for its maintenance, renewal and expansion [3].

This chapter will discuss the issue of power quality, starting with the definition of electric power quality. The classification of power quality disturbances including the phenomenons, the sources, the impacts to electric equipment, and the indices of quantification are presented hereafter. Finally, the technologies used to mitigate the effects of the power quality problems are also briefly reviewed.

1.2 Definition of power quality

In [38] the electric power quality can be defined as the goodness of the electric power quality supply in terms of its voltage wave shape, its current wave shape, its frequency, its voltage regulation, as well as level of impulses, and noise, and the absence of momentary outages.

[3] In the context of the European exchange of electricity, transmission system operators and main electricity grid companies are member of the European Network of Transmission System Operators for Electricity (ENTSO-E, http://www.entsoe.eu).

Besides, according to [38] there are different points of view and therefore different definitions of power quality.

Some utilities consider power quality as *reliability*. The equipment manufacturers may indicate power quality as *those characteristics of the power supply that enable their equipment to work properly* [38].

For customers, *any power problem manifested in voltage, current, or frequency deviations that result in failure or unsatisfactory operation of customer's equipment* is a power quality problem [38].

1.3 Power quality disturbances

For one phase power systems, in ideal conditions, the voltage and current are represented as sinusoidal waves with rated frequency and amplitude. In digital forms, the signals are expressed as:

$$\begin{cases} v(k) = V\sin(\omega k T_s + \phi_v) \\ i(k) = I\sin(\omega k T_s + \phi_i) \end{cases} \tag{1.1}$$

where

- T_s is sampling time,
- $v(k)$ is the voltage signal at instant k, $i(k)$ is the current signal at instant k,
- ω is the angular frequency of the sinusoidal signals, their fundamental frequency f_o is calculated by:
$$f_o = \frac{\omega}{2\pi}$$
- V is the amplitude of the single phase voltage, I is the amplitude of the single phase current,
- ϕ_v and ϕ_i are respectively the phase angles of the voltage signal and the current signal,
- $(\omega k T_s + \phi_v)$ is the phase of the voltage, and $(\omega k T_s + \phi_i)$ is the phase of the current.

For three phase power systems, besides requirements for single phase systems, the ideal three phase currents/voltages are represented as sinusoidal waves equal in amplitudes and displaced 120° from each other:

$$\begin{cases} i_a(k) = I\sin(\omega k T_s + \phi_i) \\ i_b(k) = I\sin(\omega k T_s + \phi_i - 2\pi/3) \\ i_c(k) = I\sin(\omega k T_s + \phi_i + 2\pi/3) \end{cases} \tag{1.2}$$

and

$$\begin{cases} v_a(k) = V\sin(\omega k T_s + \phi_v) \\ v_b(k) = V\sin(\omega k T_s + \phi_v - 2\pi/3) \\ v_c(k) = V\sin(\omega k T_s + \phi_v + 2\pi/3) \end{cases} \tag{1.3}$$

with $i_a(k), i_b(k), i_c(k)$ three-phase currents and $v_a(k), v_b(k), v_c(k)$ three-phase voltages.

Obviously, these definitions are directly for power distribution systems. It can be noticed that they are generic and therefore can be applied to all type of power systems, i.e., to isolated micro grids, and moreover to any electric drive or generator with sinusoidal signals.

In the following, several important power quality problems and signal distortions are analyzed.

1.3.1 Reactive power

Definition of reactive power under sinusoidal conditions

Single-phase systems, assuming that the voltage and current are sinusoidal waves, can be represented by:

$$\begin{cases} v(k) = V\sin(\omega k T_s) \\ i(k) = I\sin(\omega k T_s - \phi) \end{cases} \tag{1.4}$$

The instantaneous power $p(k)$ is the product of the instantaneous voltage and the instantaneous current [5]:

$$p(k) = v(k)\,i(k) = VI\sin(\omega k T_s)\sin(\omega k T_s - \phi) = \frac{VI}{2}\cos(\phi) - \frac{VI}{2}\cos(2\omega k T_s - \phi) \tag{1.5}$$

The expression of $p(k)$ in (1.5) includes two components: The first is constant and the second is oscillating. Decomposing the oscillating component and re-arranging (1.5) yields to:

$$p(k) = \frac{VI}{2}\cos(\phi)[1 - \cos(2\omega k T_s)] - \frac{VI}{2}\sin(\phi)\sin(2\omega k T_s) \tag{1.6}$$

Expression (1.6) also contains two components. Based on (1.6), traditional concept of active, reactive and apparent power are derived: The active power P is the average of the first components of the expression of $p(k)$ at (1.6)

$$P = \frac{VI}{2}\cos(\phi) \tag{1.7}$$

The reactive power Q is the peak value of the second component in (1.6):

$$Q = \frac{VI}{2}\sin(\phi) \tag{1.8}$$

The apparent power S is defined as:

$$S = \frac{VI}{2} \tag{1.9}$$

The active power is the actual amount of power being dissipated by an electrical circuit. The reactive power Q is referred as 'the portion of power that does not realize work' or 'oscillating power' [5]. It represents the power component that has zero average value [5]. Apparent power represents 'maximum reachable active power at unity power factor' [5]. The definition of power factor will be introduced later.

Origins

The existence of the reactive power in a electric circuit relates to the load characteristics [5]:

- For resistive load only, $Q = 0$ and $P = S$.
- If the load is not purely resistive, $Q \neq 0$ and $P < S$.
- Inductive loads and capacitive loads are sources of reactive power generation.

Effects

With reactive power, the power lines have to carry more current than what would be necessary to supply an amount of active power, resulting in heating, broken isolation and inefficient power delivery systems [103].

Power factor

The power factor is an efficient indicator to quantify the amount of the reactive power filter of a power system. The power factor (PF) λ is defined as the portion of active power from apparent power:

$$\lambda = PF = \cos(\phi) = \frac{P}{S} \tag{1.10}$$

Obviously, the power factor λ varies from zero to one. The power factor is zero when all power supply is reactive and there is no actual work done. A unit value of power factor indicates that all the power supply is consumed by loads. The power factor can be used to evaluate how efficiently a devices is able to use and consume the power.

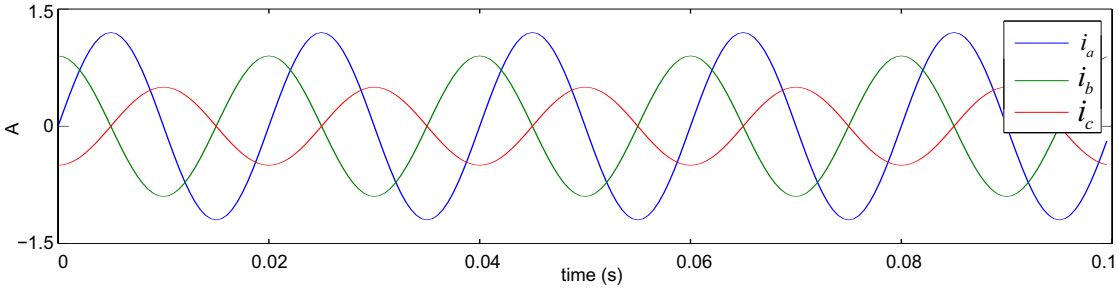

Figure 1.4 – Example the signals of an unbalanced three phase power system

1.3.2 Unbalance in three phase power systems

Phenomenon

A power system is balanced if its three phase currents (and three phase voltages) are equal in magnitudes and phase-shifted by 120° from each other (like (1.2) and (1.3)); if not, the system is unbalanced. The following equations are the expression of an unbalanced three phase system.

$$\begin{cases} i_a(k) = I_a \sin(\omega k T_s + \phi_a) \\ i_b(k) = I_b \sin(\omega k T_s + \phi_b) \\ i_c(k) = I_c \sin(\omega k T_s + \phi_c) \end{cases} \tag{1.11}$$

I_a, I_b, I_c are the amplitudes of the three phases respectively which can be different from each other. ϕ_a, ϕ_b, ϕ_c are the phase angles of the three phases that might not be shifted by 120° from each other. Fig 1.4 illustrates the unbalanced three phase signals $i_a(k), i_b(k), i_c(k)$ of an unbalanced three phase power system, with $I_a = 1.2, I_b = 0.9, I_c = 0.5$ and $\phi_a = 0, \phi_b = \frac{\pi}{2}, \phi_c = -\frac{\pi}{2}$.

Origins of unbalance

According to [110], the unbalance in a three phase power system can come from the different following causes:

- uneven distribution of single-phase loads;
- asymmetrical transformer winding impedances;
- asymmetrical transmission impedances;
- unbalanced and overloaded equipment;
- blown fuses on three-phase capacitor banks.

Besides, asymmetrical faults such as line to ground, two lines to ground, and line to line connections cause the unbalance too.

Effects

Current unbalance incurs the following problems [12]:

- increase in power losses
- additional heating which limit the line transmission capacity

Voltage unbalance adversely affects the performance of electrical equipment [12]:

- To asynchronous motors and synchronous generators, it causes power losses, heating, reduced productivity and vibration
- To converters, it generates an additional variable component of a rectified voltage (current), and harmonics that are not characteristic of a given converter.

In order to compensate for the effects of the unbalance in a power system, it is important to be able to analyze the unbalance. 'Symmetrical components' presented in the next section can be used for that purpose.

Symmetrical components to quantify the unbalance

The theory of symmetrical components was first introduced by [33] in the form of phasors and is a powerful tool to analyze unbalance conditions. In [5], it is presented in the time domain. According to the theory of symmetrical components from [5], the set of three phase signals (1.11) can be represented as sum of three sets:

$$\begin{bmatrix} i_a(k) \\ i_b(k) \\ i_c(k) \end{bmatrix} = \begin{bmatrix} i_a^+(k) \\ i_b^+(k) \\ i_c^+(k) \end{bmatrix} + \begin{bmatrix} i_a^-(k) \\ i_b^-(k) \\ i_c^-(k) \end{bmatrix} + \begin{bmatrix} i_a^o(k) \\ i_b^o(k) \\ i_c^o(k) \end{bmatrix}. \tag{1.12}$$

In (1.12), the set

$$\begin{bmatrix} i_a^+(k) \\ i_b^+(k) \\ i_c^+(k) \end{bmatrix} = \begin{bmatrix} I_+ \sin(\omega k T_s + \phi_+) \\ I_+ \sin(\omega k T_s + \phi_+ - \frac{2\pi}{3}) \\ I_+ \sin(\omega k T_s + \phi_+ + \frac{2\pi}{3}) \end{bmatrix} \tag{1.13}$$

is the positive sequence including three phase signals equal in magnitudes and displaced 120° from each other.

The set

$$\begin{bmatrix} i_a^-(k) \\ i_b^-(k) \\ i_c^-(k) \end{bmatrix} = \begin{bmatrix} I_- \sin(\omega k T_s + \phi_-) \\ I_- \sin(\omega k T_s + \phi_- + \frac{2\pi}{3}) \\ I_- \sin(\omega k T_s + \phi_- - \frac{2\pi}{3}) \end{bmatrix} \tag{1.14}$$

is the negative sequence including three phase signals equal in magnitudes and displaced 120° from each other.
Finally the set

$$\begin{bmatrix} i_a^o(k) \\ i_b^o(k) \\ i_c^o(k) \end{bmatrix} = \begin{bmatrix} I_o \sin(\omega k T_s + \phi_o) \\ I_o \sin(\omega k T_s + \phi_o) \\ I_o \sin(\omega k T_s + \phi_o) \end{bmatrix} \tag{1.15}$$

is the zero sequence including three phase signals equal in magnitudes and in phase with each other.

It can be observed that the positive sequence has clockwise rotation of a-b-c and the negative sequence has counter clockwise rotation of a-b-c. Let's take an example to understand the meaning of the components. In a motor, the unbalanced motor voltages are also composed of symmetrical components. The positive sequence voltage produces the desired positive torque, whereas the flux produced by the negative sequence voltage rotates against the rotation of the rotor and generates an unwanted reversing torque [110]. The zero sequence voltage does not produce rotating flux, hence, does not contribute to the torque.

The theory of symmetrical components can be applied for any general case of n-phase power systems, see [33] for more information.

A three phase power is balanced when the decomposition of its three phase signals into symmetrical components is composed of only a positive component. The existence of negative components and/or zero components in the decomposition shows that the system is unbalanced.

1.3.3 Harmonics

Phenomenon

In a power system, the voltage produced by the generation system can be considered sinusoidal. "However, when a source of sinusoidal voltage is applied to a nonlinear device or load, the resulting current is not perfectly sinusoidal. In the presence of system impedance this current causes a non-sinusoidal voltage drop and, therefore, produces voltage distortion at the load terminal, i.e. the latter contains harmonics" [12].

"Power system harmonics are defined as sinusoidal voltages and currents at frequencies that are integer multiples of the main generated (or fundamental) frequency. They constitute the major distorting components of the main voltage and load current waveforms" [12].

For example, in [12], harmonic analysis of the current of a TV receiver shows the main harmonics of the orders third, fifth, seventh and ninth as followed:

$$i(k) \approx I_o \sin(\omega k T_s + \phi_o) + I_3 \sin(3\omega k T_s + \phi_3) + I_7 \sin(7\omega k T_s + \phi_7) + I_9 \sin(9\omega k T_s + \phi_7) \tag{1.16}$$

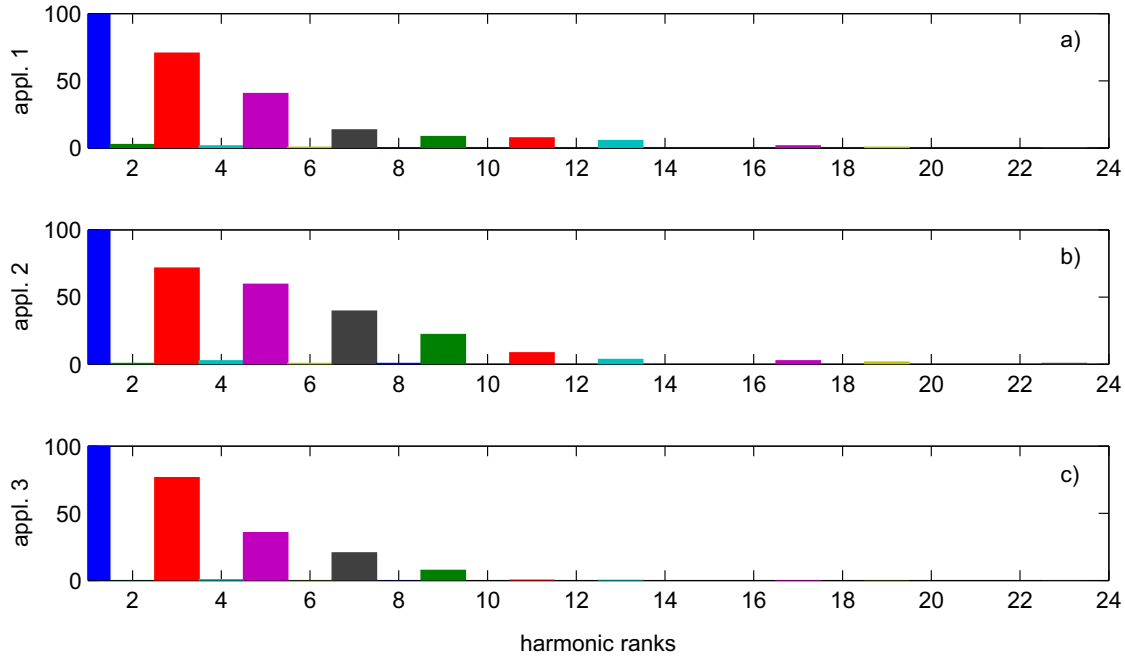

Figure 1.5 – Harmonic components caused by a) TV receiver, b) PC and printer, c) microwave oven

where $i(k)$ is current of the TV set, $i_{(o)}(k)$ is fundamental component, $i_{(3)}(k)$ is called harmonics order 3 (the component's frequency is equal three times of the fundamental frequency), $i_{(5)}(k), i_{(7)}(k), i_{(9)}(k)$ are harmonics orders 5, 7, 9 respectively.

The current of PC and printer combined together contains the main harmonics as the third, fifth, seventh and ninth, and the current of a microwave oven contains the third, fifth and seventh. Fig. 1.5 shows the harmonics spectrum generated by those devices.

Harmonic sequence and origins

From [34], harmonic components can be considered as symmetrical components. One can consider a balanced three phase power system with the fundamental currents in positive sequence as follow:

$$\begin{aligned} i_{a1}(k) &= I_1 \sin(\omega k T_s) \\ i_{b1}(k) &= I_{(1)} \sin(\omega k T_s - 2\pi/3) \\ i_{c1}(k) &= I_{(1)} \sin(\omega k T_s + 2\pi/3) \end{aligned} \tag{1.17}$$

Its third order harmonics are determined as:

$$\begin{aligned} i_{a3}(k) &= I_3 \sin 3(\omega k T_s) \\ i_{b3}(k) &= I_3 \sin 3(\omega k T_s - 2\pi/3) = I_{(3)} \sin(3\omega k T_s - 2\pi) = I_3 \sin(3\omega k T_s) \\ i_{c3}(k) &= I_3 \sin 3(\omega k T_s + 2\pi/3) = I_{(3)} \sin(3\omega k T_s + 2\pi) = I_3 \sin(3\omega k T_s) \end{aligned} \tag{1.18}$$

Type	Frequency	Source
DC	0	Electronic switching devices, half-wave rectifiers, arc furnaces, geomagnetic induced currents (GICs)
Odd harmonics	$h.f_o$ (h=odd)	Nonlinear loads and devices
Even harmonics	$h.f_o$ (h=even)	Half-wave rectifiers, geomagnetic induced currents (GICs)
positive sequence harmonics	$h.f_1$ (h = 1, 4, 7, 10, ...)	Operation of power system with nonlinear loads
negative sequence harmonics	$h.f_o$ (h = 2, 5, 8, 11, ...)	Operation of power system with nonlinear loads
zero sequence harmonics	$h.f_o$ (h = 3, 6, 9, 12, ...)	Unbalanced operation of power system

Table 1.1 – Several types and Sources of Power System Harmonics [34]

From equations (1.18), the three phase signals of the third order harmonics are in phase with each other, therefore the third harmonic components are known as zero sequence harmonics. The fifth order harmonics are expressed as:

$$\begin{gathered} i_{a5}(k) = I_5 \sin 5(\omega k T_s) = I_5 \sin(5\omega k T_s) \\ i_{b5}(k) = I_5 \sin 5(\omega k T_s - 2\pi/3) = I_5 \sin(5\omega k T_s - 10\pi/3) = I_5 \sin(5\omega k T_s + 2\pi/3) \\ i_{c5}(k) = I_5 \sin 5(\omega k T_s + 2\pi/3) = I_5 \sin(5\omega k T_s + 10\pi/3) = I_5 \sin(5\omega k T_s - 2\pi/3) \end{gathered} \tag{1.19}$$

From (1.19), the phase sequence of the fifth harmonic is counter clockwise, hence, the fifth harmonic is known as negative sequence harmonic.

Similarly, other harmonic orders can be classified as positive, negative, or zero sequence harmonic. Table 1.1 displays different types of harmonics, their order, and the sources of them [57].

In this table, f_o represents the fundamental frequency of a power system, and h represents the harmonic order.

Effects

Among power quality problems, the issue of harmonics draws much concern because of many negative effects it gives rise to. We can cite:

- Heating in rotating machinery (induction and synchronous) due to iron and copper losses, and mechanical oscillations as a consequence of pulsating torques;
- Heating in transformers due to an increase in copper losses and stray flux losses;

- Dielectric (insulation) failure in power cables causing by skin effect and proximity effect;
- Increase of heating and voltage stress to capacitors resulting in a shorten capacitor life;
- Electronic equipment mis-operation and/or malfunction;
- Erroneous operation of metering devices;
- Decrease in response speed and mis-operation of relays;
- Communication system disturbance due to magnetic and electric fields produced by harmonic currents or voltages;
- Others.

Indices to quantify harmonic contamination of a signal

The most popular index to measure the quantity of harmonic distortion is the Total Harmonic Distortion (THD), which is quantified as root mean square (rms) of the harmonics expressed as a percentage of the fundamental component [12]:

$$\mathrm{THD} = \frac{\sqrt{\sum_{n=2}^{N} V_n{}^2}}{V_1} \tag{1.20}$$

where V_1 is the rms value of the fundamental voltage, while V_n, $n = 2,3,..,N$ is the rms voltage of harmonic n. This index can also be applied for a current to evaluate its harmonic distortion level. More information of causes, effects and control of harmonics is available in [1, 2, 98]. Identifying harmonics is also very important for optimal control of electrical drives and this is illustrated in [117] for induction machines.

1.3.4 Fundamental frequency variations

Phenomenon

Frequency is a very important parameter to stable and reliable operation of electrical equipment in power systems. A frequency's low value can lead to abnormal performance of electrical devices, for example, disturbing variations of the luminous flux of incandescent lamps. On the other hand, it's high value increases losses due to skin effect. Ideally, the frequency should be kept at a constant value which is 50 Hz in Europe and 60 Hz in USA [13]. However, the frequency value rarely stays constant and varies in time. The record of variation of the fundamental frequency of power systems in various countries and areas during two days are represented on Fig. 1.6 [4]. Fig. 1.7 illustrates a fluctuating frequency during a short time in Mulhouse, France.

[4] according to wikipedia https://en.wikipedia.org/wiki/Power_quality

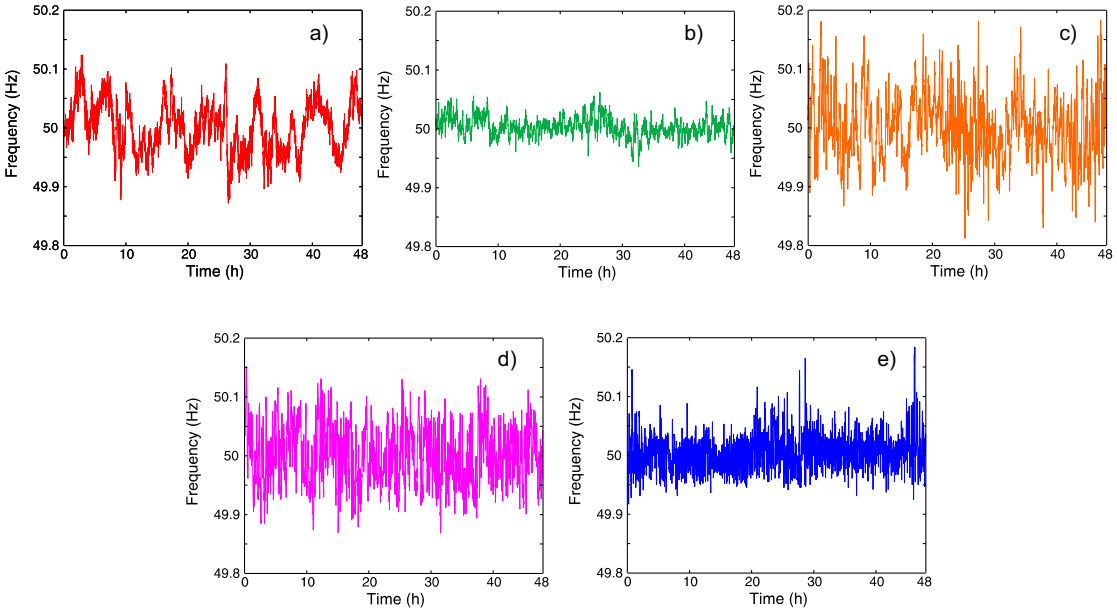

Figure 1.6 – Frequency deviations of power systems of different countries: a) Sweden, b) Central Europe, c) Greate Britain, d) Singapore, e) China (East), recording during two days

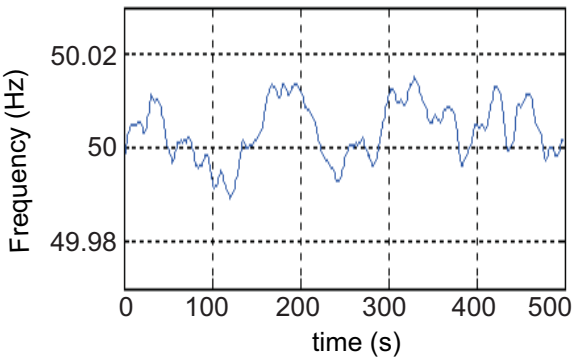

Figure 1.7 – Estimation of a fluctuating frequency during 500 s [75]

Origins

Since the fundamental frequency is directly related to the rotational speed of the generator in a power system, its value depends on the balance between the power generation and the power demand: The frequency rises if the power generation is higher than the power demand and falls otherwise.

From [50], the quantity of the frequency shift and its duration depend on the load characteristics and the response of the generation system. The continuous variation of power demand, i.e. load switching leads to small fundamental frequency variation. The frequency variation outside of the accepted limit for steady-state normal operation are normally caused by faults on the bulk power transmission system, a large block of load being disconnected, or a large source of generation going off line [50].

Effects

Frequency variation has great impact to normal operation of electrical devices, among them:

- Protection algorithms used in protective relays require the calculation in the values for amplitudes, impedances, power, phase angle, etc which can result in large errors due to frequency variation [95];
- The operation of rotating machinery, or processes using their timing from the power frequency will be affected when the frequency changes [50];
- In harmonic filters, the circuit impedance, which is designed to be equal to zero for a harmonic at the norminal frequency, becomes other than zero because of frequency variation [13];
- The magnetic characteristic of transformers can get into non-linear zones when the fundamental frequency varies in time, resulting in the increase of the transformer's no-load losses [13].

Indices

According to standard EN 50160/2006 [31], the nominal frequency of the supply voltage shall be 50 Hz. Under normal operating conditions the mean value of the fundamental frequency measured over 10 s shall be within a range of

- for systems with synchronous connection to an interconnected system
  50 Hz $\pm 1\%$ (i.e. 49.5 - 50.5 Hz) during 99.5% of a year
  50 Hz + 4%/ − 6% (i.e. 47 - 52 Hz) during 100% of the time

- for systems with no synchronous connection to an interconnected system (e.g., supply systems on certain islands)
  50 Hz ±2% (i.e. 49 - 51 Hz) during 95% of a week
  50 Hz ±15% (i.e. 42.5 - 57.5 Hz) during 100% of the time

1.3.5 Short-duration voltage variations

Interruptions

Interruption, which is illustrated in Fig. 1.8 a), occurs when the supply voltage (or load current) decreases to less than 0.1 pu for less than 1 minute. After a while after the interruption happens, the supply is restored automatically. Equipment failures, control malfunction, and blown fuse or breaker opening are some causes of interruptions [34].

Sags

Reductions in the rms voltage between 0.1 and 0.9 pu in a short duration (usually between 0.5 cycles and 1 minute.) are called sags [34], its phenomenon is illustrated at Fig. 1.8 b). According to [34], the power quality problem can be consequence of:

- energization of heavy loads,
- starting of large induction motors,
- single line-to-ground faults,
- load transferring from one power source to another

Sags are reason for malfunctions of electrical low-voltage devices.

Swells

Swells are the increases of voltage magnitude between 1.1 and 1.8 pu during the most accepted duration from 0.5 cycles to 1 minute [34], as shown in Fig. 1.8 c). Main causes of swells are [34]:

- switching off of a large load,
- energizing a capacitor bank,
- voltage increase of the unfaulted phases during a single line-to-ground fault

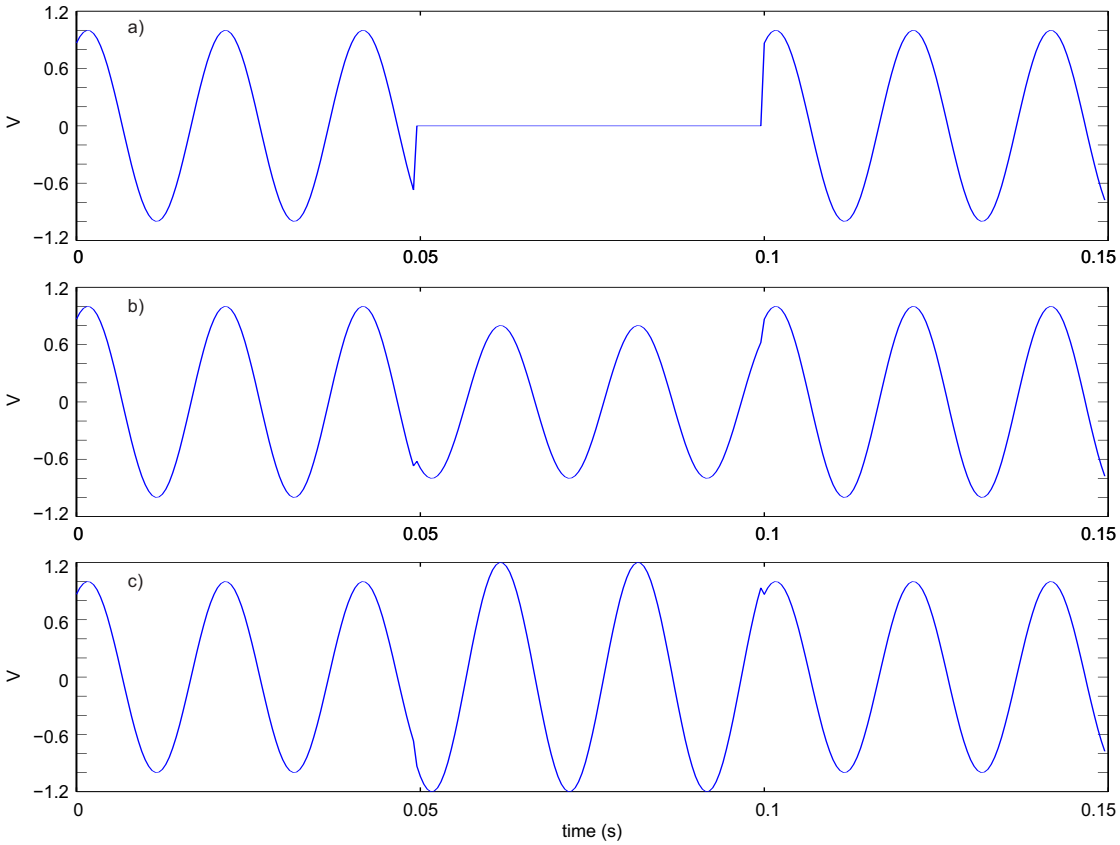

Figure 1.8 – Short duration voltage variations: a) Interruption, b) Sag, c) Swell

1.3.6 Long-duration voltage variations

Long Interruptions

Long interruption is a phenomenon at which voltage drops to zero and does not return automatically [34]. According to the IEEE definition, the duration of this type of interruption is more than 1 minute [34]. There are several causes of long interruptions:

- fault occurrence in a part of power systems with no redundancy or with the redundant part out of operation,
- an incorrect intervention of a protective relay leading to a component outage,
- scheduled (or planned) interruption in a low-voltage network with no redundancy.

Under voltage and over voltage

The undervoltage condition occurs when the rms voltage decreases to 0.8-0.9 pu for more than 1 minute.

Overvoltage is an increase in the rms voltage to 1.1-1.2 pu for more than 1 minute. This phenomenon could happen because of:

- an insulation fault, ferroresonance, faults with the alternator regulator, tap changer transformer, or overcompensation,
- an incorrect intervention of a protective relay leading to a component outage,
- scheduled (or planned) interruption in a low-voltage network with no redundancy.

1.3.7 Other power quality problems

Besides the power quality problems discussed above, there are others such as electrical transients and inter harmonics. More details of different power quality phenomena, their types and origins, and their indice of evaluation are available in [50, 29] for reference.

1.4 Power quality monitoring and control

Power quality disturbances result in power loss, heating, and bad performance of electrical devices. Further, they may propagate to the entire power system and cause more serious consequences.

Power quality monitoring indicates measuring power quality parameters of a power grid, evaluation and diagnosis of the power system's conditions. Power quality control relates to the activities of compensation power quality disturbances and/or isolation the infected area from the power grid [119]. The Flexible AC Transmission System (FACTS) is an application of power electronics revolution in areas of electric energy in order to enhance controllability, stability, and power transfer capability of AC transmission systems [43].

The followings present some methods to monitor and control power quality of power grids: frequency control, compensation of power quality problems, protection of power systems from failures.

1.4.1 Frequency Control

As stated previously, the fundamental frequency is related to the stability of a power system and the stable operation of all the electrical devices connecting to the system. The frequency value rarely stays constant and depends on the power generation and the power demand which vary and lead to fundamental frequency variations. Energy management strategies are also necessary to control and to optimize the power flow in a grid [111].

According to [104], Automatic Generation Control (AGC) is important in controlling the fre-

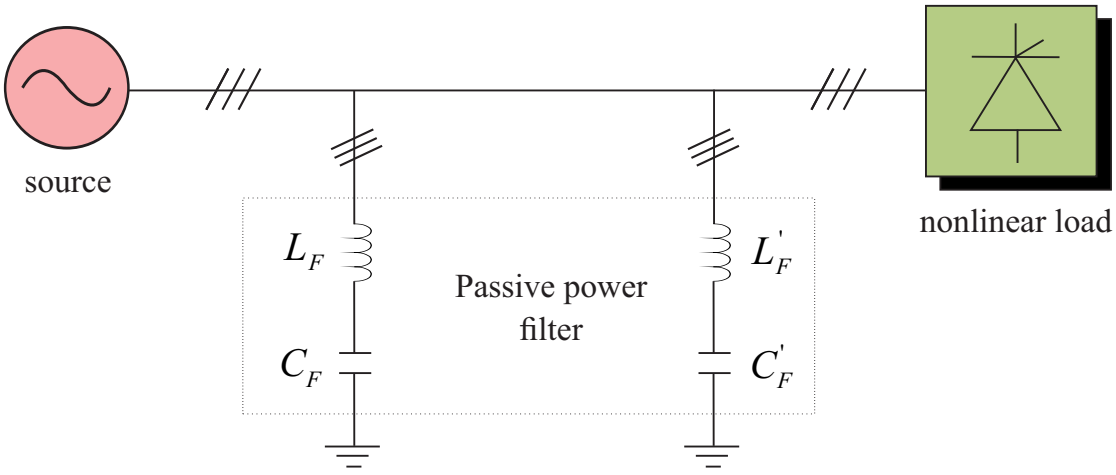

Figure 1.9 – Principle of a passive power filter [71]

quency of power systems. AGC contains three levels:

- Primary control is to perform the speed control of the generating units in order to response immediately to sudden change of load (or change of frequency). A deviation in system frequency is compensated by adjusting the unit power generation.
- Secondary control has function of restoring the frequency to its nominal value while maintaining power interchange among areas by regulating the output of selected generators [91].
- Tertiary control helps the system operate as economically as possible and restore security level if necessary.

Secondary control is referred as Load Frequency Control (LFC) [65]. For more information about LFC in interconnected power systems, one can refer to [76, 47].

1.4.2 Compensation

Passive power filters and active power filters are typical compensators of power quality disturbances.

Passive filters consist of capacitors, inductors and/or resistors. The functions of passive filters are correcting power factor and filtering high order harmonics [4]. Fig. 1.9 shows an example of passive filters applied for harmonic filtering. Such a passive filter is installed in the vicinity of a nonlinear load to absorb the dominant harmonic currents flowing out of the load.

The performance of passive power filters depends on the source impedance, however, the impedance may be not well determined and may vary as the grid topology changes [5]. Parallel

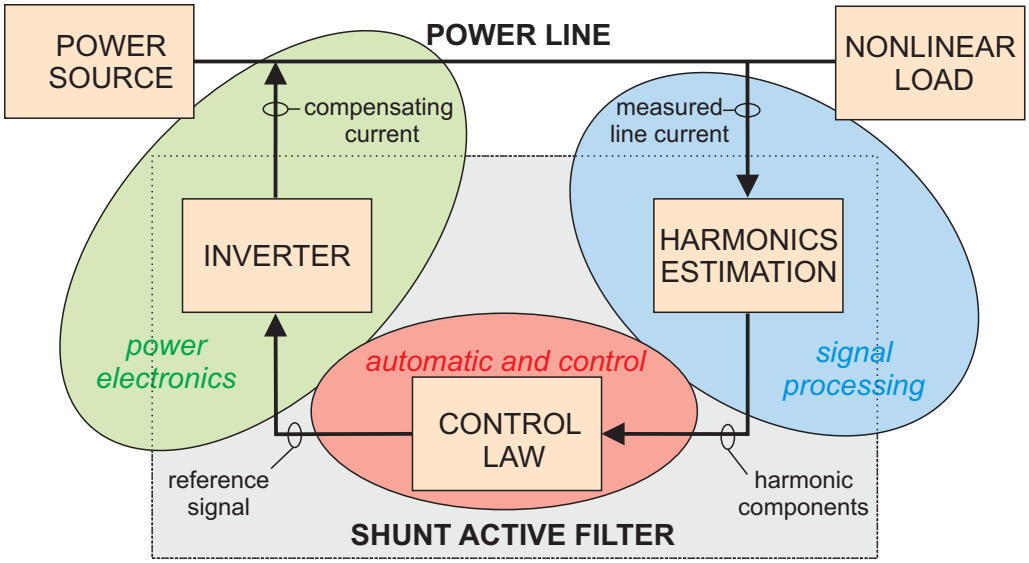

Figure 1.10 – Main parts of an active power filter with associated scientific skills

resonance between the source impedance and the shunt filter impedance produces harmonic magnifying phenomenon [5]. One can refer to IEEE Std 1531-2003 [49] for instructions on how to install passive power filters to meet certain standards.

Active power filters (APF) were developed to overcome disadvantages of passive power filter by providing dynamic and flexibly adjustable compensation for power quality problems [99]. A review of active filters for power quality is provided in [100]. An APF is able to measure harmonic currents and harmonic voltages caused by nonlinear loads and eliminate them to ensure the THD of grid voltages and currents and the power factor with sufficient capacity and low background harmonics. It can also compensate for negative component sequence, reduce power off loss caused by resonance phenomenons and improve the reliability of the power supply system. This is achieved by injecting compensating currents/voltages into the grid and these currents/voltages are calculated from important estimated parameters. APF have to be adaptive because of the load changes, energy generation variations, and non-stationary properties of the power system's signals. Adaptive AFP strategies can be found in [72].

An APF is composed of three steps: Signal processing, control, and generation of compensating currents and/or voltages, as shown in Fig. 1.10.

The step of signal processing is to measure the power signals (voltages, currents) from a power grid then to process these signals in order to estimate the power system's parameters and states and to calculate the compensating current (voltage) references. These functions can be implemented on a digital controller using DSPs, FPGAs, and A/D converters for digital signal processing, together with operational and isolation amplifiers for analog signal processing, and Hall-effect voltage/current sensors [4]. Examples of a signal processing methods used to calculate harmonic-compensating currents with ANNs are presented in [114].

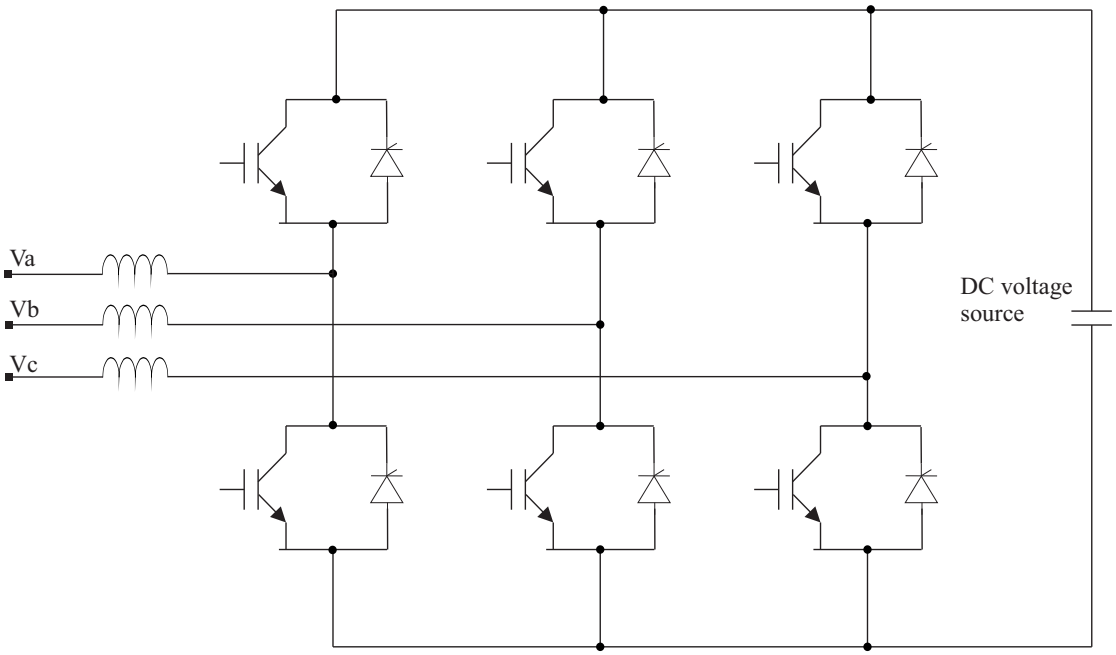

Figure 1.11 – A typical architecture of a Voltage Source Inverter (VSI)

The compensating currents or voltages are generated by controlling on/off switch of semiconductor devices such as IGBT of an inverter. Fig. 1.11 presents a Voltage Source Inverter (VSI). For how an inverter works to generate a desired analog current or voltage, one can refer to [18].

In the APF family, there are shunt APF and series APF. The shunt active filter is designed to compensate all current disturbances, for example, harmonics, unbalance, and voltage sag [71, 74, 113]. The filter, which is connected in parallel with a nonlinear load to filter harmonics, operates in the following steps [5]:

- Measure the instantaneous load current and voltage;
- Extract the harmonics current by digital signal processing;
- Inject the current equal to the harmonic current extracted from the load current but opposite in phase, so that the current supply by the network is sinusoidal

The series active filter is designed to compensate for all voltage disturbances like harmonics, unbalance, and voltage sag [71] [74]. The configuration of a three-phase series APF for harmonic-voltage filtering is shown in Fig. 1.12. In this example the filter is connected in series with the utility supply voltage through a three-phase transformer or three single-phase transformers [5]. The series APF works according to the following steps:

- Measure the instantaneous load voltage and current;

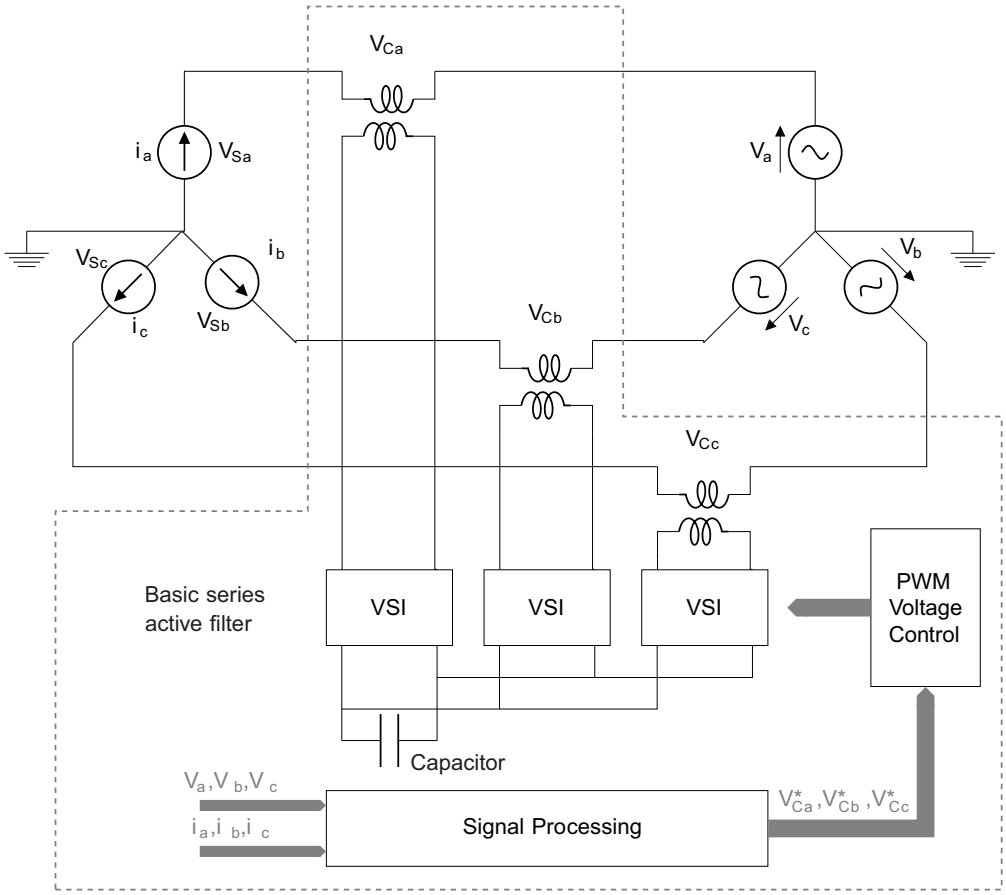

Figure 1.12 – Basic series active filter [5]

- Calculate the compensating voltage for the harmonic voltage components in the load by digital signal processing;
- Apply the compensating voltage across the primary of the transformer.

More information of series active filter can be found at [66] Futher more, an UPQC (Unified Power Quality Conditioner) is the integration of a shunt APF and a series APF to benefit from the advantages of each of the two filters [51].

Hybrid APF is a shunt or series active filter combined with a passive filter. Here, the active filter plays a role as an active impedance to help to overcome the dependence of the passive filter on the source impedance. More information of hybrid APF can be found in [77] [92] [62] [35]. APF architectures are listed in Table 1.2 for some specific applications.

The guidance notes [2] introduce different types of equipment for measuring, analyzing and compensating for harmonics. More recently, power quality enhancement and renewable energy control can be associated in APF schemes for a better use of these resources [17, 115]. It can be noticed that identifying the harmonic content of signals measured on drives allows to

Compensation for specific applications	Active Power Filters Topologies			
	Active series	Active shunt	Hybrid of active series and passive shunt	UPQC
Current harmonics		••	•••	•
Reactive power Load balancing		••• •	••	••
Neutral current		••	•	
Voltage harmonics	•••		••	•
Voltage regulation	•••	•	••	•
Voltage balancing	•••		••	•
Voltage flicker	••	•••		•
Voltage sag & dips	•••	•	••	•

Table 1.2 – Selection of APF for specific application considerations [99] (a higher number of '•' is preferred)

achieve optimal control signal for torque ripple minimization in permanent magnet synchronous motors [71].

1.4.3 Power system protection

The protective relay and the circuit breaker usually works together to isolate faults in power systems. A protective relay is responsible for detecting faults and then send a signal to the circuit breaker to make a trip that isolates the faults detected. According to [9], there are different types of protective relays, below are three of them:

- Electromechanical relays: The relays base on magnetic field and mechanical movement to detect faults.
- Static relays: Without armature or other moving element, in the relays, the faults are detected by electronic components.
- Digital relays: The relays work with samples of the signal and use digital signal processing embedded in microprocessors to identify abnormalities and power quality disturbances.

According to [10], digital relays have advantages over analog relays:

- The evolution of hardware makes it possible to have different digital signal processing implemented, and to exchange date between devices, e.g., alarm signals.
- Useful information, e.g., the whole information of an event, can be stored with low cost of memory for protection engineer.
- One hardware can be programmed with different algorithms in order to implement different tasks.

1.5 Conclusion

In this chapter, an introduction to the main power quality problems has been presented. There are different types of perturbations and we focus on the reactive power, the unbalance between the phases, harmonics, the frequency deviation, the voltage variations. At the same time, their origins, their impacts to end-user equipment and their quantifying indices are analyzed.

Passive power filters and active power filters are mentioned as solutions to mitigate the negative effects caused by the power quality problems. Most of power filters in the market today are 'closed', i.e, the parameters of the filters are fixed so that the filters are only dedicated for a specific function, like filtering the 5^{th} harmonic, but not work with other harmonics. The application of digital signal processing in active power filters makes them more flexible to varying environment. Indeed, digital signal processing allows to analyze the currents and voltages and to identify the existing harmonics in real time even with load changes. Active power filtering consists in using shunt APF, series APF, Hybrid APF, UPQC, each is appropriate for some specific applications.

The next chapter will present digital signal processing methods applicable to estimate parameters and states of a power system.

2 Advanced signal processing methods for power quality improvement

Signal processing is concerned with the representation, manipulation, and transformation of signals and the information that they carry. Typical signal processing tasks for example consist in enhancing a signal by reducing the noise or some other interference, or in extracting some information from it [41].

Analog signal processing works directly with physical signals, e.g., analog currents or analog voltages. Digital signal processing works with samples of the signals, i.e, the analog signal must be converted into a digital signal by an analog-to-digital conversion before being processed. Digital signal processing has some advantages: It is easy to implement complex algorithms and/or modify the algorithms, it is convenient to exchange information, and it is useful to store and memorize values and parameters.

Digital signal processing methods are classified into offline methods and online methods. Offline methods collect a batch of data before processing the data so that they are only applicable to non-real-time applications. Online methods update their estimation at each time that a new data is available. This type of signal processing methods is appropriate to real-time applications. Adaptive filters or adaptive methods belong to online method and are able to self-adapt to changing conditions [42]. Digital signal processing has found applications in various fields, e.g., control, communication, health care, etc. [59]. In power system applications, signal processing has been used widely to improve power quality. It is used in harmonics analysis and signal parameter estimation [11, 71, 74, 113]. Several signal processing methods can detect voltage sags and swells [68]. Other digital signal processing methods have been applied to improve and control the power quality in power grids [96].

The fundamental frequency is a very important parameter of a power system and it is often required by different other applications, e.g., harmonics analysis and unbalance conditions analysis. The frequency value rarely stays constant and varies according to the power demand. The power generation and demand vary continuously and lead to small fundamental frequency variations. There are other faults, among them unbalanced voltage situations in the case of multiphase systems. Fast and precise harmonics compensation and fault detection necessitate

an online estimation and tracking of the fundamental frequency in power lines.

The theory of symmetrical components is a powerful tool to analyze a power system in unbalanced conditions. Symmetrical components are used in fault analysis and design of protective relays [22], reactive power compensation and unbalance mitigation [101] and other applications. Therefore identifying the symmetrical components plays an important role in improving the reliability and stability of power systems.

This chapter will present some effective adaptive signal processing methods of power quality improvement, focusing on the estimation of the fundamental frequency of a power system, and on the estimation of the symmetrical components of a power system. Their advantages and disadvantages are also discussed.

2.1 Adaptive signal processing methods to estimate the fundamental frequency of a power system

Various frequency estimation techniques have been proposed for electric transmission grids. One of the earliest methods used for tracking the phase angle is the Zero Crossing (ZC) method which determines the moment the signal passes zero. The performance of ZC is badly affected by power quality disturbances such as noise and harmonics [78].

More sophisticated methods like polynomial models can be used to estimate the parameter of a typical signal issued from a power system. Thus, Auto-Regressive (AR) models, Auto-Regressive Moving Average (ARMA) models, or other polynomial signal model can be used for frequency and parameter estimation of non-stationary power signals [69]. A power system frequency estimation method using morphological prediction of Clarke components has been proposed in [28]. All these methods are able to adapt themselves to changes, but at the same time they need new measurements and time to take into account the new behavior.

Adaptive methods like Artificial Neural Networks (ANN), neuro-evolutionary approaches [86], fuzzy adaptive filter for frequency are faster in estimating parameters of non-stationary power signals [69]. In these approaches, unknown nonlinear terms are identified by artificial nonlinear units (i.e., neurons) or neuro-fuzzy networks [90, 115]. They take into account the changes through an adaptation and/or learning procedure. These approaches have also been successfully applied for estimating frequency variations of electric signals [26, 19, 39].

Filters like Adaptive Notch Filter (ANF) [70] or Adaptive Prony Method (APM) [21] are also good candidates under some conditions. For example, a specific adaptive notch filter solution under unbalanced and/or distorted conditions has been proposed in [108]. Recently, Phase Locked Loop (PLL) methods have found much attention for being applied to power systems, mainly due to their simplicity, robustness, and effectiveness [93, 58].

Extended Kalman Filter (EKF) is a well-known method that finds applications in different fields

of signal processing and control, e.g., wind generator control [7]. Kalman filtering is based on a state-space model, it is therefore a time-based method. EKF has been investigated and designed in [25, 45, 36, 56] for fundamental frequency estimation of a power system. The method is robust to noise, but the initialization remains a challenge and often requires prior knowledge of the process.

Fourier's methods and the Fast Fourier Transform (FFT) algorithms are efficient to estimate the spectrum of a signal. Obviously, the assumptions that must be made before using Fourier's theory are that the signal to be processed have to be periodical and stationary. However, one major disadvantage associated with the approaches is the leakage effect which is the spreading of energy from one frequency into adjacent ones. Due to that leakage effect, the amplitudes and phase angles of harmonics can not be determined accurately from the spectrum of the signal [37, 107]. Power quality can also be evaluated with the wavelet theory [94].

Time-frequency analysis methods are known to be efficient methods [44]. Thus, Stockwell's theory can be used and it is referred to as the s-transformation [67, 52]. Parameter estimation of frequency changing signals based on the robust s-transform algorithms is well illustrated in [24].

PLL, APM, ANF and methods of EKF are presented in the following sections and their characteristics are discussed.

2.1.1 Phase-locked Loop (PLL)

PLL was introduced by de Bellescize in 1936 [6]. Since that time, PLL has found applications in various fields such as communication, signal processing and control [6]. *"A PLL is defined as a circuit that enables a particular system to track another one. More precisely, a PLL is a circuit synchronizing an output signal (generated by an oscillator) with a reference or input signal in the frequency as well as in phase"* [6].

In [6], the authors claim that: *"In the synchronized or the locked state, the phase error between the oscillator's output and the reference signal is either zero or an arbitrary constant. In the case of a phase error building up, the oscillator is tuned by a control mechanism in order to reduce the phase error to a minimum. In such a control system, the phase of the output signal is actually locked to the phase of the reference input"*. A basic digital structure of a PLL is shown in Fig. 2.1 and contains three basic functional components: A digital controlled oscillator to generate an oscillating signal (the output signal) to track the phase of the input signal, a phase error detector to measure the phase error of the input and output signals, and a digital filter to control the DCO (Digital Controlled Orcillator) in producing the phase-tracking output [6]. Modern power distribution systems include distributed electric power generation which is based on wind energy, fuel cells, PV, hydraulic systems, etc. and grid synchronization is one of the most important issues. Grid voltage conditions such as phase, amplitude and frequency determine the proper operation of a grid connected system. In such applications, a fast and accurate detection

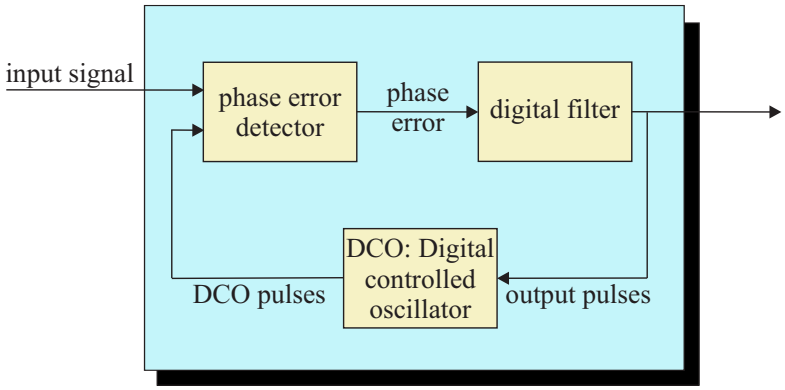

Figure 2.1 – Basic principle of a Digital PLL [6]

of the phase angle, frequency and amplitude of the grid voltage is essential. These parameters, together with the implementation simplicity and the cost are all important when examining the credibility of a synchronization scheme. Therefore an ideal phase-detection scheme must be used to promptly and smoothly track the grid phase through various short-term disturbances and long term disturbances to set the energy transfer between the grid and any power converter.

The Phasor Measurement Unit (PMU) technology can provide phase information (both magnitude and phase angle) in real-time by using a common time source for synchronization [97]. The advantage of referring phase angle to a global reference time is helpful in capturing the wide area snap shot of the power system. Effective utilization of this technology is very useful in monitoring power quality and mitigating blackouts [46].

PLL-based systems can be used to track the phase angle in order to improve the synchronization systems response in adverse grid conditions [106]. Although the implementation of PLL is simple, the drawbacks associated with the PLL are: Sensitivity to the grid voltage variations, harmonics and unbalance, difficulty to obtain an accurate tuning of the PLL parameters. PLLs are not fast because of their proportional-integral block and low-pass filters used by the phase error detector. With real-time implementations of discrete signal processing, various high performance PLL-based methods have been introduced to simplify the phase error detector. For example, the dq-PLL in [20, 116] is based on the dq-transformation to calculate the signal of the phase error. The existence of harmonic and/or unbalanced conditions can seriously affect the performance of PLL. Enhanced methods called robust PLL have been proposed to overcome this limitation [3].

2.1.2 Extended Kalman Filter for fundamental frequency estimation of balanced three phase power systems (3P EKF)

The 3P EKF is a model-based method which is based on a state-space model of the input signals and uses EKF to estimate the state variables of the model.

One can consider the following balanced three-phase signals of a power system:

$$\begin{cases} i_a(k) = I\sin(\omega k T_s + \phi) + \varepsilon_a(kT_s) \\ i_b(k) = I\sin(\omega k T_s + \phi - 2\pi/3) + \varepsilon_b(kT_s) \\ i_c(k) = I\sin(\omega k T_s + \phi + 2\pi/3) + \varepsilon_c(kT_s) \end{cases} \tag{2.1}$$

where ε_a, ε_b and ε_c are time-varying terms that can be any combination of white noise and higher-order harmonics.

Signal modeling

According to [25], the $\alpha - \beta$ components i_α and i_β of the three phases signals in (2.1) are obtained from the $\alpha\beta$-transform of the three phase signals given in (2.1), and the corresponding complex form is determined by (Appendix A.2):

$$i(k) = i_\alpha(k) + j i_\beta = A e^{j(\omega k T_s + \phi)} + \eta(k) \ , \tag{2.2}$$

where $\eta(k)$ is the noise component. Defining

$$\begin{cases} q_1(k) = e^{j\omega k T_s} \\ q_2(k) = A e^{j(\omega k T_s + \phi)} \end{cases} \tag{2.3}$$

leads to the following state-space model:

$$\begin{bmatrix} q_1(k+1) \\ q_2(k+1) \end{bmatrix} = \begin{bmatrix} 1 & 0 \\ 0 & q_1(k) \end{bmatrix} \begin{bmatrix} q_1(k) \\ q_2(k) \end{bmatrix} \ , \tag{2.4}$$

and a scalar output

$$y(k) = i(k) = q_2(k) + \eta(k) \ . \tag{2.5}$$

According to [25], the previous state-space model can be extended in order to take into account harmonics and thus to be more precise. For example, including the fifth harmonic into the state space $\mathbf{q}(k)$ is achieved with q_3 and gives:

$$\begin{bmatrix} q_1(k+1) \\ q_2(k+1) \\ q_3(k+1) \end{bmatrix} = \begin{bmatrix} 1 & 0 & 0 \\ 0 & q_1(k) & 0 \\ 0 & 0 & q_1^5(k) \end{bmatrix} \begin{bmatrix} q_1(k) \\ q_2(k) \\ q_3(k) \end{bmatrix} \ , \tag{2.6}$$

i.e., $\mathbf{q}(k+1) = F(k, \mathbf{q}(k))$, and

$$y(k) = i(k) = q_2(k) + q_3(k) + \eta(k) = C(k, \mathbf{q}(k)) + \eta(k) \ . \tag{2.7}$$

Estimation algorithm: Extended Kalman Filter (EKF)

Before presenting the Extended Kalman Filter (EKF), we first introduce the Kalman Filter.

The Kalman Filter (KF) is a recursive estimation method based on a linear state-space model of the dynamics of the plant, i.e., the system [42].

$$\mathbf{q}(k+1) = \mathbf{F}(k+1,k)\mathbf{q}(k) + \boldsymbol{\nu_1}(k) \quad , \tag{2.8}$$

$$\mathbf{y}(k) = \mathbf{C}(k)\mathbf{q}(k) + \boldsymbol{\nu_2}(k) \quad , \tag{2.9}$$

where $\mathbf{F}(k+1,k)$ is a known state transition matrix, $\mathbf{C}(k)$ is a known measurement matrix. $\boldsymbol{\nu_1}$ and $\boldsymbol{\nu_2}$ are uncorrelated, zero-mean, white noises.

The KF is used to estimate the state vector by minimizing the Mean Squared Error (MSE) based on the real values of the state vector. This error is updated iteratively and error correction can be taken online for estimating the states. Below the update equations are presented, in which the input of the filter is $\mathbf{y}(k)$, and the output is the estimate $\widehat{\mathbf{q}}(k|\mathbf{Y}_k)$ of the state vector [42]:

$$\mathbf{K}(k) = \mathbf{F}(k+1,k)\mathbf{P}(k,k-1)\mathbf{C}^H(k)[\mathbf{C}(k)\mathbf{K}(k,k-1)\mathbf{C}^H(k) + \mathbf{Q_2}(k)]^{-1} \tag{2.10a}$$

$$\boldsymbol{\alpha}(k) = \mathbf{y}(k) - \mathbf{C}(k, \widehat{\mathbf{q}}(k|\mathbf{Y}_{k-1})) \tag{2.10b}$$

$$\widehat{\mathbf{q}}(k+1|\mathbf{Y}_k) = \mathbf{F}(k+1,k)\widehat{\mathbf{q}}(k|\mathbf{Y}_{k-1}) + \mathbf{P}(k)\boldsymbol{\alpha}(k) \tag{2.10c}$$

$$\mathbf{P}(k) = \mathbf{P}(k,k-1)[\mathbf{I} - \mathbf{F}(k+1,k)\mathbf{K}(k)\mathbf{C}(k)] \tag{2.10d}$$

$$\mathbf{P}(k+1,k) = \mathbf{F}(k+1,k)\mathbf{P}(k)\mathbf{F}^H(k+1,k) + \mathbf{Q_1}(k) \tag{2.10e}$$

Table 2.1 below defines the variables used in equations (2.10). To start the one-step filtering algorithm, the initial conditions must be specified. In [42], the initialization is:

$$\widehat{\mathbf{q}}(1|\mathbf{Y}_0) = E[\mathbf{q}(1)] \tag{2.11}$$

Variable	Definition
$\mathbf{I}$	Identity matrix
$\mathbf{Q_1}(k)$	Correlation matrix of process noise vector $\boldsymbol{\nu_1}(k)$
$\mathbf{Q_2}(k)$	Correlation matrix of measurement noise vector $\boldsymbol{\nu_2}(k)$
$\mathbf{Y}(k)$	The observation set, i.e., all the measurements from the first to the actual iteration: $\mathbf{Y}(k) = [\mathbf{y}(1), \mathbf{y}(2), ..., \mathbf{y}(k)]$
$\widehat{\mathbf{q}}(k+1\|\mathbf{Y}_k)$	Predicted estimate of the state vector at iteration $k+1$, given the observation vectors $\mathbf{y}(1), \mathbf{y}(2), ..., \mathbf{y}(k)$
$\widehat{\mathbf{q}}(k\|\mathbf{Y}_k)$	The estimated state vector at iteration k, given the observation vectors $\mathbf{y}(1), \mathbf{y}(2), ..., \mathbf{y}(k)$
$\mathbf{K}(k)$	Kalman gain at iteration k
$\boldsymbol{\alpha}(k)$	Innovations vector at iteration k
$\mathbf{P}(k+1,k)$	Correlation matrix of the error in $\widehat{\mathbf{q}}(k+1\|\mathbf{Y}_k)$
$\mathbf{P}(k)$	Correlation matrix of the error in $\widehat{\mathbf{q}}(k\|\mathbf{Y}_k)$

Table 2.1 – Summary of Kalman variables

$$\mathbf{P}(1,0) = E[(\mathbf{q}(1) - E[\mathbf{q}(1)])(\mathbf{q}(1) - E[\mathbf{q}(1))^H] \tag{2.12}$$

KF is a robust and efficient method to estimate the parameters of systems represented by a linear state-space model. The convergence properties of KF are presented in [88] [89]. Different forms of Robust Kalman Filters and their applications are discussed in [60].

The EKF is the variant to handle non-linear systems. A nonlinear system can be modeled by a nonlinear state model with the following recursive expressions

$$\mathbf{q}(k+1) = \mathbf{F}(k, \mathbf{q}(k)) + \boldsymbol{\nu_1}(k) \ , \tag{2.13}$$

$$\mathbf{y}(k) = \mathbf{C}(k, \mathbf{q}(k)) + \boldsymbol{\nu_2}(k) \ , \tag{2.14}$$

where $\mathbf{q}(k)$ is state vector, $\boldsymbol{\nu_1}$ and $\boldsymbol{\nu_2}$ are uncorrelated, zero-mean, white noises. The output vector $\mathbf{y}(k)$ is supposed to be known or measured. Functions $\mathbf{F}()$ or $\mathbf{C}()$ are non-linear functions that represent the dynamics of the system whose states have to be estimated.

The EKF is based on the idea of linearizing the state-space model of equations (2.13) and (2.14) at each time instant around the most recent state estimate. For convenient reference, the recursive equations of the discrete EKF are recapitulated thereafter [42]:

$$\mathbf{K}(k) = \mathbf{P}(k, k-1)\mathbf{C}^H(k)[\mathbf{C}(k)\mathbf{P}(k, k-1)\mathbf{C}^H(k) + \mathbf{Q_2}(k)]^{-1} \tag{2.15}$$

$$\boldsymbol{\alpha}(k) = \mathbf{y}(k) - \mathbf{C}(k, \widehat{\mathbf{q}}(k|\mathbf{Y}_{k-1})) \tag{2.16}$$

$$\widehat{\mathbf{q}}(k|\mathbf{Y}_k) = \widehat{\mathbf{q}}(k|\mathbf{Y}_{k-1}) + \mathbf{K}(k)\boldsymbol{\alpha}(k) \tag{2.17}$$

$$\widehat{\mathbf{q}}(k+1|\mathbf{Y}_k) = \mathbf{F}(k, \widehat{\mathbf{q}}(k|\mathbf{Y}_k)) \tag{2.18}$$

$$\mathbf{P}(k) = [\mathbf{I} - \mathbf{K}(k)\mathbf{C}(k)\mathbf{P}(k, k-1)] \tag{2.19}$$

$$\mathbf{P}(k+1, k) = \mathbf{F}(k+1, k)\mathbf{P}(k)\mathbf{F}^H(k+1, k) + \mathbf{Q_1}(k) \tag{2.20}$$

Initial conditions can be chosen as:

$$\widehat{\mathbf{q}}(1|\mathbf{Y}_0) = E[\mathbf{q}(1)] \tag{2.21}$$

$$\mathbf{P}(1,0) = E[(\mathbf{q}(1) - E[\mathbf{q}(1)])(\mathbf{q}(1) - E[\mathbf{q}(1))^H] \tag{2.22}$$

The time-varying case, where the system matrices (i.e., functions) and noise covariances are function of k is presented for the sake of generality. $\mathbf{F}(k, \mathbf{q}(k))$ in (2.13) denotes a nonlinear transition matrix function that is time-variant and that depends on the state. The non-linear system is then simplified by a linearized model at each iteration:

$$\mathbf{F}(k+1, k) = \frac{\partial \mathbf{F}(k, \mathbf{q})}{\partial \mathbf{q}} | \widehat{\mathbf{q}}(k|\mathbf{Y}_k) \tag{2.23}$$

$$\mathbf{C}(k) = \frac{\partial \mathbf{C}(k, \mathbf{q})}{\partial \mathbf{q}} | \widehat{\mathbf{q}}(k|\mathbf{Y}_{k-1}) \tag{2.24}$$

Finally, the implementation of the discrete EKF consists in updating expressions (2.15) to (2.20), (2.23) and (2.24) on each iteration, i.e., for $k = 1, 2, 3, ...$ Initial conditions have to be set, i.e., the predicted state error correlation matrix and the predicted state: $\mathbf{K}(1,0)$ and $\mathbf{q}(1|\mathbf{Y}_0)$. One should note that using KF or EKF schemes needs some assumptions: $\boldsymbol{\nu_1}(k)$ and $\boldsymbol{\nu_2}(k)$ are white

processes that are uncorrelated with $\mathbf{q}(k)$ and with each other. The EKF algorithm is iteratively updated by using local linearized functions $\mathbf{F}()$ and $\mathbf{C}()$.

In the context of fundamental frequency estimation of a power system, the instantaneous value of the frequency is obtained from the states of the model. Indeed, the angular frequency is obtained from (2.3). This means that the state vector is estimated and the angular frequency is deduced at each instant k from the imaginary part of $q_1(k)$:

$$\hat{\omega}(k) = \frac{1}{T_s} \sin^{-1}\big(\text{img}(q_1(k))\big) \quad . \tag{2.25}$$

The fundamental frequency then can thus be determined by:

$$\hat{f}_o(k) = \frac{1}{2\pi\omega} = \frac{1}{2\pi T_s} \sin^{-1}\big(\text{img}(q_1(k))\big) \quad . \tag{2.26}$$

The efficiency of this EKF method in estimating the states of a nonlinear and dynamic power system and in tracking its fundamental frequency has be evaluated [78].

2.1.3 Extended Kalman Filter for fundamental frequency estimation of single phase power systems (1P EKF)

Another method tries to estimate the fundamental frequency of a power system from only the measured voltage from one phase as follow [45]:

$$i(k) = I\sin(\omega k T_s + \phi) + \varepsilon(kT_s) \tag{2.27}$$

where $\varepsilon(kT_s)$ is zero-mean white Gaussian noise.

Signal modeling

The signal $i(k)$ in (2.27) can be decomposed as:

$$i(k) = -0.5jIe^{j(\omega k T_s+\phi)} + 0.5jIe^{-j(\omega k T_s+\phi)} + \varepsilon(kT_s) \tag{2.28}$$

Defining $q_1(k) = e^{j\omega T_s}$, $q_2(k) = Ie^{j(\omega k T_s+\phi)}$ and $q_3(k) = Ie^{-j(\omega k T_s+\phi)}$ leads to the following equation:

$$\begin{bmatrix} q_1(k+1) \\ q_2(k+1) \\ q_3(k+1) \end{bmatrix} = \begin{bmatrix} 1 & 0 & 0 \\ 0 & q_1(k) & 0 \\ 0 & 0 & \frac{1}{q_1}(k) \end{bmatrix} \begin{bmatrix} q_1(k) \\ q_2(k) \\ q_3(k) \end{bmatrix} \quad . \tag{2.29}$$

The scalar output associated to (2.29) is the measurement of $v_a(k)$:

$$y(k) = \begin{bmatrix} 0 & -0.5j & 0.5j \end{bmatrix} \begin{bmatrix} q_1(k) & q_2(k) & q_3(k) \end{bmatrix}^T . \tag{2.30}$$

It is obvious that (2.29) is a state-space model composed of the three state variables $q_1(k)$, $q_2(k)$, and $q_3(k)$.

Algorithm: EKF

Since equations (2.29) is nonlinear, the EKF in [45] is employed for the model to estimate the fundamental frequency of the power system. When $q_1(k)$, $q_2(k)$, and $q_3(k)$ are determined at each instant k, the fundamental frequency also obtained from the imaginary part of $q_1(k)$:

$$\hat{f}_o(k) = \frac{1}{2\pi T_s} \sin^{-1}\big(\text{img}(q_1(k))\big) \ . \tag{2.31}$$

2.1.4 Adaptive Notch Filter

One can consider a power current as:

$$i(k) = I\sin(\omega k T_s + \phi) + \varepsilon(k) \ , \tag{2.32}$$

where $\varepsilon(k)$ is zero-mean white noise.

Adaptive Notch filters (ANF) are frequently used to eliminate narrow-band or sinusoidal wave disturbances with unknown frequencies from observed time series [70]. In [105], ANF is used to estimate the fundamental frequency of a signal.

Signal modeling

In [105], a single ANF is represented in a form of a transfer function as follow:

$$H(z,\theta,\rho) = \frac{1 - 2\cos(\theta)z^{-1} + z^{-2}}{1 - 2\cos(\theta)\rho z^{-1} + \rho^2 z^{-2}} \ . \tag{2.33}$$

where $H(z,\theta,\rho)$ is an ANF; θ is called a 'notch', i.e., any sinusoidal component of an input signal that has frequency angular equal to θ will be eliminated when the signal passes the filter; ρ represents the bandwidth β of the filter with the following relationship:

$$\beta = \pi(1-\rho).$$

If the single sinusoidal signal $i(k)$ from (2.32) is taken as the input of $H(z,\theta,\rho)$ and if its parameter θ is adjusted to be close to the frequency angular ω of $i(k)$, then we have the

following relationship:

$$i(k)H(z,\theta,\rho) \approx \varepsilon(k) \quad . \tag{2.34}$$

Expression (2.34) means that in order to estimate the fundamental frequency of $i(k)$, we consider the signal as the input of $H(z)$ and estimate the value of parameter θ of the filter so that the output of the filter approximates a zero mean white noise.

If $i(k)$ is disturbed by harmonics and if the harmonic terms are multiple of the fundamental frequency, a single ANF $H(z,\theta,\rho)$ in (2.33) can be expanded to a cascade of single ANFs to take into account the harmonic components [105]. A cascade of single ANF can be expressed by $H(z,\theta,\rho)$:

$$H(z,\theta,\rho) = \frac{Y(z)}{X(z)} = \prod_{m=1}^{M} H_m(z) \quad , \tag{2.35}$$

where M is the number of frequency terms to be taken into consideration, $H_m(z)$ are the m-th sub-filter of $H(z)$ and has the following expression:

$$H_m(z,\theta,\rho) = \frac{1-2\cos(m\theta)z^{-1}+z^{-2}}{1-2\cos(m\theta)\rho z^{-1}+\rho^2 z^{-2}} \quad . \tag{2.36}$$

m represents the harmonic order and is considered to be known in advance.

The transfer function $H(z,\theta,\rho)$ has two parameters θ and ρ. Similar to (2.32) in the case of a single-sinusoid signal, if $\theta \approx \omega$, then

$$i(k)H(z,\theta,\rho) \approx \varepsilon(k) \quad . \tag{2.37}$$

From (2.37) and (2.34), the problem of estimating the fundamental frequency of $i(k)$ can become a problem of estimating the optimal value of θ which minimizes the output of $H(z,\theta,\rho)$ according to a certain cost function (ρ that represents the bandwidth of $H(z,\theta,\rho)$ can be assigned a fixed value).

Algorithm: Least Mean Squares (LMS)

The Least Mean Squares method (LMS) is based on steepest descent algorithm to iteratively update the estimation of the parameters of a mean squared function in order to minimize that function [41].

In (2.37), $y_m(k)$ denotes the output of the m-th sub-filter, so $y_M(k)$ is the output of $H(z,\theta,\rho)$. LMS are used in [105] to iteratively estimate θ in (2.37) that minimizes the mean squared function $E\left|y_M(k)\right|^2$. The update equations of estimating θ by LMS is shown below [105]:

$$\theta(k+1) = \theta(k) - 2\mu y_M(k)\beta_M(k) \quad , \tag{2.38}$$

with μ a simple adaptation rate, and $\beta_m(k) = \frac{\delta y_m(k)}{\delta \theta(k)}$ the gradient term of the m-th sub-filter.

At each iteration k, $y_M(k)$ and $\beta_M(k)$ in (2.38) are determined by the following recursive equations:

$$\begin{aligned} y_m(k) = {} & y_{m-1} - 2\cos(m\theta) y_{m-1}(k-1) + y_{m-1}(k-2) \\ & + 2\rho\cos(m\theta) y_m(k-1) - \rho^2 y_m(k-1) \ , \end{aligned} \tag{2.39}$$

$$\begin{aligned} \beta_m(k) = {} & \beta_{m-1}(k) - 2\cos(m\theta(k))\beta_{m-1}(k-1) \\ & + 2m\sin(m\theta(k)) y_{m-1}(k-1) + \beta_{m-1}(k-2) \\ & + 2\rho\cos(m\theta(k))\beta_m(k-1) - \rho^2\beta_m(k-2) \\ & - 2\rho m\sin(m\theta(k)) y_m(k-1) \ . \end{aligned} \tag{2.40}$$

with $m = 1, 2, ..., M$ and $y_0(k) = i(k)$ and $\beta_0(k) = 0$.

The estimated fundamental frequency is thus obtained with:

$$\hat{f}_o(k) = \frac{\theta(k)}{2\pi} \ . \tag{2.41}$$

2.1.5 Adaptive Prony's method

Signal modeling

According to [87], Prony's method is a signal processing technique which approximates a signal by a sum of exponential functions. A power signal $i(k)$ can thus be approximated as a sum of M exponential terms:

$$\hat{i}(k) = \sum_{m=1}^{M} h_m \, z_m^{k-1} \ , \tag{2.42}$$

where:

$$h_m = A_m \cdot e^{j\psi_m} \ , \tag{2.43}$$

$$z_m = e^{(\alpha_m + j\omega_m)T_s} \ , \tag{2.44}$$

and with A_m, ψ_m, ω_m and α_m respectively the amplitudes, the phases, the frequencies and the damping factors of each frequency contribution of $i(k)$. The complete signal is estimated with each of its M frequency contributions and the fundamental frequency will be deduced from the first one.

Algorithm: Least square

The values of the parameters A_m and ψ_m of h_m and α_m and ω_m of z_m with $m = 1, 2, \ldots, M$ are determined by solving two sets of equations in order to minimize the following square error:

$$\varepsilon = \sum_{k=1}^{N} \left| i(k) - \hat{i}(k) \right|^2 \quad , \tag{2.45}$$

where $\hat{i}(k)$ is the estimation of $i(k)$ using model (2.42) in which its parameters are assigned to certain values, and || is modulus of a complex number.

One can consider a polynomial $P(z)$ whose roots are z_m with $m = 1, 2, \ldots, M$:

$$P(z) = \prod_{m=1}^{M} (z - z_n) \tag{2.46}$$

The polynomial can be represented as:

$$P(z) = \sum_{m=0}^{M} a_m z^{M-m} \quad , \tag{2.47}$$

The first set of equations is to determine coefficients a_m ($m = 1, 2, \ldots, M$) of the polynomial. They are the solution of the following set of linear equations:

$$\sum_{m=0}^{M} a_m i(k-m) = 0 \quad , \tag{2.48}$$

for $k = M+1, M+2, \ldots, N$.

In (2.48), if $N = 2M$, the number of equations is equal to the number of variables. If $N > 2M$, the number of equations is more than the number of variables and the variables need to be estimated as the least square solution.

When z_m is determined, α_m and ω_m can be deduced from z_m.

After z_m is determined, h_m corresponds to the least square solution of another set of linear equations:

$$\sum_{m=1}^{M} h_m z_m^{k-1} = i(k) \quad . \tag{2.49}$$

with $k = 1, 2, \ldots, N$.

A_m and ψ_m can be deduced from h_m.

Prony's method is only applicable for approximating signals with constant parameters . For signals with time-varying parameters, an adaptive variant of Prony's method has been proposed in [21] and [87]. This APM defines a mean square relative error over the L last passed samples,

i.e., L defines a short-time window:

$$\varepsilon^2_{curr} = \frac{1}{L}\sum_{l=1}^{L} \frac{\left|i(l) - \hat{i}(l)\right|^2}{i(l)^2} \quad . \tag{2.50}$$

This error is iteratively compared to a threshold in order to detect if the parameters' values correspond to the measures. If not, a new short-time windows is considered and the signal is thus separated into contiguous short-time windows where the signal is supposed to have constant model parameters.

Applying the APM consists in the following steps:

1. Chose a starting length L_{min} for a short-time window;
2. Apply Prony's method over the samples in the short-time window in order to obtain the values of the model's parameters;
3. Calculate ε^2_{curr} from these values;
4. Compare ε^2_{curr} with a predetermined threshold ε^2_{thr} and:
   (a) if $\varepsilon^2_{curr} \leq \varepsilon^2_{thr}$, store the Prony model parameters and increase the window length (and then the subset of the data segment) with a new measure of the signal until $\varepsilon^2_{curr} > \varepsilon^2_{thr}$ and, then, go to step 2 to analyze the next contiguous short-time window.
   (b) if $\varepsilon^2_{curr} > \varepsilon^2_{thr}$, increase the short-time window length (and then the subset of the data segment) with a new value of the signal and go to step 2

The steps finish at the end of the signal. The estimated fundamental frequency is thus obtained from z_r in (2.44) where r is the index at which $\|A_r\|$ is the largest of $\|A_m\|$ with $m = 1, 2, \ldots, M$:

$$\hat{f}_o(k) = \frac{1}{2\pi}\omega_r \quad . \tag{2.51}$$

2.1.6 Performances and comparison of well-known methods

In this section, simulation results are shown to confirm the performance of the four methods APM, ANF, 1P EKF, and 3P EKF under many different conditions of the three phase power signals, these conditions are: Balanced sinusoidal signals disturbed by noise, balanced sinusoidal signals disturbed by harmonics, and unbalanced sinusoidal signals. The comparison is made through simulation results of the techniques under the same type of disturbances. The simulations were implemented in Matlab/Simulink and the parameters used in each simulation were set aiming for the best performance under each situation.

In the simulation test with sinusoidal signals disturbed by noise, the APM uses an initial short-time window of length L_{min}=20, the order is set to p=10 and the threshold to ε^2_{thr}=0.005. In the test with harmonics, the window length, the order, and the threshold employed by the APM correspondingly are L_{min}=34, p=16, $\varepsilon^2_{thr} = 0.001$. In the test with unbalanced signals, L_{min}=15, p=6, $\varepsilon^2_{thr} = 0.001$ are chosen.

The ANF uses a transfer function of order 8 for the test with harmonic disturbance and a transfer function of order 2 for the other tests. Besides, the ANF uses μ=0.0004 and ρ=0.88 for the test with noise disturbance, μ=0.0002 and ρ=0.88 for the test with harmonic disturbance, and μ=0.0007 and ρ=0.88 for the test with unbalanced signals.

With 3P EKF and 1P EKF, their initial state variables should be close enough to the true values to prevent the estimation from converging to local minima. The initial state variables $q_1(k)$ and $q_2(k)$ of 3P EKF and the initial state variables $q_1(k)$, $q_2(k)$ and $q_3(k)$ of 1P EKF are chosen so that parameters I, f, ϕ of system (2.52) are initialized at 0.8A, 45Hz, and $\pi/6$rad) respectively.

Test with balanced three phase signals

In the first test, the three phase balanced sinusoidal signals of (2.52) are taken into account.

$$\begin{cases} i_a(k) = I\sin(\omega k T_s + \phi) \\ i_b(k) = I\sin(\omega k T_s + \phi - \frac{2\pi}{3}) \\ i_c(k) = I\sin(\omega k T_s + \phi + \frac{2\pi}{3}) \end{cases} \tag{2.52}$$

with $I = 1$A, $\omega = 2\pi f_o = 100\pi$ rad/s is the signal's pulsation, $\phi = 0$rad. In this case $f_o = 50$Hz, but all the approaches are able to tackle any other values of the main frequency.

The estimated frequencies of the four methods are illustrated by Fig. 2.2, a) and the results are presented in Table 2.2. In the case of balanced sinusoidal signals with a constant fundamental frequency, the frequencies estimated by APM and ANF quickly converge to the true value with very high accuracy (the MSE in the range of 10^{-25}). On the other hand, the 3P EKF and 1P EKF provide the frequency estimation with a MSE in the range of 10^{-6}. The initial conditions impact the convergence speed and the accuracy of the estimated frequencies of the two EKF methods.

Test with balanced three phase signals disturbed by noise with the fundamental frequency of step changes

A zero-mean white Gaussian noise with a signal-to-noise (SNR) ratio of 40 dB is added to the signals in (2.52) in order to investigate the degree of noise immunity of the methods. In addition, the fundamental frequency changes from 50Hz to 50.1Hz at instant 0.2s and from 50.1Hz to 50.2Hz at instant 0.35s.

Fig. 2.2 b) shows the real fundamental frequency of the testing signals and the estimated

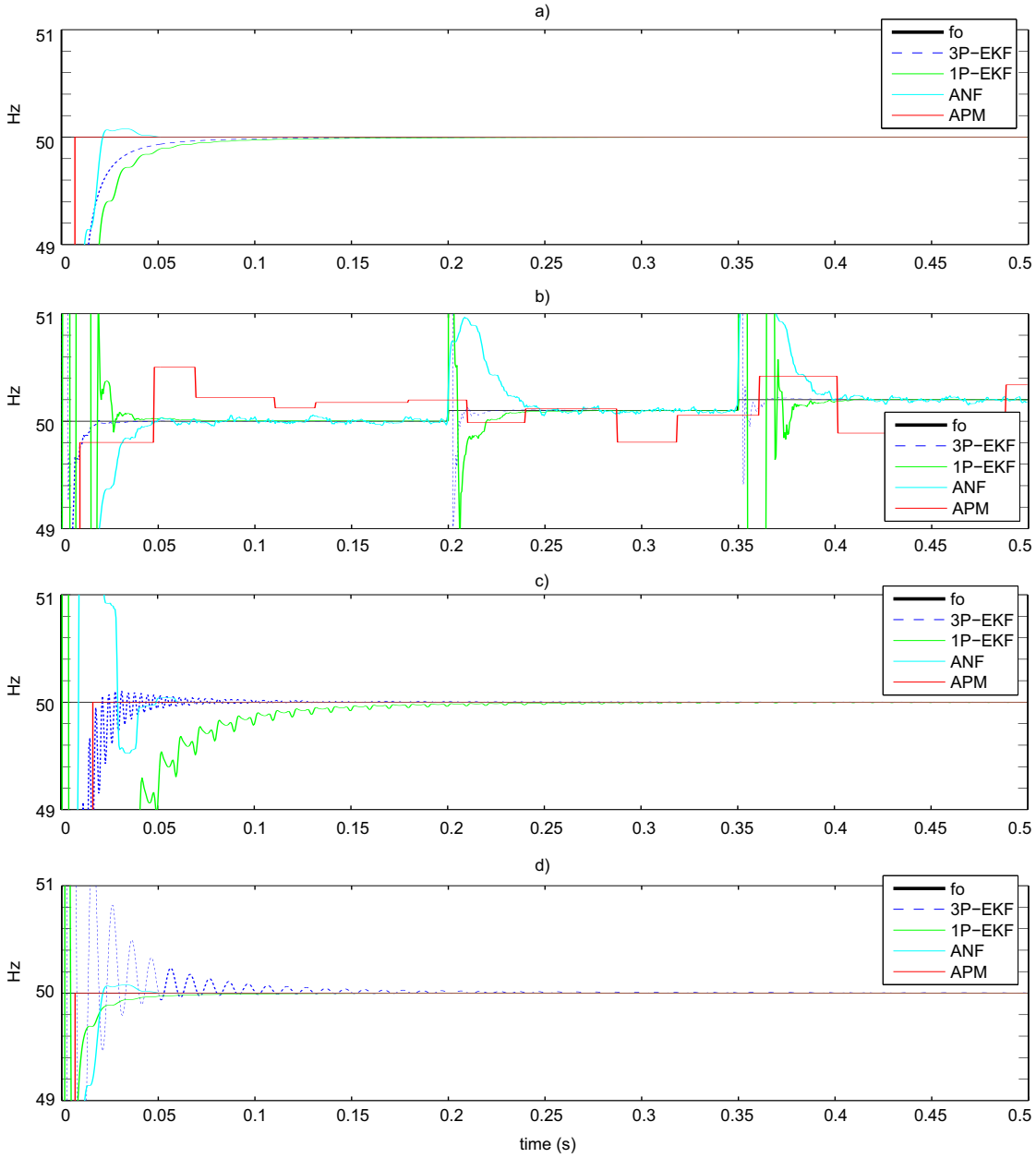

Figure 2.2 – Performance of the four considered methods in estimating the fundamental frequency of a power system under different conditions, a) signals (2.52), b) signals (2.52) with a 40 dB noise, c) signals (2.52) disturbed by harmonics, d) unbalanced three phase signals

frequencies by the four considered methods. The numerical results are presented in Table 2.3. The presence of the noise makes the estimated frequency of the APM unable to converge. Because of the noise, the MSE of the estimated frequency by the ANF increases largely, from the range of 10^{-6} to the range of 10^{-4}. The 3P EKF and the 1P EKF provide the estimated frequencies with MSEs in the range of 10^{-6} and 10^{-5} respectively. One can see that among the four methods, the two EKF methods are the most robust to noises.

Test with balanced three phase signals distorted by harmonics

This second test consists in evaluating the robustness of the four methods against harmonic distortions. For that purpose, harmonic components of orders 3^{th}, 5^{th} and 7^{th} are introduced in the power system. This results in the test signals described in (2.53):

$$\begin{cases} v_a(k) = \sin(\omega k T_s) + \frac{1}{5}\sin(3\omega k T_s) + \\ \qquad \frac{1}{5}\sin(5\omega k T_s) + \frac{1}{9}\sin(7\omega k T_s) \\ v_b(k) = \sin(\omega k T_s - \frac{2\pi}{3}) + \frac{1}{5}\sin(3\omega k T_s) + \\ \qquad \frac{1}{5}\sin(5\omega k T_s + \frac{2\pi}{3}) + \frac{1}{9}\sin(7\omega k T_s - \frac{2\pi}{3}) \\ v_c(k) = \sin(\omega k T_s + \frac{2\pi}{3}) + \frac{1}{5}\sin(3\omega k T_s) + \\ \qquad \frac{1}{5}\sin(5\omega k T_s - \frac{2\pi}{3}) + \frac{1}{9}\sin(7\omega k T_s + \frac{2\pi}{3}) \end{cases} \tag{2.53}$$

Considering the signals in (2.53), it can be noticed that the harmonic of order 3 is in the zero sequence, harmonic of order 5 is in the negative sequence, and harmonic or order 7 in the positive sequence.

The results are shown in Table 2.4 and Fig. 2.2, c). The frequencies estimated by APM and ANF converge to the the real value in a short time with high accuracy (the MSEs are in the range of 10^{-27} and 10^{-21} respectively). Compared to the first test, the performance of 1P EKF and 3P EKF shows degradation in the frequency estimation (the MSEs are in the range of 10^{-5} and 10^{-6} in order). The model errors clearly affect to the performance of EKF methods (the harmonic components are not taken into account in the state-space models used by the methods).

Test with unbalanced three phase signals

The last test verifies the performance of the four methods in estimating the fundamental frequency of a power system under unbalanced conditions, i.e., the amplitude of phase b in system (2.52) is equal to 0.3A, and the one of the other phases of the system are equal to 1A. The estimated frequencies are illustrated in Fig. 2.2, d) and Table 2.5 provides the estimation errors and convergence time. The results show that the estimated frequency by 3P EKF oscillates and its accuracy is worsened compared to the three first tests (the MSE is in the range of 10^{-5}). The performance of the other methods are not affected.

methods	time to reach the reference frequency with +/- 0.1 Hz (ms)	MSE at steady-state (Hz)	Error max. at steady-state (Hz)
APM	0.0069	$1.0683\ 10^{-25}$	$3.2685\ 10^{-13}$
ANF	0.0204	$2.6849\ 10^{-25}$	$7.2617\ 10^{-12}$
3-phase EKF	0.0420	$2.8992\ 10^{-6}$	0.0038
1-phase EKF	0.0563	$7.3860\ 10^{-6}$	0.0061

Table 2.2 – Performance of the four methods in estimating the frequency of three phase sinusoidal signals

methods	time to reach the reference frequency with +/- 0.1 Hz (ms)	MSE at steady-state (Hz)	Error max. at steady-state (Hz)
APM	Oscillates	0.0307	0.2954
ANF	0.0368	$2.9575\ 10^{-4}$	0.0522
3-phase EKF	0.0064	$4.9076\ 10^{-6}$	0.0064
1-phase EKF	0.0198	$1.4147\ 10^{-5}$	0.0099

Table 2.3 – Performance of the four methods in estimating the frequency of three phase sinusoidal signals disturbed by a noise of 40 dB

methods	time to reach the reference frequency with +/- 0.1 Hz (ms)	MSE at steady-state (Hz)	Error max. at steady-state (Hz)
APM	0.0165	$8.5323\ 10^{-27}$	$9.2371\ 10^{-14}$
ANF	0.0399	$1.1513\ 10^{-21}$	$3.3441\ 10^{-10}$
3-phase EKF	0.0401	$2.9783\ 10^{-6}$	0.0062
1-phase EKF	0.1207	$7.3469\ 10^{-5}$	0.0394

Table 2.4 – Performance of the four methods in estimating the frequency of three phase sinusoidal signals disturbed by higher-order harmonics

methods	time to reach the reference frequency with +/- 0.1 Hz (ms)	MSE at steady-state (Hz)	Error max. at steady-state (Hz)
APM	0.0070	$1.0683\ 10^{-25}$	$3.2685\ 10^{-13}$
ANF	0.0204	$2.6849\ 10^{-25}$	$7.2617\ 10^{-12}$
3-phase EKF	0.0874	$3.5027\ 10^{-5}$	0.0207
1-phase EKF	0.0282	$6.4441\ 10^{-7}$	$1.7918\ 10^{-3}$

Table 2.5 – Performance of the four methods in estimating the frequency of unbalanced three phase sinusoidal signals

2.1.7 Discussion

The methods described above are online frequency estimators. We have seen that their iterative implementation allows to estimate the frequency changes in real-time respectively

from (2.51), (2.41), (2.26) and (2.31) for the APM, ANF, 3P EKF, 1P EKF. The characteristics of the methods are compared in Table 2.6. Their underlying models, adaptive parameters, and tuning ability are recapitulated. Their complexity, advantages and drawbacks are also evaluated and listed.

methods	characteristics					
	underlying model	complexity	tuning ability	parameters	advantages	drawbacks
APM	sum of exponential functions	+++	+	h_i, z_i	adaptive, fast convergence and highly accurate without noise	frame-based sensitive to noise
ANF	band-cut filter	++	+++	θ, ρ	adaptability, sample-based, simple working rule	sensitive to noise, to local minimum, and to misadjustment, slow convergence rate
3P EKF	state-space and noise models	+++	++	$\hat{F}(k)$, $\hat{H}(k)$, $\mathbf{P}(k)$	adaptability, sample-based, fast convergence, robust to noise, but sensitive to model error	steady-state error
1P EKF	state-space and noise model	++++		$\hat{F}(k)$, $\hat{H}(k)$, $\mathbf{P}(k)$	adaptability, sample-based, fast convergence, robust to noise, but sensitive to model error	steady-state error

Table 2.6 – The characteristics of the four methods APM, ANF, 3P EKF and 1P EKF

These frequency estimators are adaptive but in different ways. The APM works with specific coefficients a_n that defines constant polynomials $P(z)$ over adjustable time-windows of the signal. The ANF is like a band-cut filter where the parameters θ and ρ are adjusted. The EKF is adaptive because it relies on a local linearized state-space model and uses an automatic online reinitialization of the covariance matrix.

Moreover, it is necessary to know which harmonic term is present or not in the signal for all

of these methods. In other works, each method includes in his model the harmonic terms and estimates or rejects them separately. Obviously, the 1P EKF method does not take into account the harmonic terms supposed to be in the signal.

The simulation results indicate that [78]:

- The APM is appropriate to model signals with harmonics and inter-harmonics. However, the estimation of the fundamental frequency is very sensitive to the existence of noise in the signals.

- The ANF is able to track the fundamental frequency, even in harmonic environment. However, with disturbing noise, the performance of the method is considerably degraded. In addition, the estimated frequency easily falls into local minima due to the non-quadratic error surface. Since the fundamental frequency of power systems oscillates around a nominal value with small amplitude in power systems, the initial value of the estimated frequency can be easily chosen.

- The 3P EKF uses a state-space model in the $\alpha - \beta$ frame and thus requires three-phase measurements. The initialization of the state variables has a great impact to the performance of the method and the variables should be assigned by appropriate initial values in order to prevent divergence.

- The 1P EKF is also based on a state-space model that directly represents an one-phase power signal. Initialization of the state variables of the model is more difficult than in the 3P EKF, since the model is more complex with one more state variables compared to the model of the 3P EKF.

- The 1P EKF and the 3P EKF are robust to noise, but the estimated frequency given by the two methods are degraded due to model errors. In the 1P EKF, model errors occur in the simulation test with the appearance of harmonics, because the state-space model (2.29) of the method does not take into account harmonics components. Model (2.4) of the 3P EKF also does not consider the harmonics, so the performance of the method is also affected by harmonics, but the estimated frequency by this method is better compared to that of the 1P EKF because of the $\alpha - \beta$ transform (presented in Appendix A.2) that is used to remove the zero sequence harmonics from the input signals.

For power system applications, the selected methods have simple digital implementation and, therefore, low computational burden.

2.2 Adaptive signal processing methods to identify symmetrical components of a power system

Because of the important role of symmetrical component theory in analyzing power systems, numerous methods have been proposed to identify symmetrical components. The Kalman filter used in [102] is a dynamic method, however, in order to estimate symmetrical components, the method requires the fundamental frequency of a power system to be specified in advance. The gradient descend method in [54] and the method based on artificial neural networks in [32] allow to estimate symmetrical components and the fundamental frequency recursively at the same time. The method in [32] is time-delaying, and the one in [54] is complex. Other neural methods have been developed like in [8] or in [73]. PLL-based methods can also be used. For example in [109], vectorial properties of the three-phase input signal in the $\alpha\beta$-reference frame are taken into account but the method necessitate to converge after each nonlinear load changes.

Among all the available methods for symmetrical components estimation, the method in [64] introduces an adaptive linear combiner structure (Adaline) and is applicable to deal with multi-output systems. The method is called MO-Adaline and is investigated due to its simplicity.

2.2.1 Signal modeling

One can consider that $i_a(k), i_b(k), i_c(k)$ are the three phase signals of a power system. According to the symmetrical component theory presented in Chapter 1, the signals can be represented by a sum of symmetrical components as follow:

$$\begin{cases} i_a(k) = I_+ \sin(\omega k T_s + \phi_+ + I_- \sin(\omega k T_s + \phi_- + I_o \sin(\omega k T_s + \phi_o \\ i_b(k) = I_+ \sin(\omega k T_s + \phi_+ - \frac{2\pi}{3}) + I_- \sin(\omega k T_s + \phi_- + \frac{2\pi}{3}) + I_o \sin(\omega k T_s + \phi_o \\ i_c(k) = I_+ \sin(\omega k T_s + \phi_+ - \frac{2\pi}{3}) + I_- \sin(\omega k T_s + \phi_- - \frac{2\pi}{3}) + I_o \sin(\omega k T_s + \phi_o \end{cases} \tag{2.54}$$

The zero component is calculated by:

$$i_o(k) = \frac{i_a(k) + i_b(k) + i_c(k)}{3} \tag{2.55}$$

Subtracting the zero component from the three phase signals in (2.54) yields to:

$$\begin{cases} i_a(k) - i_o(k) = I_+ \sin(\omega k T_s + \phi_+) + I_- \sin(\omega k T_s + \phi_-) \\ i_b(k) - i_o(k) = I_+ \sin(\omega k T_s + \phi_+ - \frac{2\pi}{3}) + I_- \sin(\omega k T_s + \phi_- + \frac{2\pi}{3}) \\ i_c(k) - i_o(k) = I_+ \sin(\omega k T_s + \phi_+ - \frac{2\pi}{3}) + I_- \sin(\omega k T_s + \phi_- - \frac{2\pi}{3}) \end{cases} \tag{2.56}$$

Using the relation $\sin a + b = \sin a \cos b + \sin b \cos a$ for (2.56) yields to:

$$\begin{cases} i_a(k) - i_o(k) = \sin(\omega k T_s) I_+ \cos\phi_+ + \cos(\omega k T_s) I_+ \sin\phi_+ \\ \qquad + \sin(\omega k T_s) I_- \cos\phi_- + \cos(\omega k T_s) I_- \sin\phi_- \\ i_b(k) - i_o(k) = \sin(\omega k T_s - \frac{2\pi}{3}) I_+ \cos\phi_+ + \cos(\omega k T_s - \frac{2\pi}{3}) I_+ \sin\phi_+ \\ \qquad + \sin(\omega k T_s + \frac{2\pi}{3}) I_- \cos\phi_- + \cos(\omega k T_s + \frac{2\pi}{3}) I_- \sin\phi_- \\ i_c(k) - i_o(k) = \sin(\omega k T_s + \frac{2\pi}{3}) I_+ \cos\phi_+ + \cos(\omega k T_s + \frac{2\pi}{3}) I_+ \sin\phi_+ \\ \qquad + \sin(\omega k T_s - \frac{2\pi}{3}) I_- \cos\phi_- + \cos(\omega k T_s - \frac{2\pi}{3}) I_- \sin\phi_- \end{cases} \tag{2.57}$$

If we define:

$$\mathbf{X}(k) = \begin{bmatrix} \sin\omega k T_s & \cos\omega k T_s & \sin\omega k T_s & \cos\omega k T_s \\ \sin\omega k T_s - \frac{2\pi}{3} & \cos\omega k T_s - \frac{2\pi}{3} & \sin\omega k T_s + \frac{2\pi}{3} & \cos\omega k T_s + \frac{2\pi}{3} \\ \sin\omega k T_s + \frac{2\pi}{3} & \cos\omega k T_s + \frac{2\pi}{3} & \sin\omega k T_s - \frac{2\pi}{3} & \cos\omega k T_s - \frac{2\pi}{3} \end{bmatrix} \tag{2.58}$$

$$\mathbf{d}(k) = \begin{bmatrix} i_a(k) - i_o(k) \\ i_b(k) - i_o(k) \\ i_c(k) - i_o(k) \end{bmatrix} \tag{2.59}$$

$$\mathbf{W}(k) = \begin{bmatrix} I_+ \cos\phi_+ \\ I_+ \sin\phi_+ \\ I_- \cos\phi_- \\ I_- \sin\phi_- \end{bmatrix} \tag{2.60}$$

then, the expressions in (2.57) can be summarized under the form of a linear combiner structure:

$$\mathbf{d}(k) = \mathbf{X}^T(k)\mathbf{W}(k) \tag{2.61}$$

where $\mathbf{X}(k)$ is the input matrix, $\mathbf{d}(k)$ is the output vector, and $\mathbf{W}(k)$ is the parameter vector that needs to be estimated.

2.2.2 Multi-output Adaline (MO-Adaline) for tracking symmetrical components

The output vector $\mathbf{d}(k)$ of the linear combiner structure (2.61) can be calculated from the measurements of $i_a(k), i_b(k), i_c(k)$ as the expression (2.59).

$\mathbf{W}(k)$ represents the weight vector of the structure (2.61) that can be iteratively updated by a MO-Adaline [64] according to:

$$\mathbf{W}(k+1) = \mathbf{W}(k) + \alpha\mathbf{X}(k)[\mathbf{X}(k)^T\mathbf{X}(k)]^{-1}\mathbf{e}(k) \tag{2.62}$$

where $\mathbf{e}(k) = \mathbf{d}(k) - \mathbf{X}^T(k)\mathbf{W}(k)$ represent an error.

After the weight vector $\mathbf{W}(k)$ is estimated, parameters I_+, ϕ_+, I_-, ϕ_- can be determined and the positive and negative components can be also reconstructed.

2.2.3 Discussion

The method uses a linear combination with an input matrix of size 3×4, an output vector with 3 rows and a weight vector with 4 rows. The MO-Adaline algorithm is then applied to estimate the weight vector $\mathbf{W}(k)$ at each iteration k, however, the fundamental frequency must be provided. Besides its simplicity, the algorithm is sensitive to noise and results in mis-adjustment of the estimation.

2.3 Conclusion

The principle of four methods of fundamental frequency estimation (an adaptive method based on Prony's theory, an adaptive notch Filter, an EKF dedicated for balanced three phase power systems, and an EKF dedicated for single phase power systems) is presented specifically for estimating the frequency in grid-interconnection systems. Drawbacks and advantages are also discussed. To evaluate and confirm the performance of the methods, extensive simulation and experimental verifications were performed. The adaptive methods are also compared to the zero-crossing technique. Numerical simulations with unknown frequency variations, when harmonic terms are present and under noise condition, but also representative experiments have highlighted the performance of the methods in real-time applications.

An adaptive method based on the principle of a MO-Adaline is also presented to identify the symmetrical components of a three phase power system. Obviously, its advantages and disadvantages are discussed.

In general, each of those methods assumes a different signal model. Prony's method tries to model a single phase voltage/current as a sum of exponential functions. ANF also models a single phase signal, however, by employing a cascade of second order notch filters. The state-space model in EKF takes three phase signals into account. However, all these models only deal with either a single phase of a power system or a balanced three phase power system. Although MO-Adaline method exploits a linear combiner structure to take into account the three phase signals of a unbalanced three phase power system, the model is not sufficient to fully represent the signals since it still requires the fundamental frequency value. Besides, the algorithm used in the method is sensitive to noise.

The next chapter proposes several new state-space models which are able to model the three phase signals of a power system and thus even under unbalanced conditions. Furthermore, a system identification algorithm is proposed for estimating the states in real-time. Therefore,

the proposed model is capable of estimating the fundamental frequency and of identifying the symmetrical components of any power system, i.e., by recovering their amplitudes and phase angles.

3 New state-space representations for modeling unbalanced three phase systems

3.1 Introduction

The fact is that in real world applications, because of load variations, a three phase power system is generally always unbalanced. A balanced state is only for a limited period of time and will permanently evolve. Most of the developed models only represent power systems with only one phase and/or with three phases but balanced. As examples, four methods have been presented in Chapter 2. Those models are not capable of representing the properties of a three phase system in practical situations, thus new models are expected. Among different types of models (AR, ARMA, state-space, etc.), the state-space model is a simple and basic way of modeling a system and/or signals issued from a process. Recently, state-spaces have been developed for the modeling and forecasting of high frequency data from power systems [27], this was for short-term load forecasting issues, i.e., hourly electricity loads of the French electricity demand.

In this chapter, two new state-space models are developed to model unbalanced three phase power systems. They have been inspired by the two state-space models presented in Chapter 2. Indeed, the model given by (2.4) is for a balanced three phase power system, and the one given by (2.29) is appropriate for single phase power systems. The two new state-space models are developed to represent unbalanced three phase power systems under different assumptions (one is linear, the other one is nonlinear):

- The first state-space model we propose is able to represent any three phase power systems which can be either balanced or unbalanced. It supposes that the fundamental frequency is known in advance. According to that, the frequency is a parameter of the model and should be provided by another process.

- The second state-space model that is developed thereafter is also suitable to represent any three phase power systems either balanced or unbalanced. Furthermore, this state-space does not require the fundamental frequency to be known in advance. It is capable to instantaneously estimate the time-varying value of the fundamental frequency of the

power system. In fact, one state variable of the model is representative of the fundamental frequency because it is a function of it. The model and its performance have been published the research in [80, 81, 82].

The two new state-space models will provide to power system designers and engineers two possibilities: With the first state-space model, the fundamental frequency is supposed to be available or estimated by another method and then it is a known parameter to estimate other parameters and/or quantities of a power system, with the second state-space model it is possible to implement the estimation of the fundamental frequency at the same time with the estimation of the other quantities of the power system.

In the thereafter section, the two state-space models we propose are completely detailed. The next section presents algorithms for the online parameter estimation of a three phase power systems. Then, a discussion is proposed in a section and the solution to find initial values of the proposed nonlinear method is introduced in another section. Applications of the proposed state-space models are presented in a section for estimating power system's parameters, i.e., for fundamental frequency estimation and for symmetrical component identification in real-time. Finally, various applications of these new state-space models are briefly referred to in a section and some concluding remarks are given in the last section.

3.2 New state-space models of unbalanced three phase signals

3.2.1 A new state-space model of unbalanced three phase signals of which the fundamental frequency is an unknown parameter

One can consider unbalanced three phase power currents as:

$$\begin{cases} i_a(k) = I_a \sin(\omega k T_s + \phi_a) \\ i_b(k) = I_b \sin(\omega k T_s + \phi_b) \\ i_c(k) = I_c \sin(\omega k T_s + \phi_c) \end{cases} \tag{3.1}$$

According to the theory of symmetrical components, the set of three phase signals can be represented as a sum of three sets:

$$\begin{bmatrix} i_a(k) \\ i_b(k) \\ i_c(k) \end{bmatrix} = \begin{bmatrix} i_a^+(k) \\ i_b^+(k) \\ i_c^+(k) \end{bmatrix} + \begin{bmatrix} i_a^-(k) \\ i_b^-(k) \\ i_c^-(k) \end{bmatrix} + \begin{bmatrix} i_a^o(k) \\ i_b^o(k) \\ i_c^o(k) \end{bmatrix}. \tag{3.2}$$

In (3.2), the set

$$\begin{bmatrix} i_a^+(k) \\ i_b^+(k) \\ i_c^+(k) \end{bmatrix} = \begin{bmatrix} I_+ \sin(\omega k T_s + \phi_+) \\ I_+ \sin(\omega k T_s + \phi_+ - \frac{2\pi}{3}) \\ I_+ \sin(\omega k T_s + \phi_+ + \frac{2\pi}{3}) \end{bmatrix} \tag{3.3}$$

is the positive sequence.

Additionally, the set

$$\begin{bmatrix} i_a^-(k) \\ i_b^-(k) \\ i_c^-(k) \end{bmatrix} = \begin{bmatrix} I_- \sin(\omega k T_s + \phi_-) \\ I_- \sin(\omega k T_s + \phi_- + \frac{2\pi}{3}) \\ I_- \sin(\omega k T_s + \phi_- - \frac{2\pi}{3}) \end{bmatrix} \tag{3.4}$$

is the negative sequence.

Finally the set

$$\begin{bmatrix} i_a^o(k) \\ i_b^o(k) \\ i_c^o(k) \end{bmatrix} = \begin{bmatrix} I_o \sin(\omega k T_s + \phi_o) \\ I_o \sin(\omega k T_s + \phi_o) \\ I_o \sin(\omega k T_s + \phi_o) \end{bmatrix} \tag{3.5}$$

is the zero sequence.

The $\alpha-\beta$ components and then the complex form of the three phase signals in (3.1) are calculated from the $\alpha\beta$ transform of the corresponding symmetrical components. The $\alpha\beta$ components for the positive components are:

$$\begin{bmatrix} i_\alpha^+(k) \\ i_\beta^+(k) \end{bmatrix} = \mathbf{M}^T \begin{bmatrix} I_+ \sin(\omega k T_s + \phi_+) \\ I_+ \sin(\omega k T_s + \phi_+ - \frac{2\pi}{3}) \\ I_+ \sin(\omega k T_s + \phi_+ + \frac{2\pi}{3}) \end{bmatrix} . \tag{3.6}$$

with

$$\mathbf{M} = \sqrt{\frac{2}{3}} \begin{bmatrix} 1 & 0 \\ -\frac{1}{2} & \frac{\sqrt{3}}{2} \\ -\frac{1}{2} & -\frac{\sqrt{3}}{2} \end{bmatrix} . \tag{3.7}$$

The corresponding complex form of the positive component is determined from (3.6) as:

$$i^+(k) = i_\alpha^+(k) + j i_\beta^+(k) = A_+ e^{j\omega k T_s}. \tag{3.8}$$

Similarly, the $\alpha\beta$ components of the negative components are:

$$\begin{bmatrix} i_\alpha^-(k) \\ i_\beta^-(k) \end{bmatrix} = \mathbf{M}^T \begin{bmatrix} I_- \sin(\omega k T_s + \phi_-) \\ I_- \sin(\omega k T_s + \phi_- + \frac{2\pi}{3}) \\ I_- \sin(\omega k T_s + \phi_- - \frac{2\pi}{3}) \end{bmatrix} . \tag{3.9}$$

The complex form of the negative component is calculated from (3.9) as:

$$i^-(k) = i_\alpha^-(k) + j i_\beta^-(k) = A_- e^{-j\omega k T_s}. \tag{3.10}$$

The zero component via the $\alpha\beta$ transform is eliminated. By applying the $\alpha\beta$ transform on the three phase signals $i_a(k), i_b(k), i_c(k)$ in (3.1), the resulting complex form of the three phase signals is the sum of the complex currents corresponding to the positive, negative and zero components and is:

$$i(k) = A_+ e^{j\omega k T_s} + A_- e^{-j\omega k T_s}. \tag{3.11}$$

(3.11) can be expressed as:

$$i(k) = e^{j\omega T_s} A_+ e^{j\omega(k-1)T_s} + e^{-j\omega T_s} A_- e^{-j\omega(k-1)T_s}. \tag{3.12}$$

By defining $q_1(k) = e^{j\omega T_s} = \cos(\omega k T_s) + j \sin(\omega k T_s)$ and $q_2(k) = A_+ e^{j\omega k T_s}$ and $q_3(k) = A_- e^{-j\omega k T_s}$, and by assuming the fundamental frequency of system (3.1) is constant in one sampling period, the following equations can be deduced from (3.12):

$$\begin{bmatrix} q_1(k+1) \\ q_2(k+1) \\ q_3(k+1) \end{bmatrix} = \begin{bmatrix} q_1(k) \\ q_1(k) q_2(k) \\ \frac{q_3(k)}{q_1(k)} \end{bmatrix} , \tag{3.13}$$

with a scalar output

$$y(k) = \begin{bmatrix} 0 & 1 & 1 \end{bmatrix} \begin{bmatrix} q_1(k) & q_2(k) & q_3(k) \end{bmatrix}^T. \tag{3.14}$$

Process noises can be added to state-space model (3.13) to account for the variance of the parameters of the state variables, so the model becomes:

$$\begin{bmatrix} q_1(k+1) \\ q_2(k+1) \\ q_3(k+1) \end{bmatrix} = \begin{bmatrix} q_1(k) + \nu_1 \\ q_1(k) q_2(k) + \nu_2 \\ \frac{q_3(k)}{q_1(k)} + \nu_3 \end{bmatrix} , \tag{3.15}$$

with ν_1, ν_2, ν_3 process noises. It can be observed that state-space model (3.13) (3.14) or (3.15) (3.14)

is only one expression of the general state-space model in (2.13) (2.14) with:

$$\mathbf{F}(k,\mathbf{q}(k)) = \begin{bmatrix} q_1(k) \\ q_1(k)q_2(k) \\ \frac{q_3(k)}{q_1(k)} \end{bmatrix}, \tag{3.16}$$

and

$$\mathbf{C}(k,\mathbf{q}(k)) = [q_2(k) + q_3(k)], \tag{3.17}$$

The state equation (3.13) is nonlinear and contains three state variables $q_1(k)$, $q_2(k)$ and $q_3(k)$, here, $q_2(k)$ and $q_3(k)$ respectively represent the positive and negative components of the three phase system given by (3.1). Additionally, $q_1(k)$ represents the variation of the phase angle of $q_2(k)$ and $q_3(k)$ between two consecutive iterations.

3.2.2 A new state-space model of unbalanced three phase signals of which the fundamental frequency is a known variable

The state equation (3.13) considers the fundamental frequency of a power system as an unknown variable. However, in many applications, at each sampling time, the fundamental frequency is known or already estimated using some methods of frequency estimation. If the fundamental frequency is available at each sampling time, so that $e^{j\omega T_s}$ in (3.12) can be considered as an available parameter at each sampling time. Therefore, denote $a(k) = q_1(k) = e^{j\omega T_s}$ to represent the parameter at sampling time k, then:

$$i(k) = a(k)A_+ e^{j\omega(k-1)T_s} + \frac{1}{a(k)} A_- e^{-j\omega(k-1)T_s}. \tag{3.18}$$

By defining $q_1(k) = A_+ e^{j\omega k T_s}$ and $q_2(k) = A_- e^{-j\omega k T_s}$, a new state-space model of the complex signal of the three phase signal in (3.1) can be deduced:

$$\begin{bmatrix} q_1(k+1) \\ q_2(k+1) \end{bmatrix} = \begin{bmatrix} a(k) & 0 \\ 0 & \frac{1}{a(k)} \end{bmatrix} \begin{bmatrix} q_1(k) \\ q_2(k) \end{bmatrix}, \tag{3.19}$$

with a scalar output

$$y(k) = \begin{bmatrix} 1 & 1 \end{bmatrix} \begin{bmatrix} q_1(k) & q_2(k) \end{bmatrix}^T. \tag{3.20}$$

Model (3.19) is linear and composed of two state variables: $q_1(k)$ and $q_2(k)$ respectively represent the positive and negative components of the three phase system given by (3.1), and one parameter $a(k)$ represents the fundamental frequency. After a state-space model of the three-phase power signals of a power system has been designed, an identification algorithms is required to estimate the states of the power system.

3.3 Algorithms for online estimation of a three phase power system's parameters and states

It is easily recognized that model (3.13) is a nonlinear state-space model, and (3.19) is a linear one. Chapter 2 describes KF and EKF as effective solutions to the problem of estimating the parameters of a system based on a state-space model in case of no model error. According to that, KF and EKF are adaptive and robust to noise. The distinction of the two filters is that: KF is exclusive for linear state-space models, and EKF is an expansion of KF for applications on nonlinear state-space models.

From that facts, two proposals are elaborated:

- The first proposal is called the 'linear method': It consists in applying KF to linear model (3.19) to recursively estimate the states of a power system, the fundamental frequency is known or provided by a previous process.
- The second proposal is the 'nonlinear method': It consists in applying EKF to model (3.13) to recursively estimate the states and parameters of a power system including the fundamental frequency.

3.4 Discussion about the two proposed methods

3.4.1 Discussion of the proposed linear method

The proposed linear method requires the fundamental frequency provided by a previous process. Its model (3.19) is linear and composed of two state variables: $q_1(k)$ and $q_2(k)$ respectively represent the positive and negative components of the three phase system given by (3.1). Additionally, parameter $a(k)$ represents the fundamental frequency. The method employs KF to estimate the states and parameters of a power system, the filter is adaptive and robust to noise.

Considering the fundamental frequency as an available parameter at each iteration, it allows to utilize the available powerful methods to estimate the fundamental frequency, e.g., the PLL presented in Chapter 2.1.1.

In addition, one big advantage of model (3.19) compared to model (2.61) of MO-Adaline in Chapter 2, is that: The fundamental frequency must be constant for the MO-Adaline. If its value changes in time, the estimation given by the MO-Adaline method will not be accurate due to the error integration. In the proposed linear model, the fundamental frequency represented by parameter $a(k)$ is updated at each iteration, which satisfies the characteristic of practical power systems: The fundamental frequency is not constant but changes in time. Therefore, the proposed method is able to estimate the symmetrical components even if the fundamental frequency varies in time. The simulation tests in Chapter 4 will verify this judgment.

3.4.2 Discussion of the proposed nonlinear method

In the proposed nonlinear method with three state variables, the state equation of (3.13) is nonlinear and contains three state variables. Compared to the model (3.13), (2.4) has only two and (2.29) has three state variables. It is also important to notice that, the state variables of model (2.29) have no physical meaning while model (2.4) only represents the positive components of three phase power signals. Furthermore, the states of (3.13), $q_2(k)$ and $q_3(k)$ respectively represent the positive and negative components of the three phase system given by (3.1). Additionally, $q_1(k)$ represents the variation of the phase angle of $q_2(k)$ and $q_3(k)$ between two consecutive iterations which directly relates to the fundamental frequency. This explains why the proposed nonlinear method can identify not only balanced but also unbalanced three phase systems.

Both the proposed method and the 3P EKF (the EKF for balanced three phase signals) apply Clark's transform to transform the three phase signals measured from grids into the complex representation. Via the $\alpha - \beta$ transform, zero sequence harmonics (harmonic of orders 3, 6, 9, 12,..., as mentioned in Chapter 1) are eliminated. Therefore, the results of the two methods are not affected by zero sequence harmonics. On the other hand, the 1P EKF uses directly the signal measured from the grid as the output of its state-space model, so it is sensitive to the harmonic components.

As 3P EKF and 1P EKF, the proposed nonlinear method relies on a nonlinear state-space model so that the initial values of the state variables of the model must be selected carefully in order for their estimation to be able to converge to the right values without suffering bias and falling into local minima, e.g., the initial values should be close enough to the global minimum point. The selection of the initial conditions is a hard issue and often requires prior knowledge of the process.

Table 3.1 compares the proposed nonlinear method with the two EKF methods presented in Chapter 2 in terms of number of state variables, application ability, computation, and initialization.

	3P EKF	1P EKF	proposed nonlinear method
number of states	2	3	3
suitable for	balanced three phase systems	one phase systems	balanced and unbalanced three phase systems
computation complexity	++	+++	+++
initial condition choice	++	+++	+++

Table 3.1 – Comparison of the proposed method and the EKFs in Chapter 2

3.5 A solution to the initialization problem of the proposed nonlinear method

As mentioned in the discussion above and in Chapter 2, in order to be able to be applied in practice, the methods based on EKF, i.e, the 1P EKF, 3P EKF and the proposed nonlinear method have to deal with the difficulty of choosing initial values of the state variables. Thereafter, we propose a solution to solve the initialization problem of the proposed nonlinear method. The 1P EKF and 3P EKF can use the same strategy to get good initialization conditions.

According to Chapter 1, the real frequency should deviate around its nominal value (50Hz, for example). There are two state-space models proposed in this chapter, in which the proposed nonlinear method accompanies with the nonlinear model (3.13). If the fundamental frequency from which the state variable $q_1(k)$ of (3.13) is calculated directly is assigned to the nominal value, the estimation of the state variables $q_2(k)$ and $q_3(k)$ becomes a linear estimation using the proposed linear method, from that the two state variables can be estimated to a certain accuracy depending on the variation of the fundamental frequency from its nominal value. In addition, recalling that $q_1(k) = e^{j\omega T_s}$, the relatively small sampling time T_s makes the error of the nominal value and the real frequency negligible. Using the observations, an initialization stage can be added to the proposed nonlinear method. The method now contains two stages: Initialization and tracking.

Initialization stage consists in:

1. Fixing the fundamental frequency at its nominal value
2. Applying the proposed linear method in case of the fundamental frequency is known to estimate the state variables $q_2(k)$ and $q_3(k)$ of the model (3.13) in N_o iterations corresponding to N_o samples $y(k)$.

Here N_o is called the 'number of iterations in the initialization stage'. Two iterations that is equivalent to $N_o = 3$ are enough to calculate the initial values of state variables $q_2(k)$ and $q_3(k)$. N_o is chosen more than 3 to mitigate the bad effect of noise and outlier samples.

The tracking stage consists in:

1. Assigning the estimated state variables in the initialization stage as initial values for the state variables $q_1(k)$, $q_2(k)$ and $q_3(k)$ in this stage
2. Applying the proposed nonlinear method to estimate the state variables
3. At each iteration k, calculating the mean square relative error $\epsilon(k)$, if the error is over a threshold $\epsilon_{thr}(k)$, it means there is a big change in the signals and the estimation is out of track. The initialization stage needs to be restarted.

The mean square error $\epsilon(k)$ is determined from a number L of the last samples in the tracking stage:

$$\epsilon(k) = \frac{1}{L-1}\sum_{l=0}^{L}\left|y(l) - \hat{y}(k-l)\right|^2 \quad . \tag{3.21}$$

where $\hat{y}(k)$ is the reconstruction of the samples $y(k)$ from the estimated state variables. The value of $\epsilon_{thr}(k)$ and L can be chosen so that the effects of noises and/or outliers will be reduced.

3.6 Applications of the proposed methods for estimating power system's parameters in real-time

Based on proposed approaches, different parameters and states of power systems can be estimated.

3.6.1 Fundamental frequency estimation

The proposed nonlinear method allows to estimate the fundamental frequency of a power system iteratively. At each instant k the fundamental frequency can be estimated from the imaginary part of state $q_1(k)$ according to:

$$\hat{f}_o(k) = \frac{1}{2\pi T_s}\arcsin\big(\text{img}(q_1(k))\big) \quad . \tag{3.22}$$

The fundamental frequency can also be calculated from state variable q_2 as follow:

$$\hat{f}_o(k) = \frac{1}{2\pi T_s}(\angle q_2(k) - \angle q_2(k-1)). \tag{3.23}$$

3.6.2 Symmetrical component identification

Both the proposed methods are capable of estimating symmetrical components of a power system. The only difference is that for the proposed linear method, the positive and negative components are represented by $q_1(k)$ and $q_2(k)$ respectively, while in method with three variables, they are $q_2(k)$ and $q_3(k)$. If φ_+ is the phase of the positive components, if φ_- is the phase of the negative components, the following details how to determine the symmetrical components and their amplitudes, phase angles and phases by the proposed linear method.

The zero component is directly calculated from the three phase signals $i_a(k), i_b(k), i_c(k)$ measured on the grid at each iteration by:

$$i_a^o(k) = i_b^o(k) = i_c^o(k) = \frac{i_a(k) + i_b(k) + i_c(k)}{3} \tag{3.24}$$

The amplitude I_+, the phase angle ϕ_+, and the phase φ_+ of the positive component can be estimated at each iteration by:

$$\begin{cases} I_+(k) = \sqrt{\frac{2}{3}} \bmod (q_2(k)) \\ \phi_+(k) = \pi/2 + \angle q_2(k) - k\angle q_1(k) \\ \varphi_+(k) = \pi/2 + \angle q_2(k) \end{cases} \tag{3.25}$$

where $\bmod(z)$ is the module of z and $\angle z$ is the phase angle of z. Here $\angle q_2(k) = \omega k T_s + \phi_+(k) - \pi/2$ and $\angle q_1(k) = \omega T_s$. If $\left[i_a^+(k) \;\; i_b^+(k) \;\; i_c^+(k)\right]$ are the three phases of the positive component, then they can be reconstructed by applying the inverse $\alpha\beta$ transform:

$$\begin{bmatrix} i_a^+(k) \\ i_b^+(k) \\ i_c^+(k) \end{bmatrix} = \sqrt{\frac{2}{3}} \begin{bmatrix} 1 & 0 \\ -\frac{1}{2} & \frac{\sqrt{3}}{2} \\ -\frac{1}{2} & -\frac{\sqrt{3}}{2} \end{bmatrix} \begin{bmatrix} i_\alpha^+(k) \\ i_\beta^+(k) \end{bmatrix}, \tag{3.26}$$

$$\begin{bmatrix} i_a^+(k) \\ i_b^+(k) \\ i_c^+(k) \end{bmatrix} = \sqrt{\frac{2}{3}} \begin{bmatrix} 1 & 0 \\ -\frac{1}{2} & \frac{\sqrt{3}}{2} \\ -\frac{1}{2} & -\frac{\sqrt{3}}{2} \end{bmatrix} \begin{bmatrix} real(q_2(k)) \\ img(q_2(k)) \end{bmatrix}. \tag{3.27}$$

In the same way as for the positive component, the amplitude I_-, the phase angle ϕ_-, and the phase φ_- of the negative component are determined from state $q_3(k)$ according to

$$\begin{cases} I_-(k) = \sqrt{\frac{2}{3}} \bmod (q_3(k)) \\ \phi_-(k) = \pi/2 - \angle q_3(k) - k\angle q_1(k) \\ \varphi_-(k) = \pi/2 - \angle q_3(k) \end{cases} \tag{3.28}$$

where $\angle q_3(k) = \pi/2 - \omega k T_s - \phi_-(k)$.

The corresponding three phases $\left[i_a^-(k) \;\; i_b^-(k) \;\; i_c^-(k)\right]$ can be reconstructed by:

$$\begin{bmatrix} i_a^-(k) \\ i_b^-(k) \\ i_c^-(k) \end{bmatrix} = \sqrt{\frac{2}{3}} \begin{bmatrix} 1 & 0 \\ -\frac{1}{2} & \frac{\sqrt{3}}{2} \\ -\frac{1}{2} & -\frac{\sqrt{3}}{2} \end{bmatrix} \begin{bmatrix} i_\alpha^-(k) \\ i_\beta^-(k) \end{bmatrix}, \tag{3.29}$$

$$\begin{bmatrix} i_a^-(k) \\ i_b^-(k) \\ i_c^-(k) \end{bmatrix} = \sqrt{\frac{2}{3}} \begin{bmatrix} 1 & 0 \\ -\frac{1}{2} & \frac{\sqrt{3}}{2} \\ -\frac{1}{2} & -\frac{\sqrt{3}}{2} \end{bmatrix} \begin{bmatrix} real(q_3(k)) \\ img(q_3(k)) \end{bmatrix}. \tag{3.30}$$

Using the proposed nonlinear method, the symmetrical components can be calculated in a similar way.

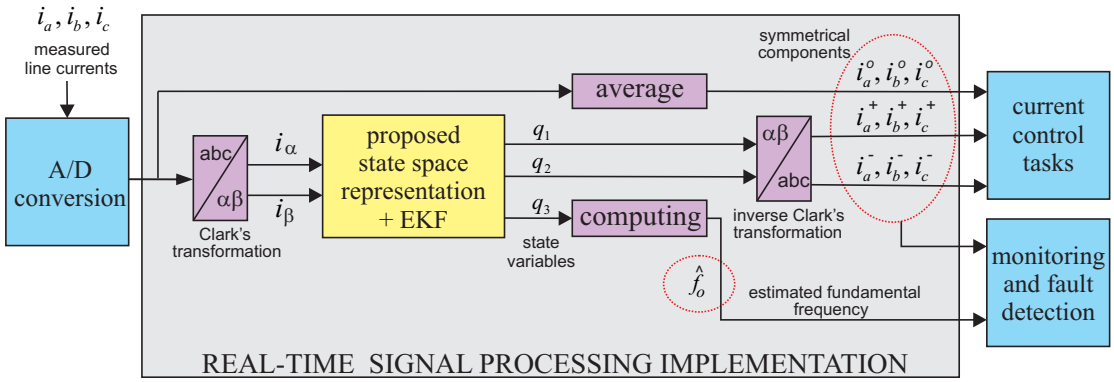

Figure 3.1 – Principles of the proposed nonlinear method

Fig. 3.1 summarizes the principle of the proposed nonlinear method. The currents and/or voltages measured from the grid are converted to digital form before being processed by the proposed methods. The output of the process is the estimated fundamental frequency and the estimated symmetrical components. For the proposed linear method, the output is only the estimated symmetrical components.

3.6.3 Discussion

Power systems are non-stationary, their parameters, e.g., the fundamental frequency, the amplitudes and phase angles of the currents and voltages are not fixed but changes in time. To represent the parameter variance, white Gaussian process noises can be integrated in model (3.13) and model (3.19) in the same way as in model (3.15). That helps to improve the tracking ability of the proposed methods.

The calculation of the phase angles of the positive and negative components by (3.25) and (3.28) is accurate when the fundamental frequency is constant all the time. For systems with a varying fundamental frequency, the phase angles can be calculated from:

$$\begin{cases} \phi_+(k) = \pi/2 + \angle q_2(k) - \sum_{i=1}^{k} \angle q_1(i), \\ \phi_-(k) = \pi/2 - \angle q_3(k) - \sum_{i=1}^{k} \angle q_1(i) \end{cases} \tag{3.31}$$

The problem with (3.31) comes from the sum up of errors of frequency angular estimation over time. The estimation of the phases does not encounter this problem, so that the phases can be used to replace the phase angles in different applications.

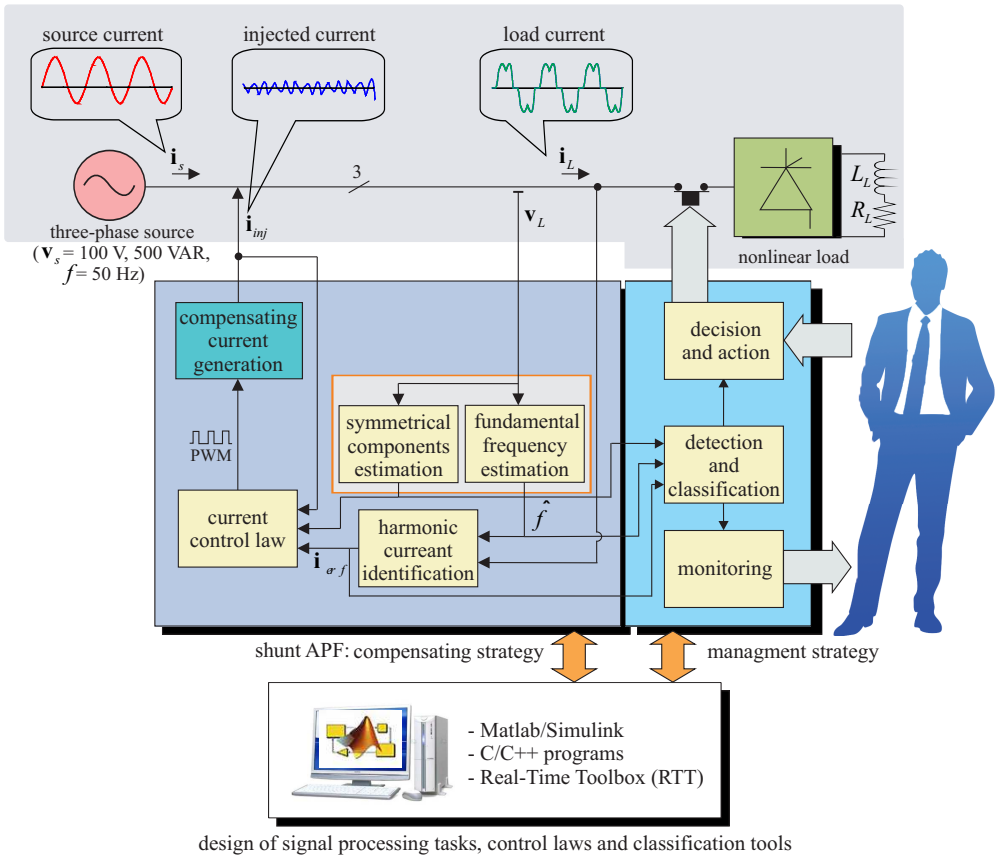

Figure 3.2 – Applications of the new methods in an APF

3.7 Applications of the ability of estimating power systems' parameters of the proposed methods in improving power quality of power systems

The estimator, i.e., the proposed state-space associated to an EKF, are implemented in a very general compensating and monitoring strategy. This context is presented by Fig. 3.2 where the orange box corresponds to Fig. 3.1. Fig. 3.2 is a detailed diagram of our shunt APF. The APF can be installed in different places of a power grid to improve power quality of the whole grid or certain areas of the grid. It can also be put next to the loads to compensate harmonics and unbalance generated by them and to prevent the disturbances from infecting the whole grid.

In fault conditions, e.g., phase-to-ground, phase-to-phase, two-phase-to-ground, etc, the symmetrical components are useful information for fault detection [22, 16]. Due to this reason, in practice, some types of protective relays are able to estimate the symmetrical-components estimation. Fig. 3.3 illustrates a structure of such a protective relays in reference of the similar structure presented in [22]. The orange box in the figure indicates the function of symmetrical component estimation that can be implemented by the proposed methods. Below are some

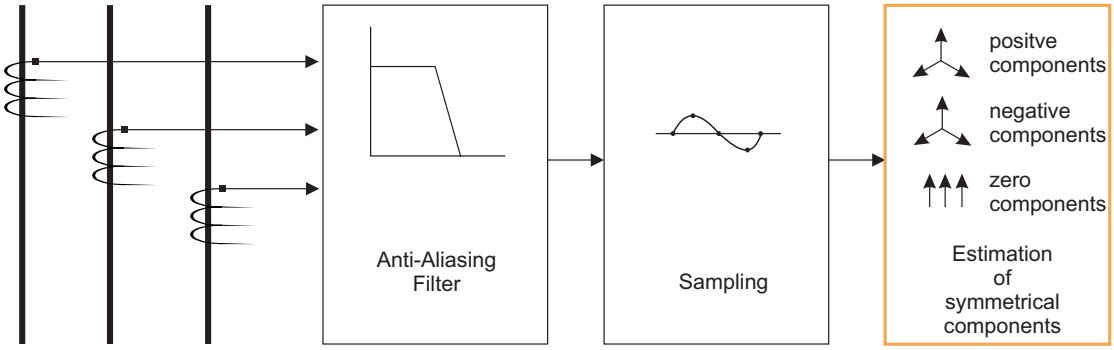

Figure 3.3 – Processes for estimating the symmetrical components of a power system in a digital protective relay

examples of using the negative components in relay applications [22]:

1. Rotating machinery applications: The information of the negative sequences is used to protect rotating machinery from damaging effect of the negative-sequence current flow,
2. Over-current protection: The relay provides sensitive backup protection against phase faults and overcurrent backup protection,
3. Directional elements: The relays provide the necessary sensitivity and direction for all unbalanced faults,
4. Line current differential relay: Negative sequence quantities are used in line current differential relays to increases the its sensibility in detecting unbalanced faults
5. Phase selection: A phase-selection algorithm based on negative-sequence and zero-sequence currents allows for implementation of sophisticated single-pole tripping relays,
6. Fault location: Fault location algorithms using negative-sequence components provide accurate solutions,
7. Other applications.

The values estimated by the proposed methods including the phase sequence, the voltage magnitudes, the frequency, and the phases or phase angles of the three-phases grid voltages of the positive sequence is useful for synchronizing the electric power of a generator to a grid.

3.8 Conclusion

Most of the modeling techniques of power systems only take into account one-phase systems or balanced three-phase systems. Therefore, in this chapter, two state-space models for unbalanced three-phase systems have been proposed. One model is linear and supposes that the estimated

frequency is provided from another estimation step. The other model is nonlinear and can handle unknown fundamental frequency. When combined with suitable algorithms, the two models allow to estimate different parameters and quantities of an unbalanced and varying three-phase system. Therefore, this chapter proposes two methods and their applications in power systems:

- The linear method consists in applying KF for the linear model (3.19) to estimate the symmetrical components of a power system;
- The nonlinear method consists in applying EKF for the nonlinear model (3.13) to iteratively estimate the fundamental frequency but also the symmetrical components of a power system.

The performance of the two proposed methods will be evaluated in the next chapter.

4 Simulations and Results

4.1 Introduction

In this chapter, a set of simulation tests has been achieved to evaluate the performance of the proposed methods for estimating the fundamental frequency and the symmetrical components of a power system under different operating conditions. These tests are for evaluating:

- The ability of the proposed linear method in estimating symmetrical components of a power system (the fundamental frequency is supposed to be known or provided by a previous process);
- The ability of the proposed nonlinear method in estimating the fundamental frequency and the symmetrical components of a power system (in these tests, the fundamental frequency is unknown).

As mentioned in Chapter 3, each of the two approaches can be useful for specific applications in practical systems. In addition, the performance of the proposed initialization scheme for the proposed nonlinear method is also evaluated.

4.2 Tests with the proposed linear method

In these tests, a sampling time T_s of 0.5ms is chosen, the value of the fundamental frequency f_o is 50Hz and will be provided for the proposed linear method to online identify the symmetrical components. The results will be compared with those of the MO-Adaline method presented in Chapter 2, in order to verify the efficiency of the linear method.

With the proposed method, the initial values of state variables $q_1(k)$ and $q_2(k)$ are respectively chosen as 0 and 0. The error covariance matrix of the state estimate of KF is initialized at $1.2\mathbf{I}$. The weight vector $\mathbf{W}(k)$ of MO-Adaline method in (2.62) is also initialized at $\mathbf{W}(0) = \mathbf{0}$.

4.2.1 Test with an unbalanced system

The following typical unbalanced three phase system is taken into account to evaluate the performance of the proposed method of two state variables.

$$\begin{cases} i_a(k) = I_+ \sin(\omega k T_s + \pi/3) + I_- \sin(\omega k T_s + \pi/6) + I_o \sin(\omega k T_s) \\ i_b(k) = I_+ \sin(\omega k T_s + \pi/3 + 2\pi/3) + I_- \sin(\omega k T_s + \pi/6 - 2\pi/3) + I_o \sin(\omega k T_s) \\ i_c(k) = I_+ \sin(\omega k T_s + \pi/3 - 2\pi/3) + I_- \sin(\omega k T_s + \pi/6 + 2\pi/3) + I_o \sin(\omega k T_s) \end{cases} \quad (4.1)$$

The following numerical values are chosen in our simulations: $I_+ = 1$A, $I_- = 0.2$A and $I_o = 0.1$A.

Applying the proposed method and MO-Adaline for estimating the symmetrical components of system (4.1), the results are shown in Fig. 4.1. Fig. 4.1 a) represents the three phase signals of (4.1), Fig. 4.1 a) represents the estimated amplitudes of the positive and negative components and Fig. 4.1 b) represents the estimated phase angles of these components. It can be seen from Fig. 4.1 that the estimated amplitudes by the two methods converge to two values 1A and 0.2A, and the estimated phase angles converge to values close to $\pi/3$rad and $\pi/6$rad. These are the amplitudes and phase angles of the positive and negative components of system (4.1). In addition, the proposed method shows much higher convergence speed than that of MO-Adaline.

Table 4.1 compares the performance of the two methods to estimate the amplitude quantities

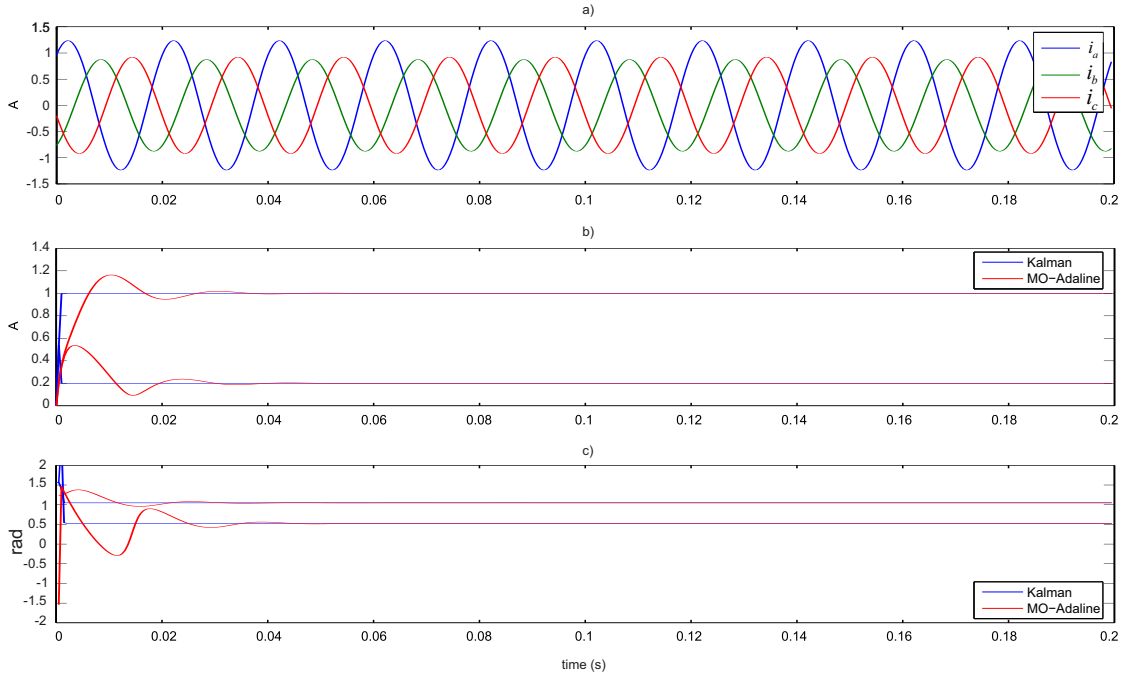

Figure 4.1 – Estimation of symmetrical components by the proposed linear method and MO-Adaline a) the unbalanced three-phase signals, b) estimated amplitudes of the positive and negative components, and c) phase angles of the positive and negative components

Amplitudes	mean at steady-state	MSE at steady-state	Error max. at steady-state
MO-Adaline	1.0000	$1.2663\ 10^{-7}$	0.0021
Proposed method	0.9999	$1.4767\ 10^{-14}$	$2.4657\ 10^{-7}$

Table 4.1 – Performance of the new method for estimating the amplitudes of the positive components of three phase signals

Amplitudes	mean at steady-state	MSE at steady-state	Error max. at steady-state
MO-Adaline	0.2000	$6.3673\ 10^{-8}$	0.0013
Proposed method	0.2000	$6.6309\ 10^{-15}$	$1.6747\ 10^{-7}$

Table 4.2 – Performance of the new method for estimating the amplitudes of the negative components of three phase signals

of the positive components, using the mean, MSE and maximum error of the estimations at steady-state. In the table, the MSE at steady-state is in the range of 10^{-7} A with the MO-Adaline and 10^{-14} A with the proposed method. Table 4.2 presents the comparison of the performance of the two methods in estimating the amplitudes of the negative components. According to the table, the MSE at steady-state of the proposed method in the range of 10^{-15} and of the MO-Adaline is in the range of 10^{-8}. Obviously, the amplitudes estimated by the proposed method shows much higher accuracy.

4.2.2 Robustness against load changes

This test is in order to verify the performance of symmetrical component estimation of the proposed linear method in an appearance of load changes. Equations (4.2) below represents a balanced system.

$$\begin{cases} i_a(k) = 1.2\sin(\omega k T_s) \\ i_b(k) = 1.2\sin(\omega k T_s - 2\pi/3) \\ i_c(k) = 1.2\sin(\omega k T_s + 2\pi/3) \end{cases} . \tag{4.2}$$

At instant 0.075s (at iteration $k = 150$), a switch in the load makes the system to become unbalanced, i.e., having the three phase signals as (4.1). The three phase signals of the power system before and after the switching are illustrated in Fig. 4.2 a).

The proposed linear method is used to estimate the system's symmetrical components. We want to evaluate its robustness to the practical problem. To improve the tracking ability of the proposed method, process noises are used to represent the variance of the state variables. The

correlation matrix of the process noise vector used by the EKF scheme is set to:

$$Q_1(k) = \begin{bmatrix} 2\ 10^{-7} & 0 \\ 0 & 2\ 10^{-7} \end{bmatrix} \tag{4.3}$$

The MO-Adaline is also employed for comparison. Fig. 4.2 b) shows the estimated amplitudes of the positive and negative components of the testing signals by the two methods. Fig. 4.3 shows the reconstructed positive components by the proposed method and the MO-Adaline, accompanied by the real ones. Fig. 4.4 shows the reconstructed negative components by the proposed method and MO-Adaline, accompanied by the real ones. According to these figures, the two methods can track the change of the signals. The proposed linear method demonstrates a better performance in comparison of the performance of MO-Adaline.

4.2.3 Tracking symmetrical components when the fundamental frequency constantly varies in time

In this test, the three-phase signals (4.1) are considered with the fundamental frequency that is not constant all the time but it varies in time at a rate of 2Hz/s, starting at 50Hz. Fig. 4.5 shows the variation of the frequency during the time from 0.8s to 0.1s. The correlation matrix of the process noise vector used by the EKF scheme is set to:

$$Q_1(k) = \begin{bmatrix} 2 & 0 \\ 0 & 2 \end{bmatrix} . \tag{4.4}$$

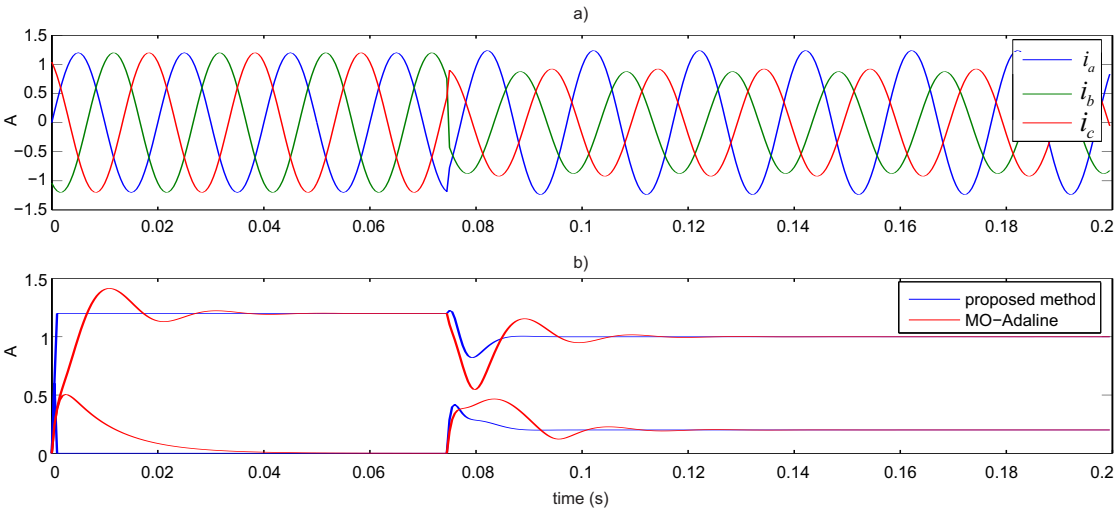

Figure 4.2 – Estimation of the symmetrical components of the power system in load changes by the proposed method and MO-Adaline a) the unbalanced three-phase signals, b) estimated amplitudes of the positive and negative components

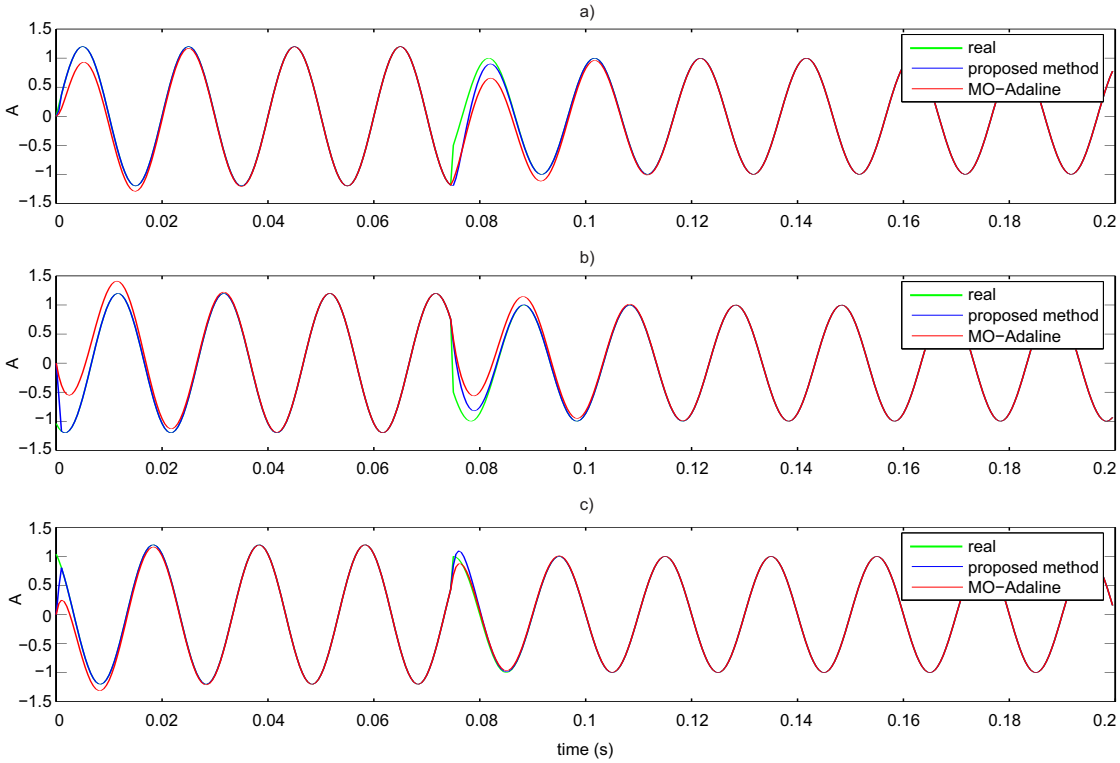

Figure 4.3 – Reconstruction of the positive components of the power system in load changes by the proposed method and MO-Adaline a) positive component in phase a b) positive component in phase b c) positive component in phase c

The estimated amplitudes of the positive and negative components of the proposed method and MO-Adaline are shown in Fig. 4.6. It can be seen from the figure that the estimation of the proposed method accurately converges to the real amplitudes of the positive and negative componets. On the other hand, the estimation of MO-Adaline shows some oscillations around the real values.

The error of the estimated three phase signals of the positive and negative components of the MO-Adaline compared to the real signals are shown in Fig. 4.7. Fig. 4.8 draws the deviation of the estimated signals of the proposed method from the real signals. The error in estimating the symmetrical components of the proposed method is less than 1.510^{-5} which is much less compared to the error of the estimated symmetrical components obtained with the MO-Adaline (more than 0.01). The bad performance of the MO-Adaline in this test with a constantly varying fundamental frequency comes from the assumption of this method for a constant fundamental frequency.

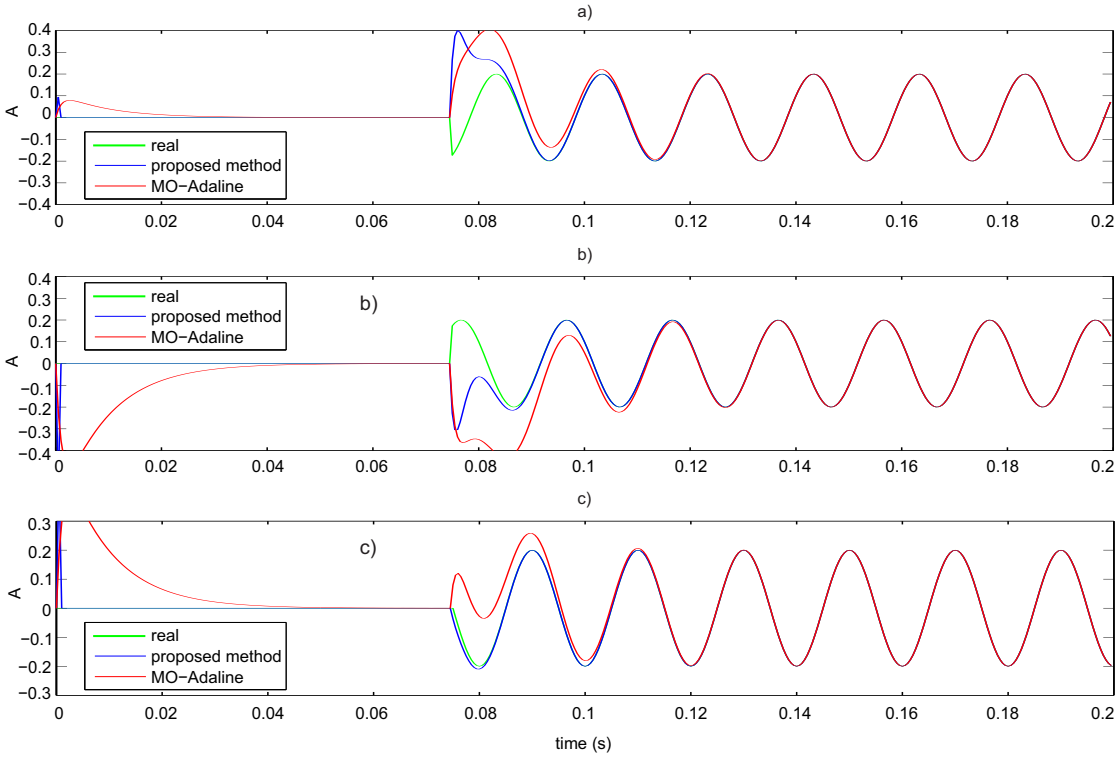

Figure 4.4 – Reconstruction of the negative components of the power system in load changes by the proposed method and MO-Adaline a) positive component in phase a b) positive component in phase b c) positive component in phase c

4.3 Test with the proposed nonlinear method

4.3.1 Fundamental frequency estimation

The proposed nonlinear method, which is able to work under balanced or unbalanced conditions, is used to estimate the fundamental frequency of a power system under different conditions. The results are compared to the one obtained with the 3P EKF method and 1P EKF method

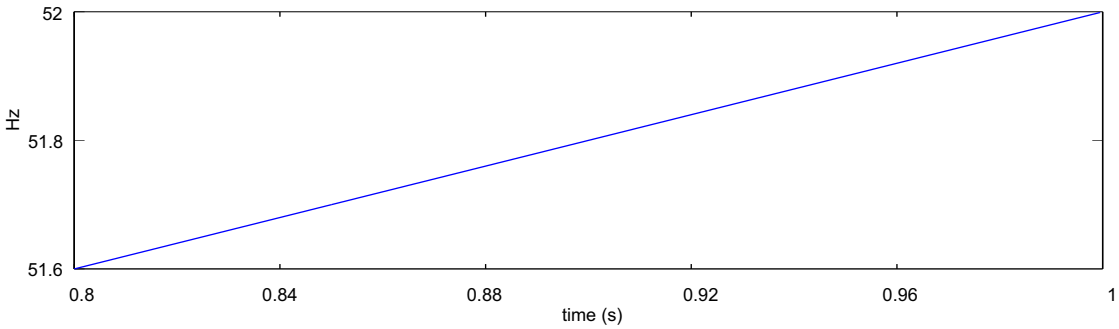

Figure 4.5 – varying fundamental frequency

presented in Chapter 2.

For each of these tests, the proposed method utilizes the state-space model (2.6) of 3 state variables including the positive and negative components, the 1P EKF employes model (2.29) also composed of three variables while the model used by the 3P EKF has only 2 variables, either the positive or negative component.

The initial conditions of the EKFs are the first estimation of the frequency $\widehat{f}(0) = 45$Hz and $1.2\mathbf{I}$ for the error covariance matrix of the state estimate, $\mathbf{I}$ is the identity matrix. The initial values of the other state variables of the three methods are chosen such that the amplitude and phase angle of the positive components are 0.8A and $\pi/6$rad and the amplitude of the negative components is equal 0A.

Frequency estimation under balanced conditions

In this test, the system that is used is composed of the following three-phase balanced sinusoidal signals with $I = 1$A, $\phi = \frac{\pi}{3}$rad, $\omega = 2\pi f_o$ with $f_o = 50$Hz:

$$\begin{cases} i_a(k) = I\sin(\omega k T_s + \phi) \\ i_b(k) = I\sin(\omega k T_s + \phi - 2\pi/3) \\ i_c(k) = I\sin(\omega k T_s + \phi + 2\pi/3) \end{cases} . \tag{4.5}$$

The fundamental frequency is estimated at the same time with the two methods. The results are presented in Table. 4.3 with the Mean Square Error (MSE), the maximum error at steady state and the time to converge. Both the proposed method and the 3P EKF method require a short transient time to converge, i.e., about 39 ms, and present a small error in estimating the

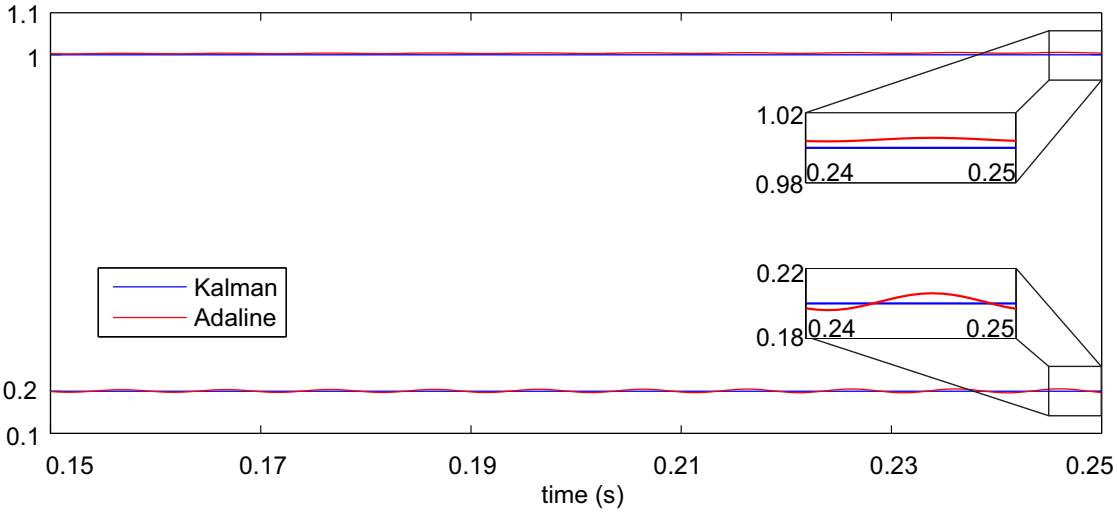

Figure 4.6 – The estimated amplitudes of the positive and negative components of the proposed method and MO-Adaline

frequency (in the range of 10^{-6} Hz). The estimated frequency given by the 1P EKF method is slightly less accurate than the other two method (in the range of 10^{-5} Hz).

Frequency estimation under unbalanced conditions

An unbalanced power system is considered in this test. The following is a typical unbalanced three phase system:

$$\begin{cases} i_a(k) = I_+ \sin(\omega k T_s + \phi_+) + I_- \sin(\omega k T_s + \phi_-) + I_o \sin(\omega k T_s + \phi_o) \\ i_b(k) = I_+ \sin(\omega k T_s + \phi_+ - 2\pi/3) + I_- \sin(\omega k T_s + \phi_- + 2\pi/3) + I_o \sin(\omega k T_s + \phi_o) \\ i_c(k) = I_+ \sin(\omega k T_s + \phi_+ + 2\pi/3) + I_- \sin(\omega k T_s + \phi_- - 2\pi/3) + I_o \sin(\omega k T_s + \phi_o) \end{cases} \quad (4.6)$$

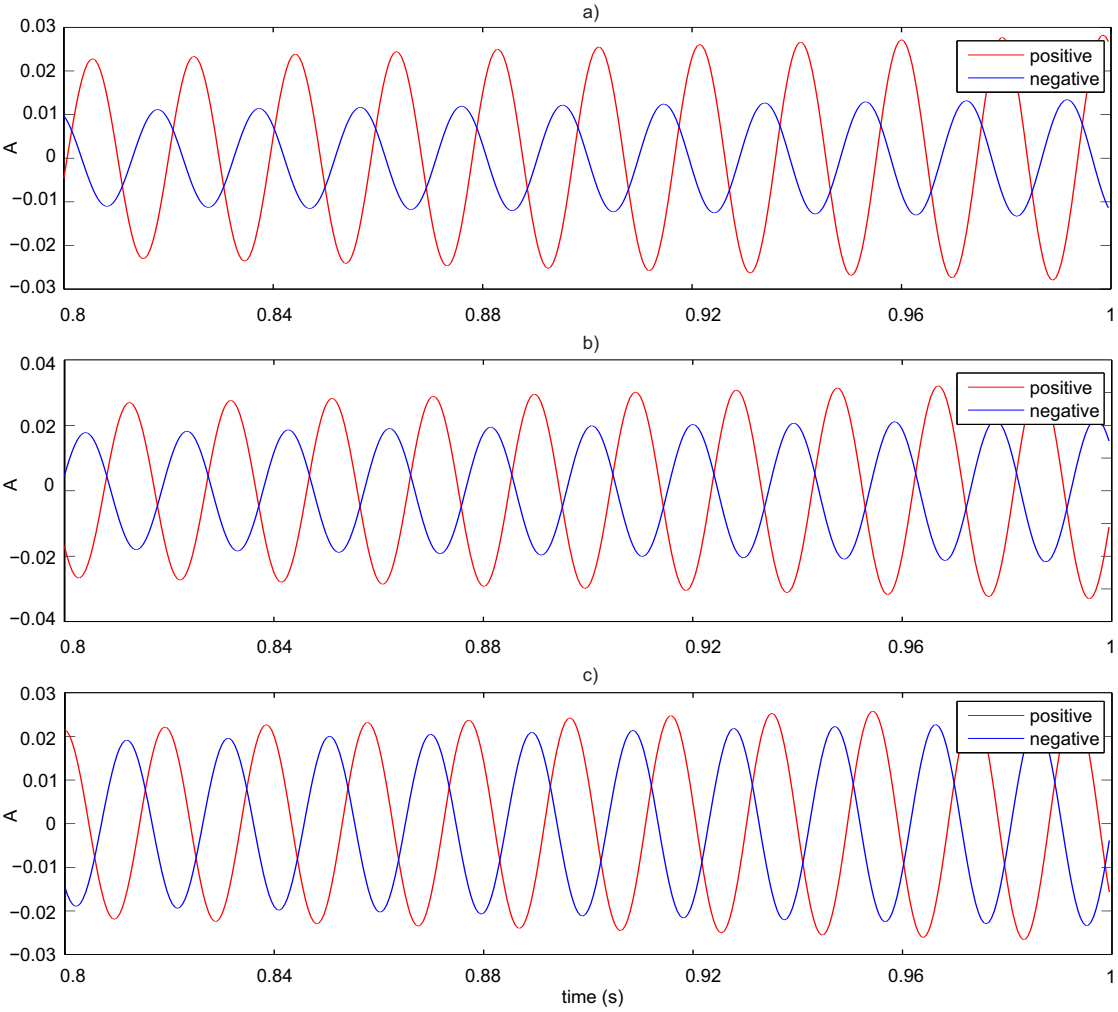

Figure 4.7 – The errors of the estimation of the positive and negative components of the signals (4.1) with the frequency varies as in Fig. 4.5 by MO-Adaline compared to the real ones: a) phase a, b) phase b, c) phase c

The following numerical values are chosen in our simulations: $f_o = 50\text{Hz}$, $I_+ = 1$, $I_- = 0.3$, $I_o = 0.1$, and $\phi_+ = 0$, $\phi_- = \pi/5$, $\phi_o = \pi/2$.

The three phase signals of this system are shown on Fig. 4.9.

The proposed method, the 3P EKF method and the 1P EKF method are applied to estimate the fundamental frequency of the system given by (4.6). The results are presented by Fig. 4.10 a). As it can be observed, the estimated frequency given by the 3P EKF method oscillates around the true value meanwhile the estimated frequencies using the proposed method and the 1P EKF converge faster without oscillation. The efficiency of the three methods in estimating the fundamental frequency is shown by Table. 4.4. It can be seen that the estimated frequency obtained with the proposed method is the most accurate (the MSE is about 10^{-7} Hz). On the

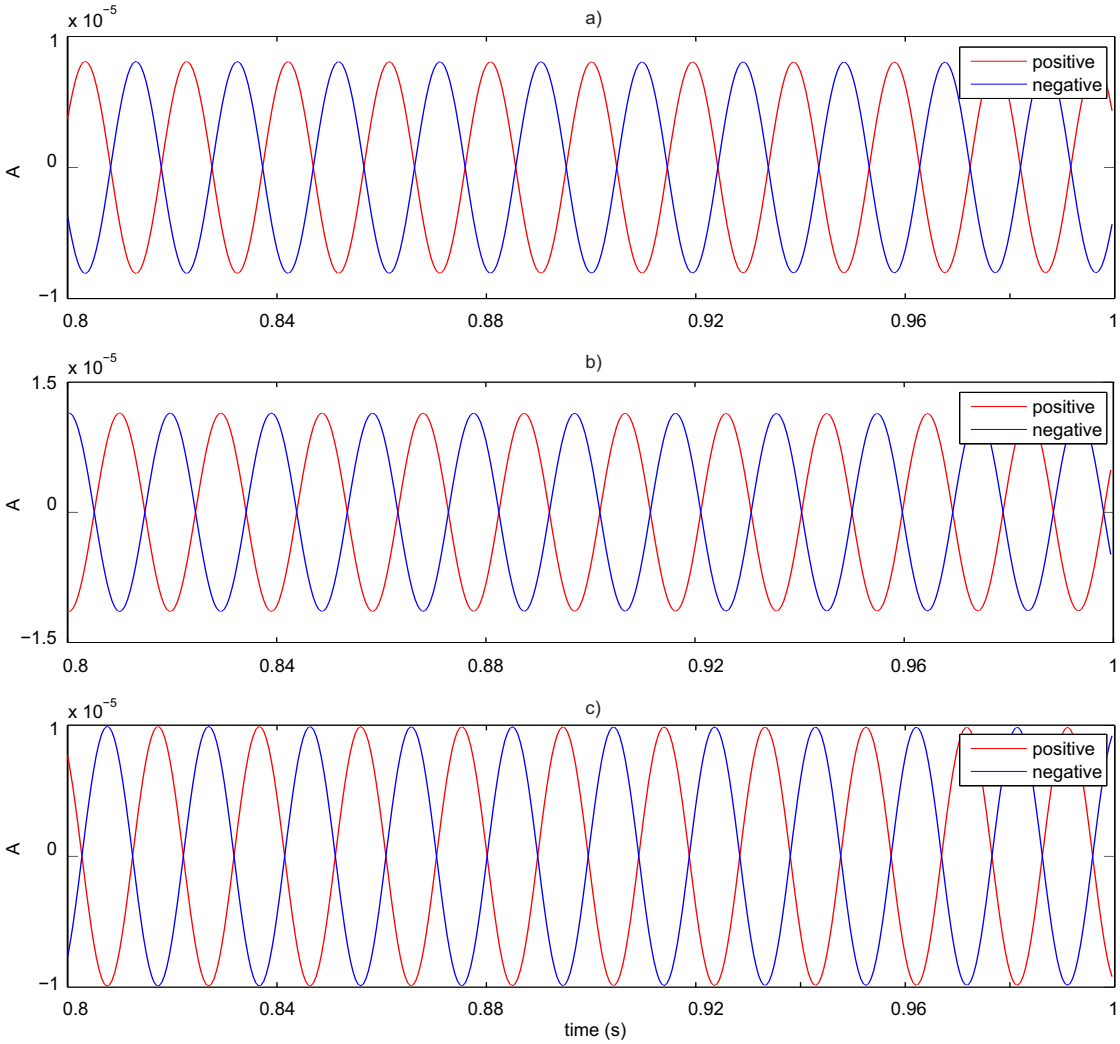

Figure 4.8 – The errors of the estimation of the positive and negative components of the signals (4.1) with the frequency varies as in Fig. 4.5 by the proposed method compared to the real ones: a) phase a, b) phase b, c) phase c

methods	time to reach the reference frequency with +/- 0.1 Hz (s)	MSE at steady-state (Hz)	max. error at steady-state (Hz)
proposed method	0.0332	$1.8350\ 10^{-6}$	0.0030
3P EKF	0.0388	$1.5620\ 10^{-6}$	0.0028
1P EKF	0.0667	$3.3167\ 10^{-5}$	0.0126

Table 4.3 – Performance of the proposed nonlinear method compared to the 3P EKF and the 1P EKF in estimating the frequency of a balanced system

methods	time to reach the reference frequency with +/- 0.1 Hz (s)	MSE at steady-state (Hz)	max. error at steady-state (Hz)
proposed method	0.049	$6.810\ 10^{-7}$	0.001
3P EKF	0.100	$1.242\ 10^{-4}$	0.015
1P EKF	0.057	$6.535\ 10^{-6}$	0.015

Table 4.4 – Performance of the proposed nonlinear method compared to the 3P EKF and the 1P EKF in estimating the frequency of an unbalanced system

methods	time to reach the reference frequency with +/- 0.1 Hz (s)	MSE at steady-state (Hz)	max. error at steady-state (Hz)
proposed method	0.049	$3.6844\ 10^{-6}$	0.0049
3P EKF	0.115	$1.8268\ 10^{-4}$	0.0368
1P EKF	0.047	$9.1296\ 10^{-6}$	0.0065

Table 4.5 – Performance of the proposed nonlinear method compared to the 3P EKF and the 1P EKF in estimating the frequency of an unbalanced system with an additional 30 dB noise

methods	time to reach the reference frequency with +/- 0.1 Hz (s)	MSE at steady-state (Hz)	max. error at steady-state (Hz)
proposed method	0.070	$7.6017\ 10^{-6}$	0.0094
3P EKF	0.135	$4.8846\ 10^{-4}$	0.0535
1P EKF	0.150	$1.0793\ 10^{-4}$	0.0435

Table 4.6 – Performance of the proposed nonlinear method compared to the 3P EKF and the 1P EKF in estimating the frequency of an unbalanced system disturbed by harmonics

other hand, the MSE with the 3P EKF method has a largest value (in the range of 10^{-4} Hz).

Evaluation of the robustness against noise

The immunity of the methods to noise is now investigated. Each of the three phase signals of the system in (4.6) is contaminated by a zero-mean white Gaussian noise with a Signal-to-Noise Ratio (SNR) of 30 dB. Table. 4.5 shows a MSE in the range of 10^{-6} Hz for the estimated frequency with the proposed nonlinear method and the 1P EKF method. At the same time, the corresponding MSE for the 3P EKF method is in the range of 10^{-4} Hz. Fig. 4.10 b) illustrates the performance of the two methods. These results prove that the proposed method and the 1P EKF are able to estimate the fundamental frequency quickly and accurately even under noisy conditions. The 3P EKF requires a longer convergence time and results in a less accurate estimation.

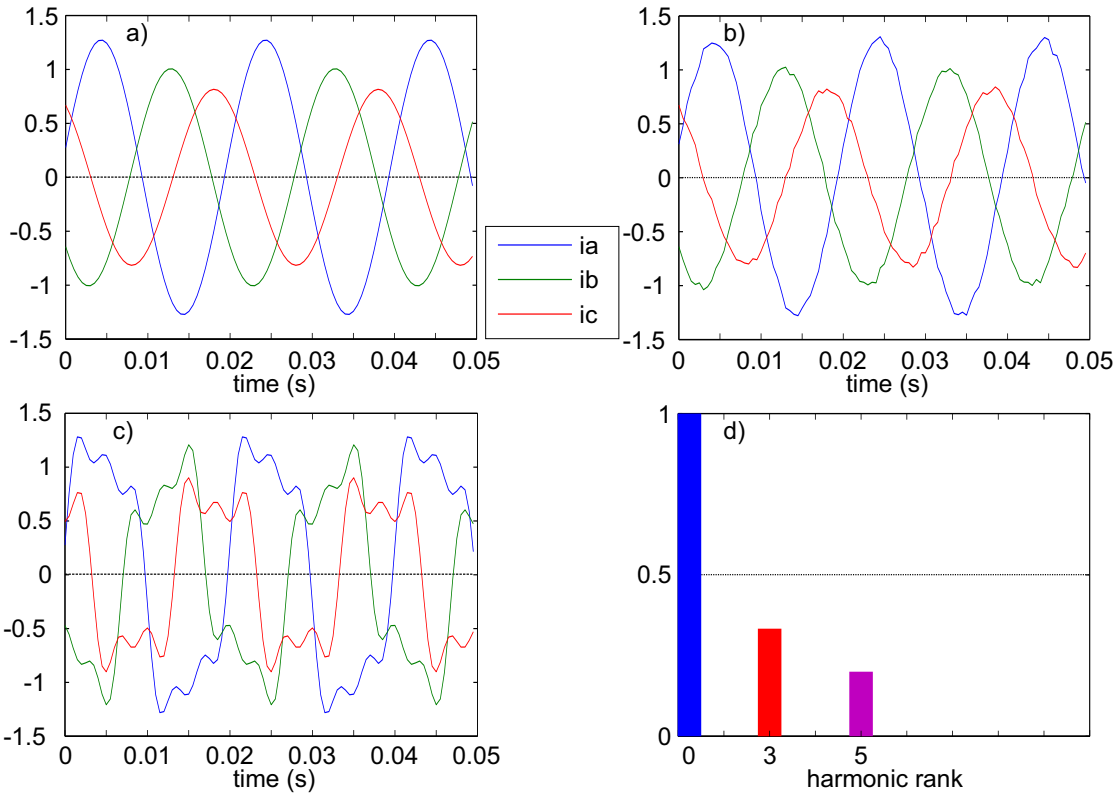

Figure 4.9 – The signals of the unbalanced three-phase system defined by (4.6), a) without noise, b) with a 30 dB noise, c) with higher-order harmonics of rank 5 and 7, d) histogram corresponding to the signal with higher-order harmonics of rank 3 and 5

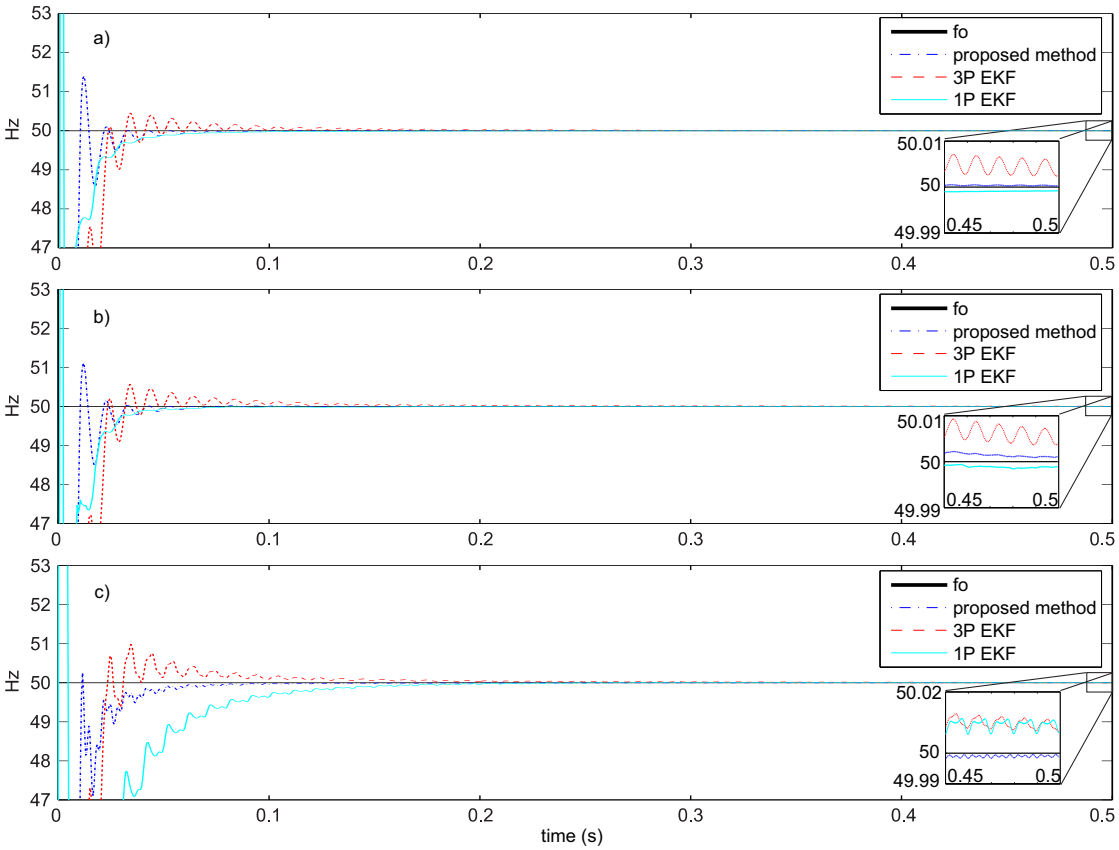

Figure 4.10 – Estimated frequencies by the three methods, a) without noise and harmonics, b) with a 30 dB noise, c) with harmonics of rank 3 and 5

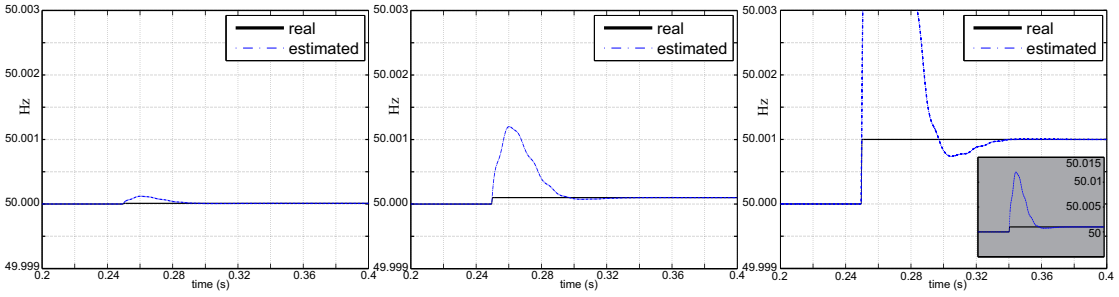

Figure 4.11 – Fundamental frequency estimation when steps appear with different amplidutes and respectively, a) of 0.00001 Hz, b) of 0.0001 Hz and c) of 0.001 Hz

Evaluation of the robustness against higher-order harmonics

The presence of harmonic terms influences the fundamental frequency estimation. This is evaluated for the three methods. Each phase signal of the system in (4.6) are therefore disturbed by adding higher order harmonics of rank 3 and 5, respectively with amplitudes of $\frac{V_+}{3}$ and $\frac{V_+}{5}$ in which harmonic of rank 3 is in the zero sequence. Results are presented in Table. 4.6 and the estimated frequencies of the two methods are shown by Fig. 4.10 c). It can be seen that the addition of harmonics strongly degrades the performance of the 1P EKF method, meanwhile the proposed method is robust against harmonic pollution.

The results of these tests can be explained as follow: The model used by the 3P EKF method is flawed for modeling unbalanced systems. Thus, estimating the frequency is even more challenging for it under severe conditions, i.e., with the presence of noise and harmonics. As a consequence, the estimation is achieved with a low convergence rate, a constant steady-state error and oscillations. On the other hand, the state-space proposed in (3.13) models power systems with their unbalance properties. Therefore, this model is efficient in estimating the frequency in an EKF scheme and is robust against noise and higher-order harmonics. The 1P EKF employs a state-space model for one phase power signal and is not affected under unbalanced conditions, however, when the other two methods apply $\alpha - \beta$ transform that helps to eliminate zero sequence harmonics, the 1P EKF method does not have the ability and hence suffers severe impact by these harmonics.

case	a)	b)	c)
freq. step amplitude (Hz)	0.00001	0.0001	0.001
peak value (Hz)	50.00012004	50.00120044	50.01200460
PO (%)	1100.45	1100.44	1100.46
first peak time (ms)	11	11	11
settling time to 5% (ms)	77.6	77.3	77.2
steady-state error (Hz)	$7.105\ 10^{-15}$	$3.553\ 10^{-13}$	$4.007\ 10^{-12}$

Table 4.7 – Performance of the proposed state-space method in tracking fundamental frequency steps

Tracking of fundamental frequency steps

Further investigations have been carried out to check the harmonic tracking ability of the proposed method. To test the speed and convergence of the proposed technique at nominal frequency conditions (the fundamental frequency is f_0 = 50 Hz but it can be any other numerical value), a signal is taken for fundamental frequency estimation where frequency steps occur under unbalanced conditions.

In this test, fundamental frequency steps appear with different amplitudes, i.e., 0.001, 0.0001 and 0.00001 Hz. The fundamental frequency is estimated by using the proposed state-space model and the EKF algorithm. The fundamental frequency step appears at instant 0.25 s, in

other words at iteration 500. The correlation matrix of the process noise vector in the EKF scheme is set to:

$$Q_1(k) = \begin{bmatrix} 5.10^{-7} & 0 & 0 \\ 0 & 1.10^{-4} & 0 \\ 0 & 0 & 1.10^{-4} \end{bmatrix} \tag{4.7}$$

The simulation results reveal that the proposed state-space method takes few iterations to reach the steady-state value of the new value of the fundamental frequency. Results are represented on Fig. 4.11. The evaluated converged results have been presented for each case in Table 4.7 which indicates the Percent Overshoot (PO), the peak value, the first peak time, the settling time to within 5% of the final value and the steady-state error. If the peak values are high in percent, frequency steps of 0.001 Hz are very severe cases and reasonably never happen in real installations, and a frequency step of 0.1 10^{-3} Hz leads to a overshoot of 11.004 10^{-4} Hz. Furthermore, the fundamental frequency estimated by the proposed state-space model and the EKF converges rapidly the real value of the frequency. In all cases, the peak value appears only 22 iterations after the fundamental frequency step, i.e., in approximately 11 ms. Table 4.7 also shows the accuracies of the proposed estimator: At steady-state, the error is almost less than 4.1 10^{-12} Hz.

All these results demonstrates that the proposed state-space method is an accurate frequency estimator even in time-varying environments and for fundamental frequency variations.

Tracking of a fundamental frequency varying constantly in time

The estimation performance of the proposed nonlinear method has been evaluated with a continuously changing fundamental frequency of the power system whose decay is 2Hz/s. The correlation matrix of the process noises is set to:

$$Q_1(k) = \begin{bmatrix} 2 & 0 & 0 \\ 0 & 2 & 0 \\ 0 & 0 & 2 \end{bmatrix} \tag{4.8}$$

Fig. 4.12 shows the tracking performance of the proposed method: Fig. 4.12 a) plots real and estimated frequency and Fig. 4.12 b) presents the frequency error (subtraction of the estimated frequency and the real frequency). The frequency error is less than 2.510^{-3}Hz which is an acceptable range in power systems applications.

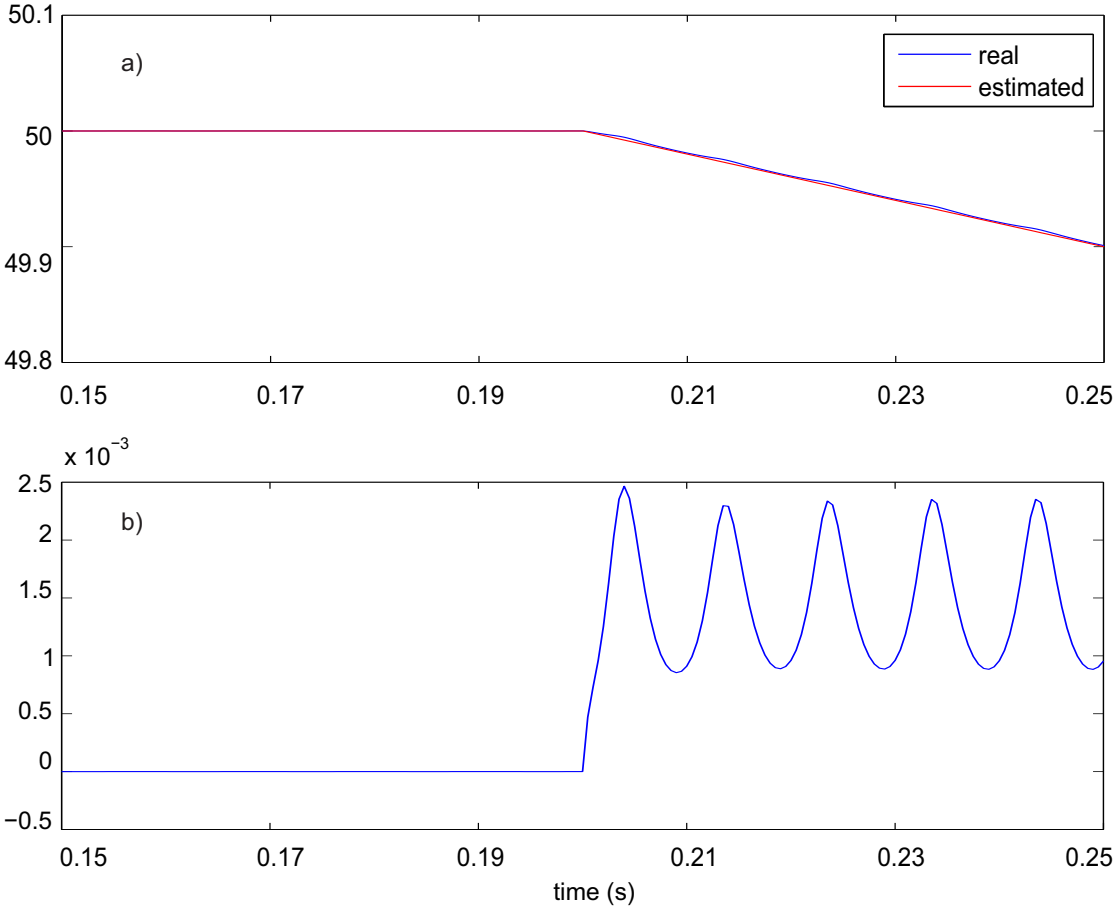

Figure 4.12 – Performance in estimating the frequency with a changing fundamental frequency, a) real and estimated frequency (Hz), b) frequency error (Hz)

4.3.2 Symmetrical component estimation

In the section, the performance of the proposed nonlinear method applyed in estimating the symmetrical components of a power system is investigated in various conditions.

Performance under unbalanced conditions

The first test works with a set of three phase signals of a unbalanced power system which can be represented as the sum of three symmetrical components as in (4.9):

$$\begin{cases} i_a(k) = I_+ \sin(\omega k T_s + \phi_+) + I_- \sin(\omega k T_s + \phi_-) + I_o \sin(\omega k T_s + \phi_o) \\ i_b(k) = I_+ \sin(\omega k T_s + \phi_+ - 2\pi/3) + I_- \sin(\omega k T_s + \phi_- + 2\pi/3) + I_o \sin(\omega k T_s + \phi_o) \\ i_c(k) = I_+ \sin(\omega k T_s + \phi_+ + 2\pi/3) + I_- \sin(\omega k T_s + \phi_- - 2\pi/3) + I_o \sin(\omega k T_s + \phi_o) \end{cases} \tag{4.9}$$

In this application, the following numerical values are used for (4.9): $f_o = 50$Hz, $I_+ = 1$, $I_- = 0.4$, $I_o = 0.1$ and $\phi_+ = \pi/3$, $\phi_- = \pi/6$, $\phi_o = 0$, the three phase signals in (4.9) are unbalanced. A zero-mean, white Gaussian noise of 30 dB is added to each of the signals.

The proposed state-space model is used in an EKF scheme, and expressions (3.25)-(3.27) and (3.28)-(3.30) are used to identify the symmetrical components at each instant. The initial values of $q_1(k)$ is chosen as $0.9891 + 0.1471i$ (this value corresponds to the fundamental frequency at 47Hz). Supposing that we do not know the existence of the negative components, $q_3(k)$ is initialized at 0. The initial value of $q_2(k)$ is chosen as $1.2 - 0.5i$ which is not far from the true value of $q_2(0)$. The error covariance matrix of the state estimate is initialized at $1.2\mathbf{I}$.

Results are presented by Fig. 4.13. Furthermore, Fig. 4.13 a) shows the evolution of the unbalanced three phase signals through time and the estimated amplitudes of the corresponding symmetrical components are presented in Fig. 4.13 b). It can be seen that, after a short time, the estimated amplitudes get close to two values 1.0 and 0.4 which are the true amplitudes of the positive and negative components. In addition, Table 4.1 evaluates the mean values, the MSE and the maximum errors of the estimated amplitudes at steady-state for the proposed method. The mean values indicate the biases from the true values. It can be explained as the result of a poor initialization of the EKF. However, the MSE is in the range of 10^{-6} and the maximum error is in the range of 10^{-3}. This demonstrates well that the deviation of the estimated amplitudes from the true ones is small and that the method provides high accuracy in estimating the amplitudes of the symmetrical components. Fig. 4.13 shows the evolution of the symmetrical components converted in the $\alpha\beta$-reference frame. It can be observed that the estimated components track the true ones very well.

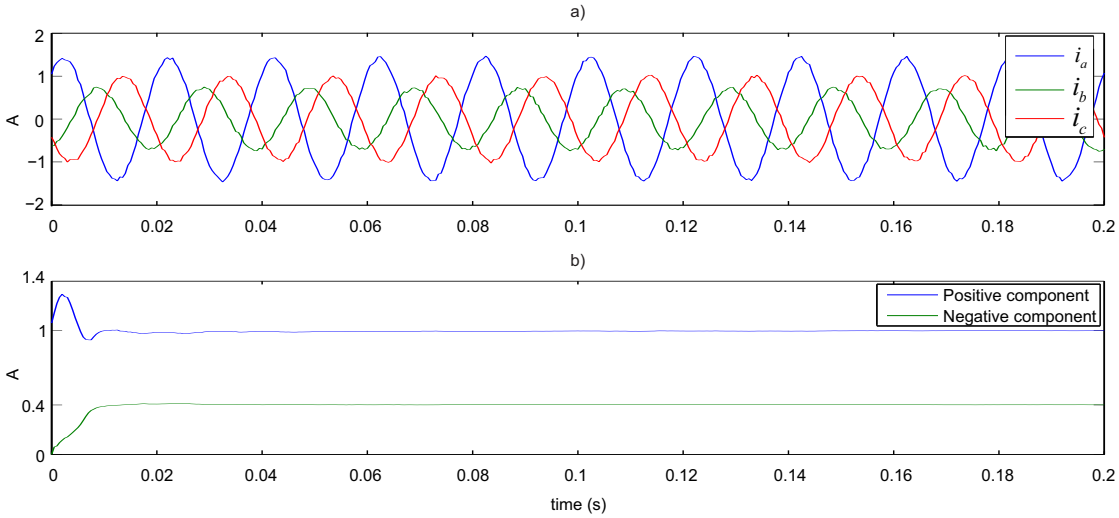

Figure 4.13 – Identification of the symmetrical components, a) the unbalanced three-phase signals, b) estimated amplitudes of the positive and negative components

Robustness against higher-order harmonics

The second test aims to demonstrate the immunity of the proposed method to harmonics. Each phase signal of the system given by (4.9) are therefore disturbed by adding higher order harmonics of rank 5 and 7, respectively with amplitudes of $\frac{I_+}{10}$ and $\frac{I_+}{15}$. The state variables $q_1(k)$, $q_2(k)$ and $q_3(k)$ are initialized with the same values as in the first test. The results are presented in Table 4.9 and are similar to the ones from the first test. There is a small bias and the MSE and maximum errors are small, i.e., in the range of 10^6 for the MSE and 10^3 for the maximum error.

Robustness against load changes

A third test is proposed to evaluate the dynamics to the proposed method. This is for examining the performance of the proposed method with time-varying processes, like changes of nonlinear loads. We propose to switch suddenly from a balanced load to an unbalanced one because this can happen in real-world applications. Therefore, the following three-phase system is considered:

$$\begin{cases} i_a(k) = \sin(\omega k T_s) \\ i_b(k) = \sin(\omega k T_s - 2\pi/3) \\ i_c(k) = \sin(\omega k T_s + 2\pi/3) \end{cases} \tag{4.10}$$

The three phase system is balanced. At instant 0.075 s (at iteration $k = 150$), it changes to become unbalanced with the signals in (4.9) with $I_+ = 0.8$, $I_- = 0.2$, $I_o = 0.1$, $\phi_+ = \frac{\pi}{3}$, $\phi_- = \frac{\pi}{2}$ and $\phi_o = 0$.

The proposed method is used to identify the symmetrical components of the changing system

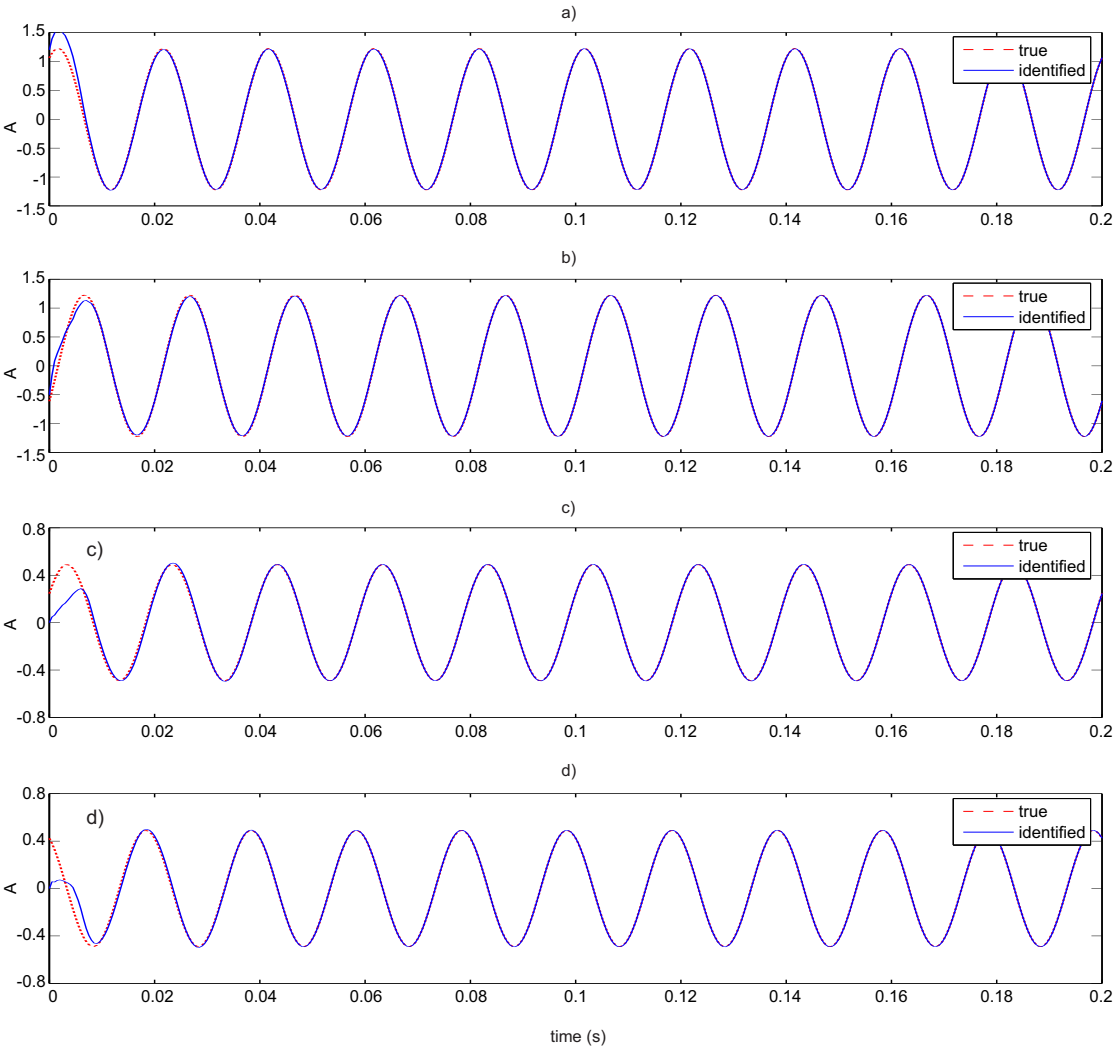

Figure 4.14 – Identified currents compared to the real ones, a) i_{α}^{+}, b) i_{β}^{+}, c) i_{α}^{-} and d) i_{β}^{-}

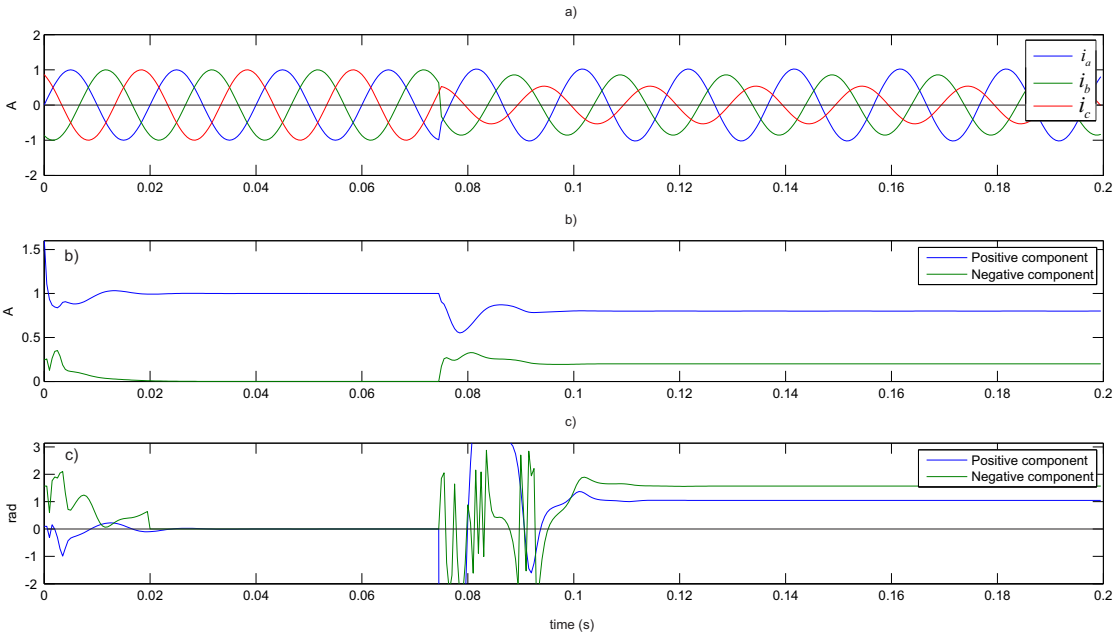

Figure 4.15 – Identification of the symmetrical components, a) the unbalanced three-phase signals, b) estimated amplitudes of the positive and negative components, and c) phase angles of the positive and negative components

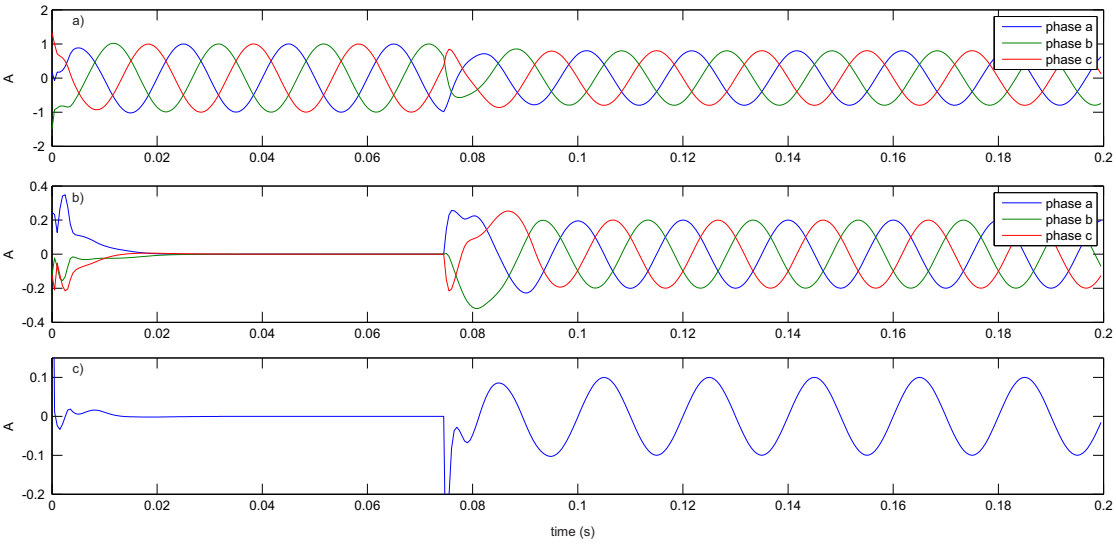

Figure 4.16 – Reconstruction of the system's symmetrical components, a) recovered positive components, b) recovered negative component, and c) recovered zero component

Amplitudes	mean at steady-state (A)	MSE at steady-state (A)	Error max. at steady-state (A)
Positive component	0.9988	$2.8627\ 10^{-6}$	0.0046
Negative component	0.4011	$1.7359\ 10^{-6}$	0.0032

Table 4.8 – Performance of the new method for estimating the amplitudes of the positive and negative components of three phase signals disturbed by noise of 30 dB

Amplitudes	mean at steady-state (A)	MSE at steady-state (A)	Error max. at steady-state (A)
Positive component	0.9981	$5.2349\ 10^{-6}$	0.0083
Negative component	0.4008	$9.2706\ 10^{-7}$	0.0031

Table 4.9 – Performance of the new method for estimating the amplitudes of positive and negative components of three phase signals disturbed by harmonics of rank 5 and 7

at each instant. The EKF scheme uses the process noises with the following correlation matrix:

$$Q_1 = \begin{bmatrix} 10^{-3} & 0 & 0 \\ 0 & 10^{-3} & 0 \\ 0 & 0 & 10^{-2} \end{bmatrix} \tag{4.11}$$

The results are presented by Fig. 4.15 and it can be seen that before the transition ($k < 150$), the estimated negative component is zero while the estimated positive component has an amplitude of 1 V and a phase angle of 0 rad at steady-state. After the failure appears at iteration $k = 150$ and after a short transient, the estimated amplitudes of the positive and negative components converge respectively to the true amplitudes 0.80 V and 0.20 V. At the same time, the estimation of the phase angles of the positive and negative components respectively converge to 1.047 and 1.571 which are approximatly the true phase angles $\frac{\pi}{3}$ and $\frac{\pi}{2}$ of the power system.

The evolution of the positive and negative components are shown on Fig. 4.16. This figure also shows the evolution of the three currents reconstructed from the symmetrical components. The results show that after a time shorter than one cycle, the estimated currents are very close to the real values. Finally, the evolution of the symmetrical components converted in the $\alpha\beta$-reference frame are shown by Fig. 4.17. It can be seen from this figure that at the beginning, the reconstructed system is balanced. After the failure appears, the negative and zero component become significant and the positive component decreases at the same time. This characterizes the behavior of the true power system.

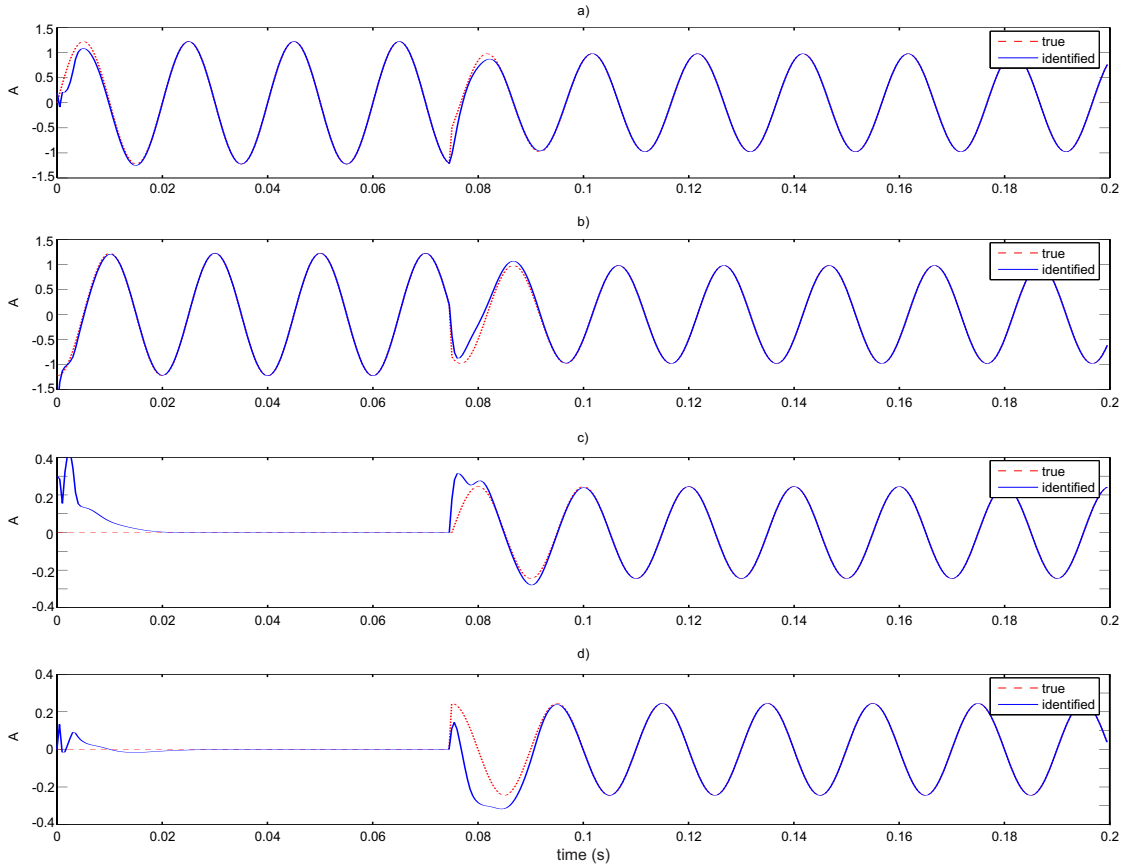

Figure 4.17 – Identified currents compared to the real ones, a) i_{α}^{+}, b) i_{β}^{+}, c) i_{α}^{-} and d) i_{β}^{-}

Robustness against varying fundamental frequency

The three phase signals with the constantly varying frequency presented in section 4.3.1 is used again in this test to evaluate the performance of the proposed method in estimating the symmetrical components. The estimated amplitudes of the positive and negative components of the proposed method are shown in Fig. 4.18, the estimations converge to 1 and 0.3 which are the exact values. Fig. 4.19 shows the errors of the estimated phases of the symmetrical components which are relatively small (in the range of 10^{-6} and 10^{-5} respectively). The errors of the estimated three phase signals of the positive and negative components compared to the real signals are indicated in Fig. 4.20. According to the figure, these errors are less than 2.10^{-5} so the estimation of the three phase signals of the symmetrical components of the proposed method is precise. The proposed method proves to perform well even in the variance of the fundamental frequency. From that, the error in estimating the symmetrical components is less than 2.10^{-5}, showing that the proposed method is able to accurately estimate the symmetrical components of the power system with a continuously varying fundamental frequency.

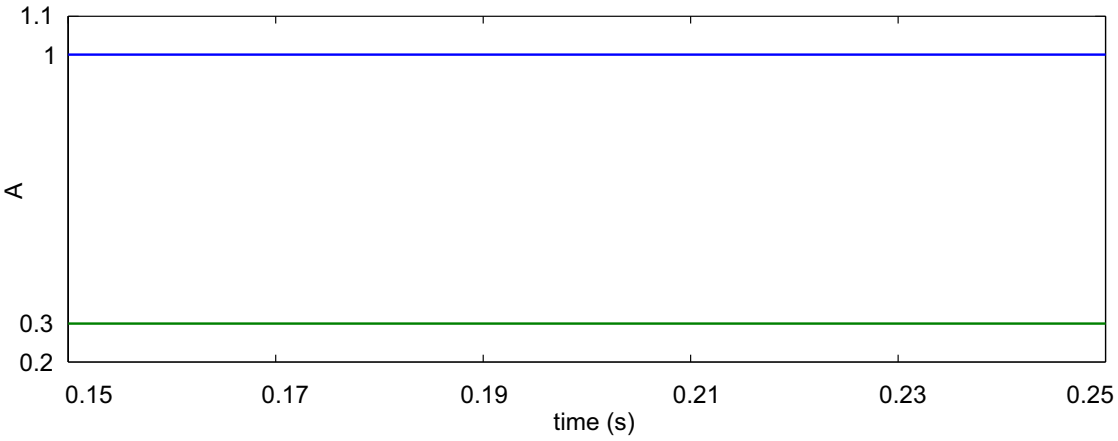

Figure 4.18 – The estimated amplitudes of the positive and negative components of the proposed nonlinear method: a) the positive, b) the negative

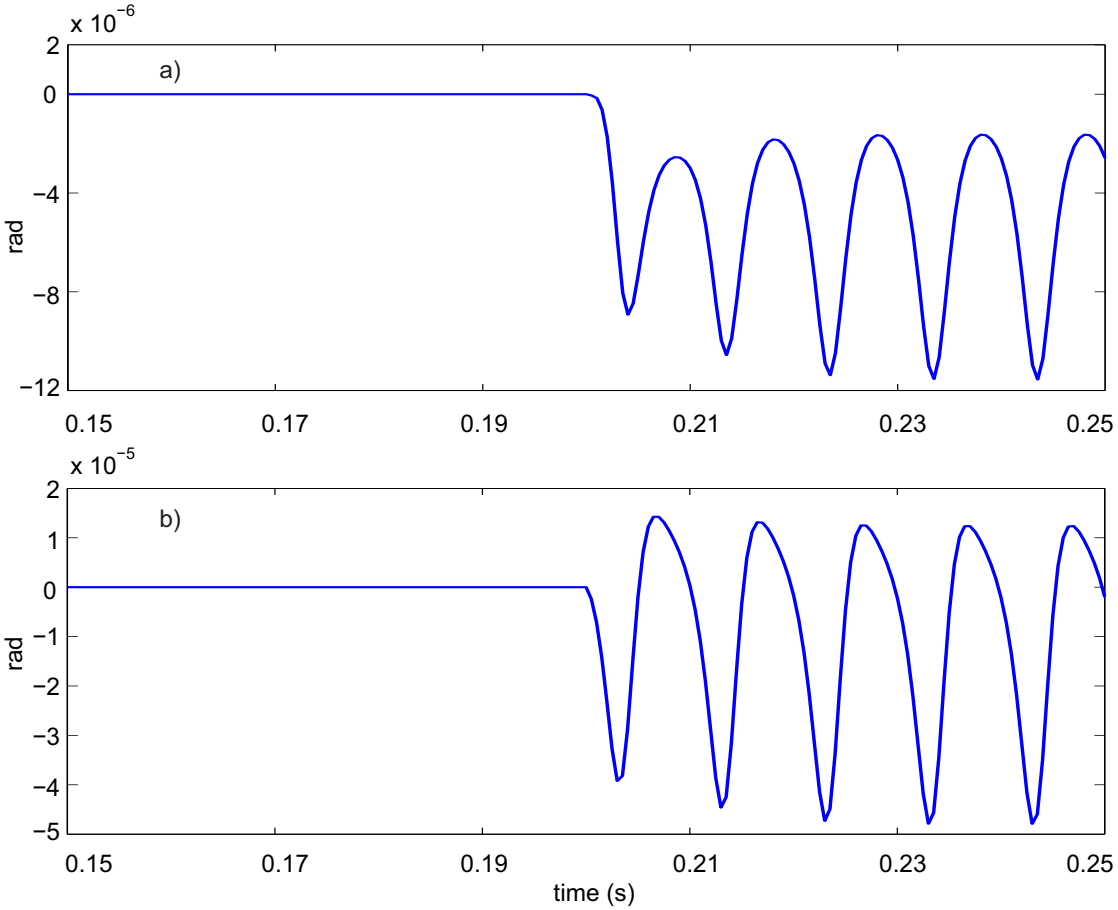

Figure 4.19 – the errors of the estimated phases of the symmetrical components: a) the phase error of the positive components b) the phase error of the negative components

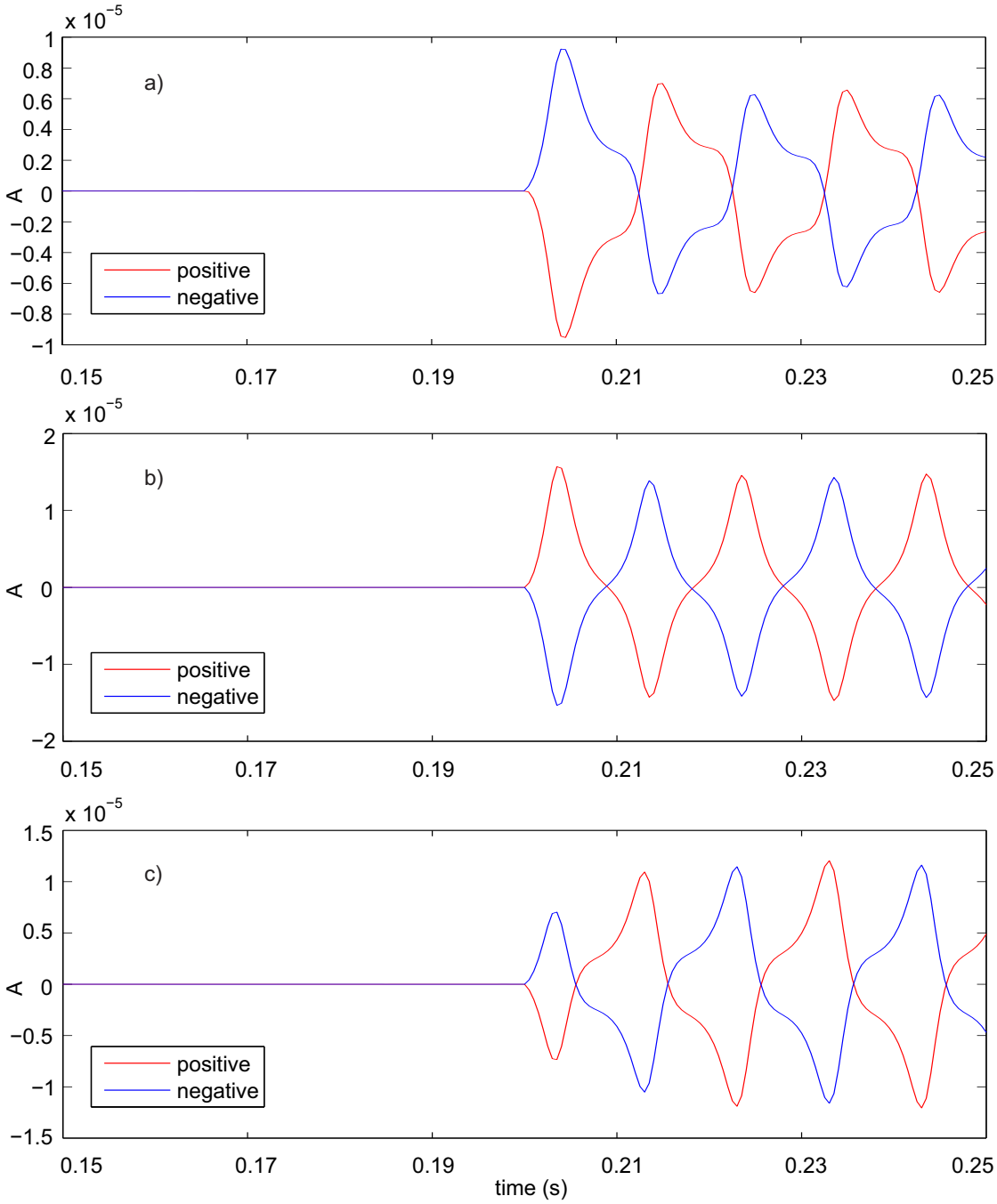

Figure 4.20 – The error of the estimated three phase signals of the positive and negative components compared to the real signals, a) phase a, b) phase b, c) phase c

4.4 Test the proposed initialization of the proposed nonlinear method

The following typical unbalanced three phase system is taken into account to evaluate the performance of the proposed nonlinear method with the addition of the initialization scheme.

$$\begin{cases} i_a(k) = I_+ \sin(\omega k T_s + \phi_+) + I_- \sin(\omega k T_s + \phi_-) + I_o \sin(\omega k T_s + \phi_o) \\ i_b(k) = I_+ \sin(\omega k T_s + \phi_+ - 2\pi/3) + I_- \sin(\omega k T_s + \phi_- + 2\pi/3) + I_o \sin(\omega k T_s + \phi_o) \\ i_c(k) = I_+ \sin(\omega k T_s + \phi_+ + 2\pi/3) + I_- \sin(\omega k T_s + \phi_- - 2\pi/3) + I_o \sin(\omega k T_s + \phi_o) \end{cases} \tag{4.12}$$

where sampling time $T_s = 0.0002$s, amplitudes $I_+ = 1$, $I_- = 0.2$, $I_o = 0.1$ and phase angles $\phi_+ = \frac{\pi}{3}$, $\phi_- = \frac{\pi}{6}$, $\phi_o = 0$. The nominal fundamental frequency is 50Hz.

4.4.1 Robustness against noises

A white Gaussian noise of 30 dB is added to each of the three phase signals in (4.12). To test the performance of the proposed nonlinear method combined with the initialization scheme in estimating the parameters of the power system, the state variables $q_1(k)$, $q_2(k)$, and $q_3(k)$ are initialized according to the following two cases:

Case 1 The initial value of the fundamental frequency is 49.5Hz, correspondingly the initial value of the state variables $q_1(k) = 0.9981 + 0.0622 * j$. Both the state variables $q_2(k)$ and $q_3(k)$ are initialized at 0A.

Case 2 The initial value of the fundamental frequency is 45Hz. Both the state variables $q_2(k)$ and $q_3(k)$ are initialized at 50A.

The number of iterations in the initialization stage N_o is chosen as 30. The estimated fundamental frequencies corresponding to the two cases are shown in Fig. 4.21 that both converge to the value 50Hz. Table 4.10 provides the details of the estimation accuracy and convergence speed. In each of the two cases, it takes approximately one cycle to reach the reference frequency with +/- 0.1 Hz, the MSE of the frequency estimation of the three cases are in the range of 10^{-6}.

Fig. 4.22 and Fig. 4.23 respectively plot the estimations of the three phases of the positive and negative components, together with their real curves, with the initialization in Case 1. In the case of a 30 dB disturbance noise, the estimations tightly track the real curves. There is no special requirement of knowledge of the initial conditions as well as no special turning in this test.

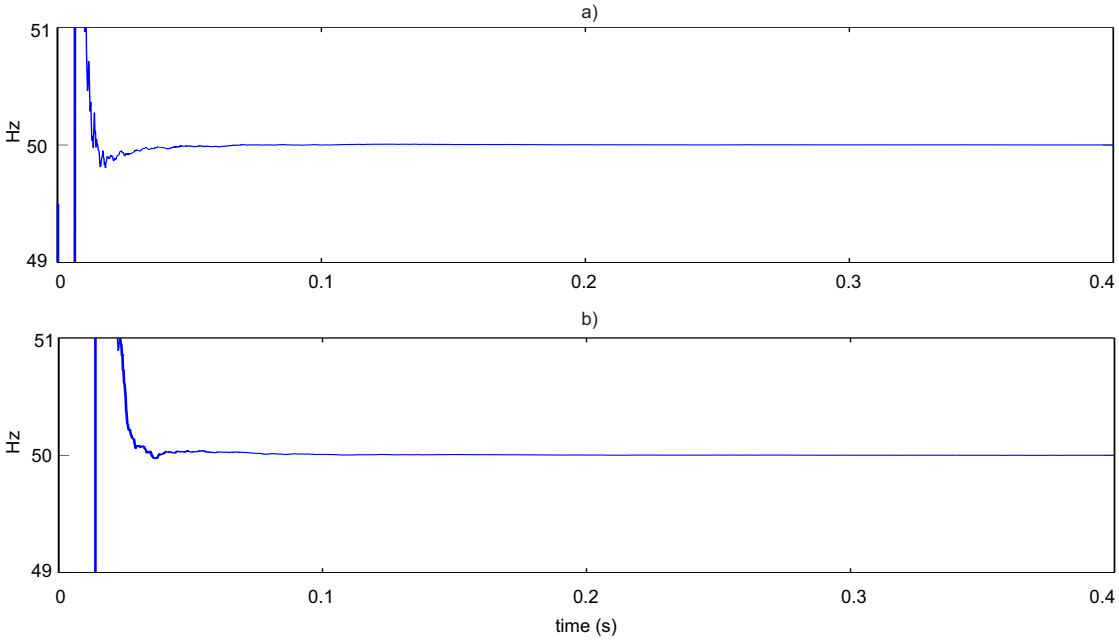

Figure 4.21 – The estimated frequency of the proposed nonlinear method combined with the initialization scheme in disturbance of 30 dB noise a) Initialization with Case 1, b) Initialization with Case 2

Initialization	time to reach the reference frequency with +/- 0.1 Hz (ms)	MSE at steady-state (Hz)	Error max. at steady-state (Hz)
Case 1	0.0220	$2.8024\ 10^{-6}$	0.0043
Case 2	0.0288	$3.4785\ 10^{-6}$	0.0056

Table 4.10 – The estimated frequencies of an unbalanced system disturbed by a noise of 30 dB of the proposed method combined with the initialization scheme corresponding to the two case of initialization

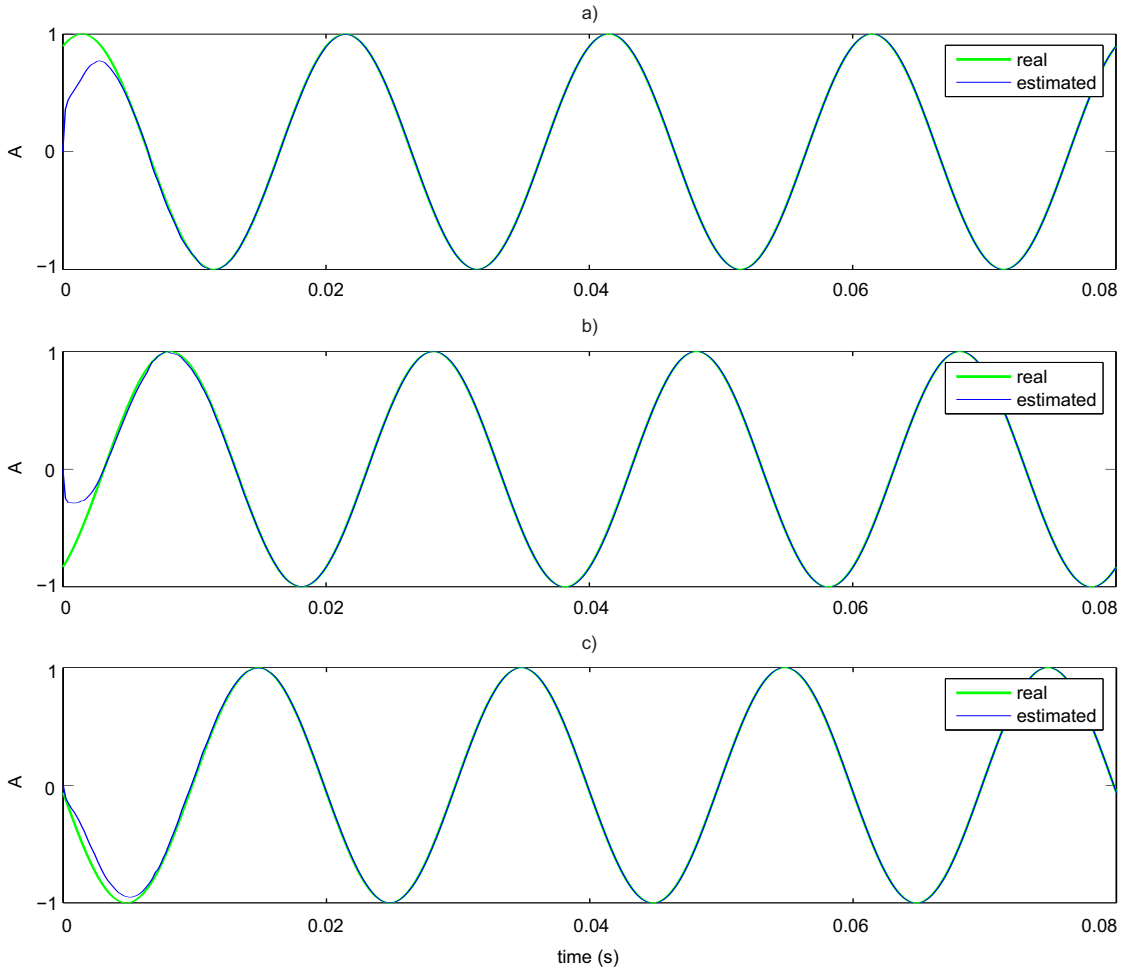

Figure 4.22 – The estimation of the three phases of the positive components of the proposed nonlinear method combined with the initialization scheme: a) phase a, b) phase b, c) phase c

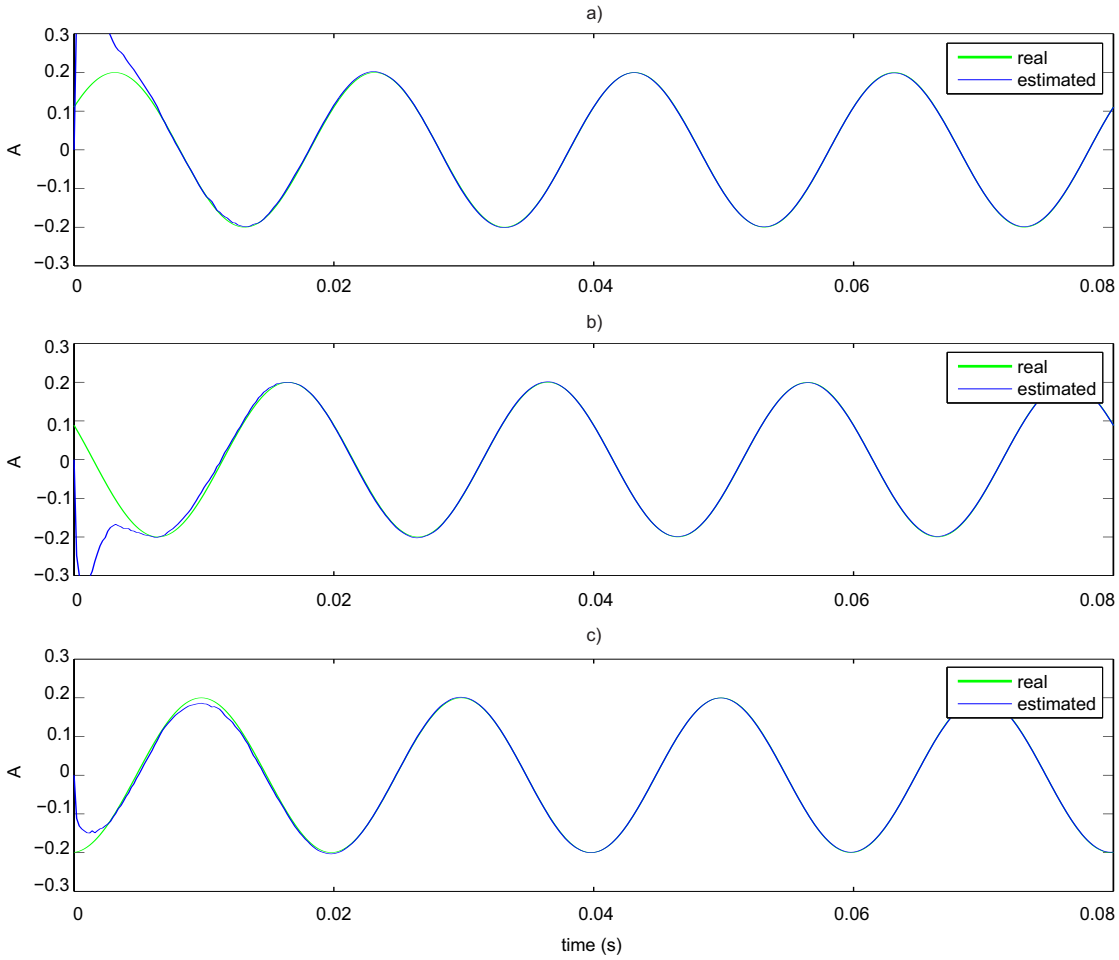

Figure 4.23 – The estimation of the three phases of the negative components of the proposed nonlinear method combined with the initialization scheme: a) phase a, b) phase b, c) phase c

Initialization	time to reach the reference frequency with +/- 0.1 Hz (ms)	MSE at steady-state (Hz)	Error max. at steady-state (Hz)
Case 1	0.0030	$3.9078\ 10^{-10}$	$4.2130\ 10^{-5}$
Case 2	0.0058	$2.9412\ 10^{-7}$	0.0011

Table 4.11 – The estimated frequencies of an unbalanced system in load changes of the proposed method combined with the initialization scheme corresponding to the two case of initialization

4.4.2 Robustness against load changes

The signals in (4.12) in the previous test are used again in this test. However, at the instant 0.1s their amplitudes and phase angles jumps to new values of $I_+ = 0.8$A, $I_- = 0.3$A, $I_o = 0.1$A and $\phi_+ = \pi/2$rad, $\phi_- = \pi/5$rad, $\phi_o = \pi/6$rad, the fundamental frequency also jumps from 50Hz to 50.5Hz at this moment, e.g., because of load changes. The signals are illustrated in Fig. 4.24.

To test the performance of the proposed nonlinear method combined with the initialization scheme in estimating the parameters of the power system, the state variables $q_1(k)$, $q_2(k)$, and $q_3(k)$ are initialized according to the following two cases:

Case 1 The initial value of the fundamental frequency is 49.5Hz, correspondingly the initial value of the state variables $q_1(k) = 0.9981 + 0.0622 * j$. Both the state variables $q_2(k)$ and $q_3(k)$ are initialized at 0A.

Case 2 The initial value of the fundamental frequency is 45Hz. Both the state variables $q_2(k)$ and $q_3(k)$ are initialized at 50A.

The number of iterations in the initialization stage N_o is chosen as 3.

Fig. 4.25 shows the estimated fundamental frequencies of the unbalance system in load changes using the proposed nonlinear method combined with the initialization scheme in the two cases of initialization. According to this figure, the estimated frequencies in both the two cases converge to the true value 50Hz of the fundamental frequency.

It can be seen from Table 4.11 that, in Case 1, after the transition, the estimated frequency takes a short time (0.003s or approximately $\frac{1}{7}$ of a cycle) to converge to the new value 50.5Hz, the MSE of the estimation is in the range of 10^{-10}. In case 2, the convergence time is 0.0058s and the MSE is in the range of 10^{-7}. The frequency estimation of the proposed method is good in the both cases.

With the initialization of Case 1, the estimated three phases of the positive and negative components of the proposed nonlinear method combined with the initialization scheme are shown in Fig. 4.26 and in Fig. 4.27 respectively which definitely track the real curves.

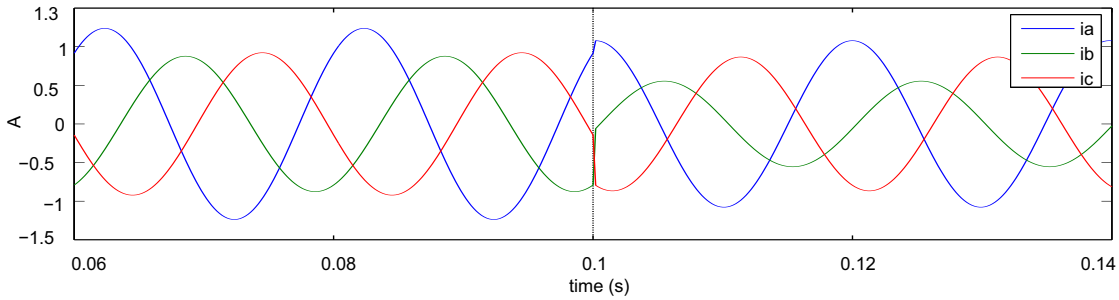

Figure 4.24 – The three phase signals with load change at time 0.1s

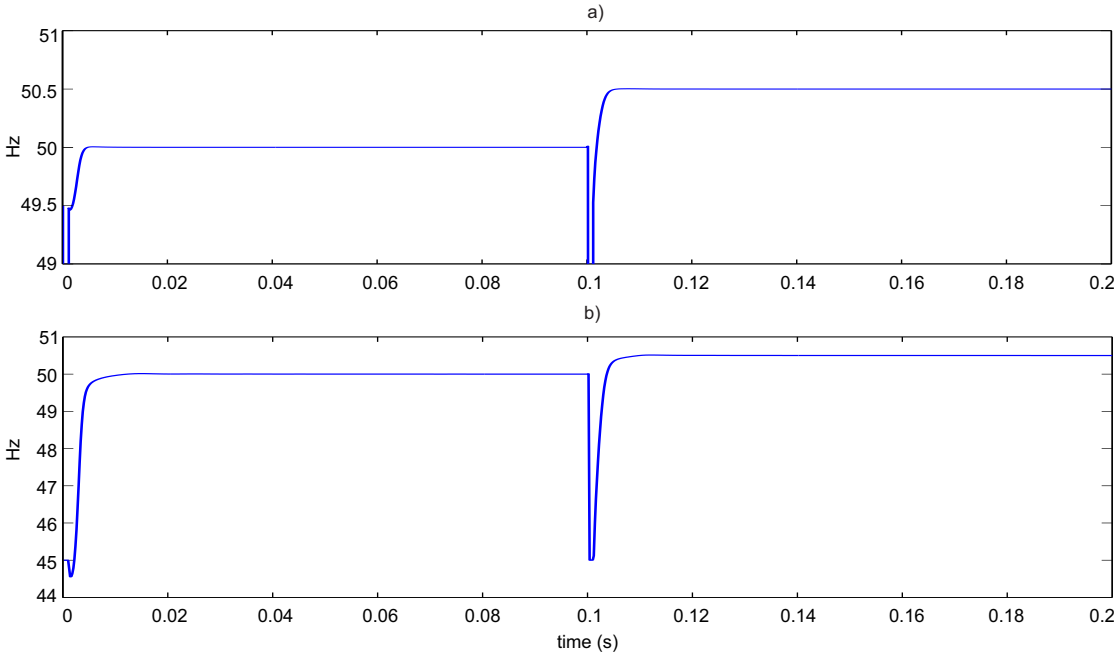

Figure 4.25 – The estimated frequency of the proposed nonlinear method combined with the initialization scheme in case of unbalanced system and load changes a) Initialization with Case 1, b) Initialization with Case 2

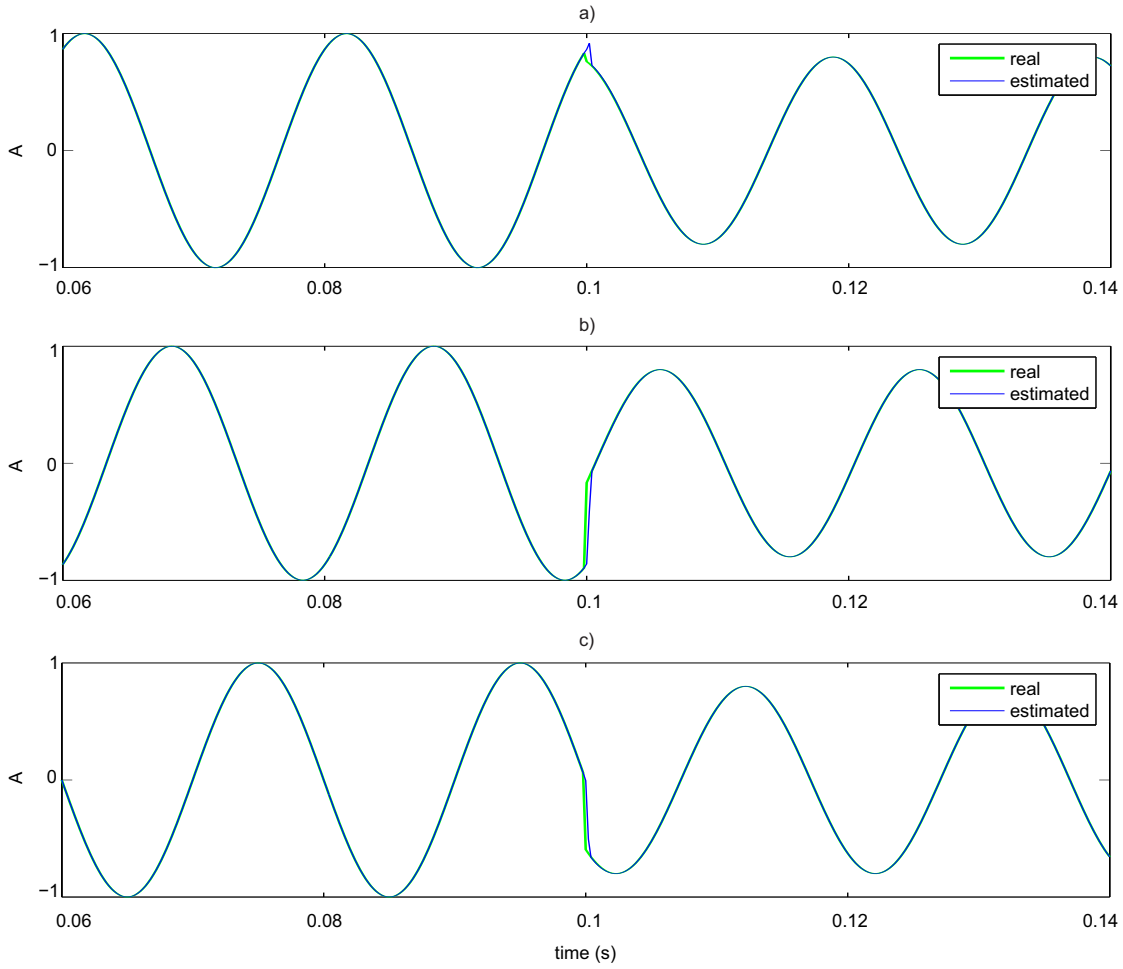

Figure 4.26 – The estimation of the three phases of an unbalanced system in load changes of the positive components of the proposed nonlinear method combined with the initialization scheme: a) phase a, b) phase b, c) phase c

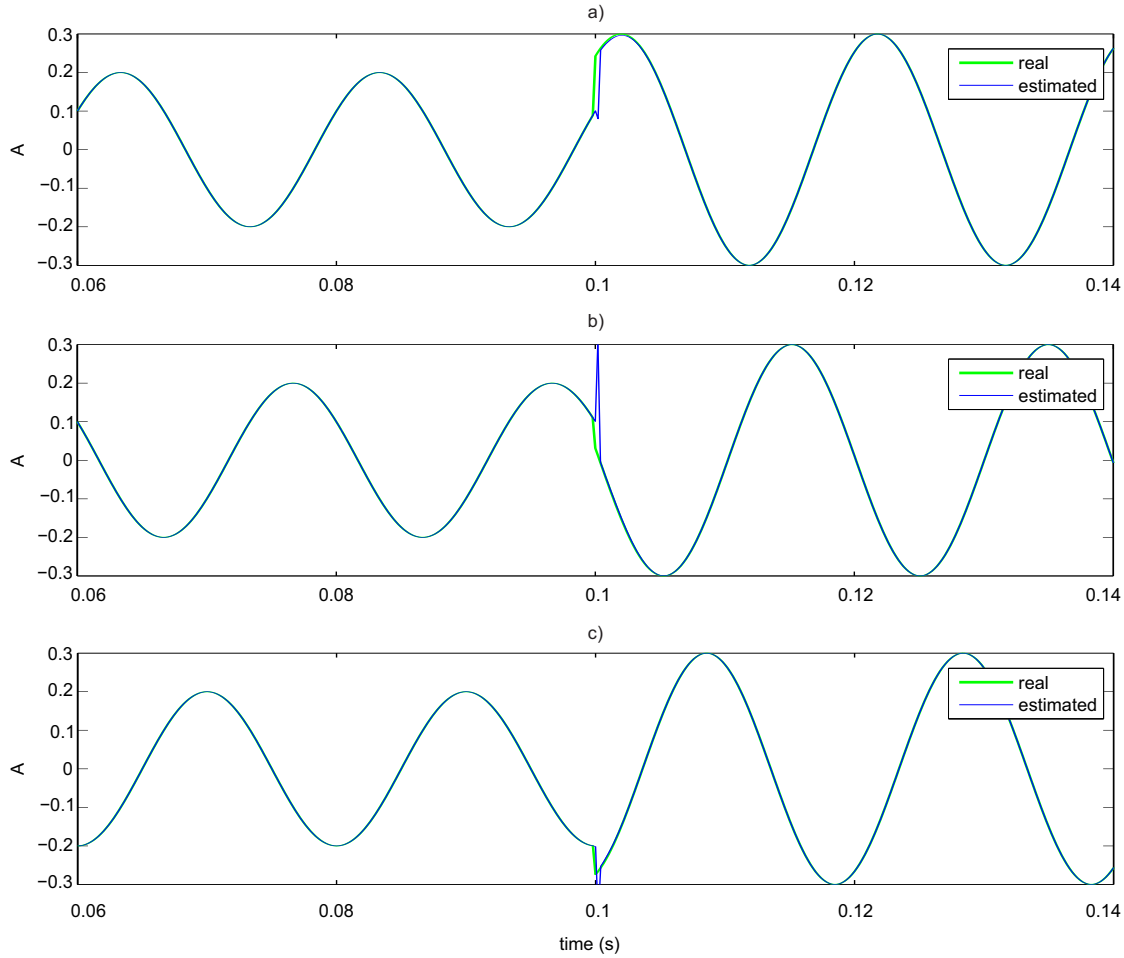

Figure 4.27 – The estimation of the three phases of the negative components of an unbalanced system in load changes of the proposed nonlinear method combined with the initialization scheme: a) phase a, b) phase b, c) phase c

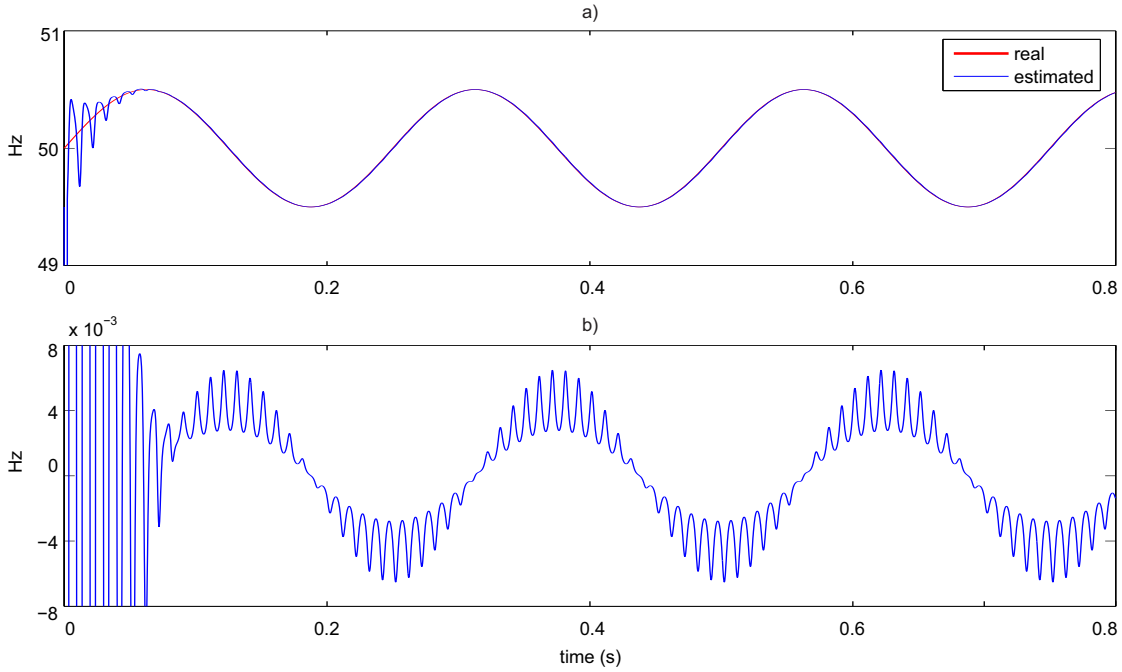

Figure 4.28 – the estimated fundamental frequency of the proposed nonlinear method combined with the initialization scheme: a) the estimated frequency and the real one, b) the estimation error

4.4.3 Frequency tracking

The signals used for this test is the unbalanced signals in (4.12) in which the fundamental frequency varies like a sinusoidal wave form of frequency 4Hz. Fig. 4.28 a) plots the real fundamental frequency and the estimated one by the proposed method combined with the initialization scheme. The error of the estimation is presented in Fig. 4.28, the error is in the range of 10^{-3}Hz which is relatively accurate in power system applications.

4.5 Conclusion

This chapter is composed of three sections to evaluate:

- The performance of the linear method in estimating the symmetrical components of a power system;
- The performance of the nonlinear method in estimating the fundamental frequency and the symmetrical components of a power system;
- The performance of the nonlinear method when combined with the proposed initialization scheme in estimating the fundamental frequency and the symmetrical components of a power system.

The simulation results show that the proposed linear method can accurately estimate the amplitudes and phase angles of the positive and negative components of an unbalanced three phase power system. The method is also able to track the amplitudes and the phase angles when the system suddenly switches from a balanced state to an unbalanced state due to a load change, and is able to reconstruct the positive, negative and zero components. The proposed method works well even when the fundamental frequency varies constantly in time. Compared to the MO-Adaline, the proposed linear method is superior in both convergence speed and accuracy.

Various simulations were performed to evaluate the performance of the proposed nonlinear method in different conditions: With balanced and unbalanced systems, with unbalanced systems with the presence of noise or with the presence of higher order harmonic terms, and with unbalanced systems with constantly varying fundamental frequency. The estimated frequency of the method is then compared to that of the 3P EKF and the 1P EKF presented in Chapter 2. According to the simulation results, the 3P EKF is efficient to estimate the fundamental frequency of a balanced system, but the performance of the method is much degraded for an unbalanced system, because of model error. The 1P EKF can handle unbalanced systems, but is unable to remove the effect of zero sequence harmonics. The proposed approach proves to be effective to estimate the fundamental frequency of an unbalanced system and to track the varying frequency. Moreover, the method is immune to the impacts of zero sequence harmonics. In additions, as the linear method, the nonlinear method is able not only to accurately estimate the amplitudes and phase angles of the positive and negative components of a power system, but also to reconstruct the symmetrical components, including the positive, negative and zero components, even when the fundamental frequency is unknown and varies constantly. However, like the 3P EKF and the 1P EKF, the proposed nonlinear method requires a careful selection of the initial conditions to prevent the results from bias and local minimum (the initial problem does not exist in the proposed linear method).

The initialization scheme proposed in Chapter 3 for the proposed nonlinear method is tested in different conditions: Disturbance of noise, load changes, and the fundamental frequency varying in sin wave. Without prior knowledge of the initial conditions, the estimation results are of fast convergence, high accuracy and high robustness to disturbances. Combining the initialization scheme with the proposed nonlinear method leads to an efficient solution for estimating the fundamental frequency and the symmetrical components of a power system.

Conclusion

Recently, securing a reliable power supply has become an important need worldwide. This is a challenging issue because of the liberalization of electricity supply, deregulation, consciousness on the impact on the environment, increase of the power demand, integration of renewable energy generation, etc. So, power distribution systems are in a period of transformation set in motion by significant changes in their concepts and in their structures. The main developments which are needed on power distribution systems are on high-speed communication, intelligent control of substations and protection devices, integrated power distribution management, monitoring, and high performance automation capabilities.

The research work proposed in this thesis aims to develop some new methods for estimating physical parameters of power systems and their signals, i.e., voltages and currents. This is directly related to power quality in electricity supply. Power quality is one key aspect in electricity transportation, in the evolution of power distribution systems toward smart grids. The proposed methods represent new tools that can be used for improving the reliability and stability of electric power systems. They are based on advanced signal processing techniques and models. The proposed methods can be implemented and applied to estimate the grid's fundamental frequency and symmetrical components in order to evaluate the operating conditions of a power system. This study is based on four chapters.

Chapter 1 discusses the issue of power quality and analyzes the symptoms, causes, and effects of several power quality problems that have bad impacts on power quality and reliability of power systems, i.e., frequency deviation, harmonics, reactive power, short voltage, long voltage, and unbalance. For each problem, the method of evaluating it is also mentioned. The chapter also mentions passive power filter and active power filter as solutions for the power quality problems, in which, the active power filter is preferable because of its flexibility to environment changes. In active power filter strategies, signal processing plays an important role in information extraction and parameter estimation from power grids.

Chapter 2 reviews signal processing methods used in power system applications to estimate a very important parameter of the system, the fundamental frequency. Four of the methods are chosen APM, ANF, 1P EKF, 3P EKF; their principles are explained and the advantages and disadvantages of each method are discussed. Further simulation tests are implemented to verify the performance of the four methods. The EKFs provide good estimation even in a

noisy environment but are sensitive to model error (the error of modeling harmonics and/or unbalance). The estimation by ANF is of low accuracy and that of the APM even does not converge in a noisy environment. This chapter also presents the principle of another method of identifying the symmetrical components of a power system, the MO-Adaline.

In chapter 3, we propose two new state-space models of an unbalanced three phase power system. The first state-space model which has been developed is linear and is able to represent an unbalanced three phase power system in the case where the fundamental frequency is available. This model is composed of two state variables representing the positive and negative components of the power systems. The second state-space model also represents an unbalanced three phase power system, however, the model uses one more state variable to represent the unknown fundamental frequency, and it is nonlinear. The nonlinear state-space model of an unbalanced three phase power system is appropriate for the situation where the fundamental frequency is not available nor estimated. Kalman filtering schemes are used with these model to estimate the power system's parameters. The linear method uses a KF to estimate the symmetrical components of a power system in real-time. On the other hand, the nonlinear method uses an EKF to estimate the fundamental frequency and the symmetrical components of the power system in real-time. The derivation of the proposed linear method is to make it possible to use any other methods for fundamental frequency estimation. The characteristics and the advantages and disadvantages of the proposed methods are discussed. The initialization procedure is pointed out as a challenge for the proposed nonlinear method as well as the other methods based on EKF. An simple scheme is also proposed in this thesis to solve the initialization problem.

Chapter 4 verifies the performance of the proposed methods in Chapter 3 with several and different simulation tests. Simulation results prove that:

- With the fundamental frequency supposed to be available, the linear method is able to estimate the amplitudes and phase angles of the positive and negative components of a power system, as well as to reconstruct the three symmetrical components, i.e., the positive, the negative and the zero components.
- The nonlinear method, with a good initialization, is efficient and robust in estimating the fundamental frequency under unbalanced conditions. This approach can be used in another application, i.e., for the identification of the symmetrical components of time-varying unbalanced power systems. It can be used to precisely estimate the value of the fundamental frequency in order to be able to identify in real-time the harmonic content of signals. When combined with the proposed initialization scheme, the proposed nonlinear method becomes more effective and robust in estimating parameters of a power system.

Both methods are efficient in cases representative of real industrial or domestic applications. It has been demonstrated that both method are robust against noise and harmonics. They are adaptive and able to handle time-varying conditions of power systems. Even under severe

conditions, the fundamental frequency and the symmetrical components are rapidly estimated with a good precision.

Perspectives

In the early future, further studies will be conducted on:

- Looking to associate to the proposed state space model another identification algorithm in order to diminish the disadvantage of EKF (model approximation error).
- Expanding the proposed state-space models in order to take into account the harmonic components, as each component of three phases could be considered as a positive or negative sequence.
- Enhancing the proposed state-space models for higher order unbalanced harmonics, the final purpose is to come up to a general and uniform state-space model able to include in one concept or model the unbalanced fundamental component, the unbalanced harmonics, and the harmonic sequences.

A Appendixes

A.1 List of Acronyms

AGC	Automatic Generation Control
ANF	Adaptive Notch Filter
ANN	Artificial Neural Network
APF	Active Power Filter
APM	Adaptive Prony's method
AR	Auto-Regressive
ARMA	Auto-Regressive Moving Average
DCO	Digital Controlled Oscillators
DSP	Digital Signal Processor
EKF	Extended Kalman Filter
FFT	Fast Fourier Transform
FPGA	A Field-Programmable Gate Array
IGBT	Insulated-Gate Bipolar Transistor
KF	Kalman Filter
LFC	Load Frequency Control
LMS	Least Mean square
MSE	Mean Squared Error
PCC	Point of Common Coupling
PF	Power Factor
PLL	Phase Locked Loop
PMU	Phasor Measurement Unit
PO	Percent Overshoot
PWM	Pulse Width Modulation
RMS	Root Mean Square (rms)
SNR	Signal-to-Noise Ratio
THD	Total Harmonic Distortion
VSI	Voltage Source Inverter
ZC	Zero crossing
EMS	Energy Management System
FACTS	Flexible ac transmission
PV	PhotoVoltaics
UKF	Unscented Kalman Filter

A.2 The $\alpha - \beta$ transform and the complex form of three phase signals

According to [25], $\alpha\beta$ transform calculates the $\alpha - \beta$ components i_α and i_β from the three phases instantaneous signals in the abc phases $i_a(k)$, $i_b(k)$, $i_c(k)$ as

$$\begin{bmatrix} i_\alpha(k) \\ i_\beta(k) \end{bmatrix} = \mathbf{M}^T \begin{bmatrix} i_a(k) \\ i_b(k) \\ i_c(k) \end{bmatrix} , \tag{A.1}$$

with

$$\mathbf{M} = \sqrt{\frac{2}{3}} \begin{bmatrix} 1 & 0 \\ -\frac{1}{2} & \frac{\sqrt{3}}{2} \\ -\frac{1}{2} & -\frac{\sqrt{3}}{2} \end{bmatrix} . \tag{A.2}$$

The corresponding complex form of the positive component is determined from (A.1) as

$$i(k) = i_\alpha(k) + j i_\beta(k) \tag{A.3}$$

Bibliography

[1] ABB. Electrical installation handbook - protection, control and electrical devices. Technical guide, ABB, 2010.

[2] ABS. Control of harmonics in electrical power systems. Guidance notes, American Bureau of Shipping, May 2006.

[3] Tadjer Sid Ahmed, Habi Idir, El Ganaoui Mohamed, and Angel Scipioni. Direct components extraction of voltage in photovoltaic active filter connected in a perturbed electrical network (based on robust pll algorithm). *Energy Procedia*, 74:966–972, 2015.

[4] H. Akagi. Modern active filters and traditional passive filters. *Bulletin of the Polish Academy of Sciences. Technical Sciences*, 54(3):255–269, 2006.

[5] Hirofumi Akagi, Edson Hirokazu Watanabe, and Mauricio Aredes. *Instantaneous Power Theory and Applications to Power Conditioning*. Wiley, 2007.

[6] Saleh R. Al-Araji, Zahir M. Hussain, and Mahmoud A. Al-Qutayri. *Digital phase lock loops*. Springer, 2006.

[7] Hossam Al-Ghossini, Fabrice Locment, Manuela Sechilariu, Laurent Gagneur, and Christophe Forgez. Adaptive-tuning of extended kalman filter used for small scale wind generator control. *Renewable Energy*, 85:1237–1245, 2016.

[8] F.J. Alcantara and P. Salmeron. A new technique for unbalance current and voltage estimation with neural networks. *IEEE Transactions on Power Systems*, 20(2):852–858, 2005.

[9] Paul M. Anderson. *Protective Device Characteristics*, pages 43–96. Wiley-IEEE Press, 1999.

[10] Paul M. Anderson. *Relay Logic*, pages 97–146. Wiley-IEEE Press, 1999.

[11] Jos Arrillaga, Bruce C. Smith, Neville R. Watson, and Alan R. Wood. *Power System Harmonic Analysis*. John Wiley and Sons, 1997.

[12] Jos Arrillaga and Neville R. Watson. *power system harmonics*. WILEY, 2 edition, 2003.

[13] Angelo Baggini. *Handbook of Power Quality*. John Wiley and Sons, 2008.

[14] David Bakken and Krzysztof Iniewski. *Smart Grids: Clouds, Communications, Open Source, and Automation.* Devices, Circuits, and Systems. CRC Press, 2014.

[15] Thomas Bier. *Disaggregation of Electrical Appliances using Non-Intrusive Load Monitoring.* Thèse de doctorat, Université de Haute Alsace, 2014.

[16] J. Lewis Blackburn. *Symmetrical Components for Power Systems Engineering.* CRC Press, 1993.

[17] Ayman Blorfan. *Contribution à l'étude de l'association d'une source photovoltaïque et d'un filtre actif.* Thèse de doctorat, Université de Haute Alsace, 2013.

[18] B. K. Bose. *Modern Power Electronics and AC Drives.* Prentice Hall, 2002.

[19] Bimal K. Bose. Neural network applications in power electronics and motor drives - an introduction and perspective. *IEEE Transactions on Industrial Electronics*, 54(1):14–33, 2007.

[20] K. De Brabandere, T. Loix, K. Engelen, B. Bolsens, J. Van den Keybus, J. Driesen, and R. Belmans. Design and operation of a phase-locked loop with kalman estimator-based filter for single-phase applications. In *IECON 2006 - 32nd Annual Conference on IEEE Industrial Electronics*, pages 525–530, Nov 2006.

[21] A. Bracale, P. Caramia, and G. Carpinelli. Adaptive prony method for waveform distortion detection in power systems. *International Journal of Electrical Power and Energy Systems*, 29(5):371–379, 2007.

[22] F Calero and Bolivia La Paz. Rebirth of negative-sequence quantities in protective relaying with microprocessor-based relays. In *57th Annual Conference for Protective Relay Engineers, 2004*, pages 190–219, 2004.

[23] C. Cecati, Geev Mokryani, A. Piccolo, and P. Siano. An overview on the smart grid concept. In *36th Annual Conference of the IEEE Industrial Electronics Society (IECON 2010)*, pages 3322–3327, 2010.

[24] P.K. Dash, K.B. Panigrahi, and G. Panda. Power quality analysis using s-transform. *IEEE Transactions on Power Delivery*, 18(2):406–411, 2003.

[25] P.K. Dash, A.K. Pradhan, and G. Panda. Frequency estimation of distorted power system signals using extended complex kalman filter. *IEEE Transactions on Power Delivery*, 14(3):761–766, 1999.

[26] P.K. Dash, D.P. Swain, A. Routray, and A.C. Liew. An adaptive neural network approach for the estimation of power system frequency. *Electric Power Systems Research*, 41(3):203–210, 1997.

[27] Virginie Dordonnat. *State-space modelling for high frequency data – Three applications to French national electricity load.* PhD thesis, University of Amsterdam, Amsterdam, Netherlands, 2009.

[28] E. M. dos Santos, J. P. Juchem Neto, G. Marchesan, and G. Cardoso. Power system frequency estimation using morphological prediction of clarke components. *Electric Power Systems Research*, 122:208–217, 2015.

[29] Roger C. Dugan, Mark F. McGranaghan, Surya Santoso, and H. Wayne Beaty. *Electrical Power Systems Quality.* McGraw-Hill Professional, 3 edition, 2012.

[30] Mohamed A. El-Sharkawi. *Electric Energy: An Introduction.* CRC Press, 3rd edition, 2012.

[31] EN. En 50160 : Voltage characteristics of electricity supplied by public distribution system. *EN 50160/2006*, 2006.

[32] Damien Flieller, Djaffar Ould Abdeslam, Patrice Wira, and Jean Mercklé. Distortions identification and compensation based on artificial neural networks using symmetrical components of the voltages and the currents. *Electric Power Systems Research*, 79(7):1145–1154, 2009.

[33] C. L. Fortescue. Method of symmetrical coordinates applied to the solution of polyphase networks. *Transactions of The American Institute of Electrical Engineers*, XXXVII(2):1027–1140, 1918.

[34] Ewald F. Fuchs and Mohammad A.S. Masoum. Chapter 1 - introduction to power quality. In *Power Quality in Power Systems and Electrical Machines*, pages 1–54. Academic Press, Burlington, 2008.

[35] H. Fujita and H. Akagi. A practical approach to harmonic compensation in power systems; series connection of passive and active filters. *IEEE Transactions on Industry Applications*, 27(6), 1991.

[36] Richard G. Gibbs. New kalman filter and smoother consistency tests. *Automatica*, 49(10):3141–3144, 2013.

[37] A. A. Girgis and F. M. Ham. A quantitative study of pitfalls in the fft. *IEEE Transactions on Aerospace and Electronic Systems*, AES-16(4):434–439, July 1980.

[38] Turan Gonen. *Electric Power Distribution Engineering.* CRC Press, 2008.

[39] D. Halbwachs, P. Wira, and J. Mercklé. Adaline-based approaches for time-varying frequency estimation in power systems. In *2nd IFAC International Conference on Intelligent Control Systems and Signal Processing (ICONS 2009)*, Istanbul, Turkey, 2009.

[40] L. H. Hansen, L. Helle, F. Blaabjerg, E. Ritchie, S. Munk-Nielsen, H. Bindner, P. Sorensen, and B. Bak-Jensen. Conceptual survey of generators and power electronics for wind turbines. Report Riso-R-1205(EN), Riso National Laboratory, 2001.

[41] Monson H. Hayes. *Statistical digital signal processing and modeling*. Wiley, 1996.

[42] Simon S. Haykin. *Adaptive Filter Theory*. Prentice Hall Information and System Sciences Series. Prentice Hall, 3rd edition, 1996.

[43] N. G. Hingorani and L. Gyugyi. *Understanding FACTS: concepts and technology of flexible AC transmission Systems*. IEEE Press, New York, 2002.

[44] Franz Hlawatsch and Francois Auger. *Time-Frequency Analysis*. Wiley-ISTE, 2008.

[45] Chien-Hung Huang, Yunlin, Chien-Hsing Lee, Kuang-Jung Shih, and Yaw-Juen Wang. Frequency estimation of distorted power system signals using robust extended complex kalman filter. In *International Conference on Intelligent Systems Applications to Power Systems (ISAP 2007)*, Niigata, Japan, 2007.

[46] Y. F. Huang, S. Werner, J. Huang, N. Kashyap, and V. Gupta. State estimation in electric power grids: Meeting new challenges presented by the requirements of the future grid. *IEEE Signal Processing Magazine*, 29(5):33–43, 2012.

[47] Ibraheem, P. Kumar, and D. P. Kothari. Recent philosophies of automatic generation control strategies in power systems. *IEEE Transactions on Power Systems*, 20(1):346–357, Feb 2005.

[48] IEEE. Ieee recommended practices and requirements for harmonic control in electrical power systems. *IEEE Std 519-1992*, pages 1–112, 1993.

[49] IEEE. Ieee guide for application and specification of harmonic filters. *IEEE Std 1531-2003*, 2003.

[50] IEEE. Ieee recommended practice for monitoring electric power quality. *IEEE Std 1159-2009 (Revision of IEEE Std 1159-1995)*, pages c1–81, 2009.

[51] Gu Jianjun, Xu Dianguo, Liu Hankui, and Gong Maozhong. Unified power quality conditioner (upqc): the principle, control and application. In *Power Conversion Conference, 2002. PCC-Osaka 2002. Proceedings of the*, volume 1, pages 80–85 vol.1, 2002.

[52] Yan Jin and Jie Liu. Parameter estimation of frequency hopping signals based on the robust s-transform algorithms in alpha stable noise environment. *AEU - International Journal of Electronics and Communications*, 70(5):611–616, 2016.

[53] Andreas Kamilaris, Yiannis Tofis, Chakib Bekara, Andreas Pitsillides, and Elias Kyriakides. Integrating web-enabled energy-aware smart homes to the smart grid. *International Journal on Advances in Intelligent Systems*, 5(1 and 2):15–31, 2012.

[54] M. Karimi-Ghartemani and H. Karimi. Analysis of symmetrical components in time-domain. In *48th Midwest Symposium on Circuits and Systems*, volume 1, pages 28–31, 2005.

[55] Philipp Klein. *Non-Intrusive Information Sources for activity Analysis in Ambient Assisted Living Scenarios*. Thèse de doctorat, Université de Haute Alsace, 2015.

[56] Neslihan Köse, Özgül Salor, and Kemal Leblebicioğlu. Interharmonics analysis of power signals with fundamental frequency deviation using kalman filtering. *Electric Power Systems Research*, 80(9):1145 – 1153, 2010.

[57] Tony R. Kuphaldt. *Lessons In Electric Circuits, Volume II – AC*. Open Book Project, Design Science License, 6 edition, 2007.

[58] Kyoung-Jun Lee, Jong-Pil Lee, Dongsul Shin, Dong-Wook Yoo, and Hee-Je Kim. A novel grid synchronization pll method based on adaptive low-pass notch filter for grid-connected pcs. *IEEE Transactions on Industrial Electronics*, 61(1):292–301, 2014.

[59] F. L. Lewis. *Applied Optimal Control and Estimation, Digital Design and Implementation*. Texas Instruments Digital Signal Processing Series. Prentice Hall Press, Texas Instruments, Englewood Cliffs, 1992.

[60] Frank L. Lewis, Lihua Xie, and Dan Popa. *Optimal and Robust Estimation: With an Introduction to Stochastic Control Theory*. CRC Press, 2 edition, 2007.

[61] M. Liserre, T. Sauter, and J.Y. Hung. Future energy systems: Integrating renewable energy sources into the smart power grid through industrial electronics. *IEEE Industrial Electronics Magazine*, 4(1):18–37, 2010.

[62] S. P. Litran, P. Salmeron, J. R. Vazquez, and R. S. Herrera. A new control for a combined system of shunt passive and series active filters. In *2007 IEEE International Symposium on Industrial Electronics*, pages 2463–2468, June 2007.

[63] M. Manic, D. Wijayasekara, K. Amarasinghe, and J. J. Rodriguez-Andina. Building energy management systems: The age of intelligent and adaptive buildings. *IEEE Industrial Electronics Magazine*, 10(1):25–39, Spring 2016.

[64] M.I. Marei, E.F. El-Saadany, and M.M.A. Salama. A processing unit for symmetrical components and harmonics estimation based on a new adaptive linear combiner structure. *IEEE Transactions on Power Delivery*, 19(3):1245–1252, 2004.

[65] Tarek Hassan Mohamed, Gaber Shabib, and Hossam Ali. Distributed load frequency control in an interconnected power system using ecological technique and coefficient diagram method. *International Journal of Electrical Power & Energy Systems*, 82:496–507, 2016.

[66] L. Moran, I. Pastorini, J. Dixon, and R. Wallace. Series active power filter compensates current harmonics and voltage unbalance simultaneously. *IEE Proceedings - Generation, Transmission and Distribution*, 147(1):31–36, Jan 2000.

[67] Ali Moukadem, Djaffar Ould Abdeslam, and Alain Dieterlen. *Time-Frequency Domain for Segmentation and Classification of Non-Stationary Signals*. Wiley and Sons, 2014.

[68] R. Naidoo and P. Pillay. A new method of voltage sag and swell detection. *IEEE Transactions on Power Delivery*, 22(2):1056–1063, April 2007.

[69] Sarita Nanda, P. K. Dash, Tatiana Chakravorty, and Shazia Hasan. A quadratic polynomial signal model and fuzzy adaptive filter for frequency and parameter estimation of nonstationary power signals. *Measurement*, 2016.

[70] Arye Nehorai. A minimal parameter adaptive notch filter with constrained poles and zeros. *IEEE Transactions on Acoustics, Speech and Signal Processing*, 33(4):983–996, 1985.

[71] Ngac Ky Nguyen. *Approche neuromimétique pour l'identification et la commande des systèmes électriques : application au filtrage actif et aux actionneurs synchrones.* Thèse de doctorat, Université de Haute Alsace, 2010.

[72] Ngac Ky Nguyen, Damien Flieller, Patrice Wira, and Djaffar Ould Abdeslam. Neural networks for phase and symmetrical components estimation in power systems. In *35th Annual Conference of the IEEE Industrial Electronics Society (IECON09)*, Porto, Portugal, 2009.

[73] D. Ould Abdeslam, P. Wira, J. Merckle, and D. Flieller. A unified artificial neural network architecture for active power filters. *Electric Power Systems Research*, 54(1):61–76, 2007.

[74] Djaffar Ould Abdeslam. *Techniques neuromimétiques pour la commande dans les systèmes électriques : application au filtrage actif parallèle dans les réseaux électriques basse tension.* Thèse de doctorat, Université de Haute Alsace, 2005.

[75] Djaffar Ould Abdeslam, Patrice Wira, Damien Flieller, and Jean Mercklé. New methods for time-varying frequency estimation from distorted harmonic signals in power systems. In *IAR Workshop*, pages 223–228, 2005.

[76] Shashi Kant Pandey, Soumya R. Mohanty, and Nand Kishor. A literature survey on load–frequency control for conventional and distribution generation power systems. *Renewable and Sustainable Energy Reviews*, 25:318–334, 2013.

[77] F. Z. Peng, H. Akagi, and A. Nabae. A new approach to harmonic compensation in power systems-a combined system of shunt passive and series active filters. *IEEE Transactions on Industry Applications*, 26(6):983–990, Nov 1990.

[78] Anh Tuan Phan, Gilles Hermann, and Patrice Wira. Online frequency estimation in power systems: A comparative study of adaptive methods. In *40th Annual Conference of the IEEE Industrial Electronics Society (IECON 2014)*, pages 4352–4357, 2014.

[79] Anh Tuan Phan, Gilles Hermann, and Patrice Wira. Advanced techniques in power transmission system enhancement and smart grid development. In *Journée des Ecoles Doctorales à l'Université de Haute Alsace, Poster, 2 juillet, Mulhouse*, 2015.

[80] Anh Tuan Phan, Gilles Hermann, and Patrice Wira. Kalman filtering with a new state-space model for three-phase systems: Application to the identification of symmetrical components. In *IEEE Conference on Evolving and Adaptive Intelligent Systems (EAIS 2015)*, pages 216–221, 2015.

[81] Anh Tuan Phan, Gilles Hermann, and Patrice Wira. A new state-space for unbalanced three-phase systems: Application to fundamental frequency tracking with kalman filtering. In *18th IEEE Mediterranean Electrotechnical Conference (MELECON 2016)*, 2016.

[82] Anh Tuan Phan, Duc Du Ho, Gilles Hermann, and Patrice Wira. A new state-space model for three-phase systems for kalman filtering with application to power quality estimation. In *11th International Conference of Computational Methods in Sciences and Engineering (ICCMSE 2015)*, 2015.

[83] Anh Tuan Phan, Patrice Wira, and Gilles Hermann. Adaptive observer with a enhanced state-space representation for frequency tracking and unbalance current and voltage estimation in power systems. *Evolving Systems*, submitted, 2016.

[84] Kathy Pretz. Standards for a connected home. *The Institute - IEEE*, 39(4):14, 2015.

[85] Kathy Pretz. Ieee standards for greener ict. *The Institute - IEEE*, 40(1):12, 2016.

[86] Pravat Kumar Ray, Pratap Sekhar Puhan, and Gayadhar Panda. Improved recursive newton type algorithm based power system frequency estimation. *International Journal of Electrical Power & Energy Systems*, 65:231–237, 2015.

[87] M.S. Reza, M. Ciobotaru, and V.G. Agelidis. Power quality analysis using piecewise adaptive prony's method. In *2012 IEEE International Conference on Industrial Technology (ICIT)*, Athens, Greek, 2012.

[88] Matthew B. Rhudy and Yu Gu. Online stochastic convergence analysis of the kalman filter. *International Journal of Stochastic Analysis*, 2013:9, 2013.

[89] Isabel Ribeiro. Kalman and extended kalman filters: Concept, derivation and properties. Report, Instituto de Sistemas e Robótica, Instituto Superio Técnico, 2004.

[90] G. Rigatos, P. Siano, and P. Wira. Flatness-based adaptive fuzzy control for active power filters. In *41st Annual Conference of the IEEE Industrial Electronics Society (IECON 2015)*, pages 004247–004252, 2015.

[91] Nathalie Saker. *The contribution of load control in increasing electric system flexibility*. Thesis, Supélec, Paris, France, 2013.

[92] P. Salmeron and S. P. Litran. Improvement of the electric power quality using series active and shunt passive filters. *IEEE Transactions on Power Delivery*, 25(2):1058–1067, April 2010.

[93] R.M. Santos Filho, P.F. Seixas, P.C. Cortizo, L.A.B. Torres, and A.F. Souza. Comparison of three single-phase pll algorithms for ups applications. *IEEE Transactions on Industrial Electronics*, 55(8):2923–2932, 2008.

[94] S. Santoso, E. J. Powers, W. M. Grady, and P. Hofmann. Power quality assessment via wavelet transform analysis. *IEEE Transactions on Power Delivery*, 11:924–930, 1996.

[95] T. Sezi. A new method for measuring power system frequency. In *IEEE Transmission and Distribution Conference*, volume 1, pages 400–405, 1999.

[96] P. J. Shah, Rakesh Saxena, and M. P. S. Chawla. Digital control technologies for improving the power quality of power supplies. *Neural Computing and Applications*, 22(1):235–248, 2013.

[97] M. Shiroei, B. Mohammadi-Ivatloo, and M. Parniani. Low-order dynamic equivalent estimation of power systems using data of phasor measurement units. *International Journal of Electrical Power and Energy Systems*, 74:134–141, 2016.

[98] Siemens. Harmonics in power systems - causes, effects and control. Whitepaper, Siemens, May 2013.

[99] Bhim Singh, K. Al-Haddad, and A. Chandra. A review of active filters for power quality improvement. *IEEE Transactions on Industrial Electronics*, 46(5):960–971, 1999.

[100] Santosh Kumar Singh, Nilotpal Sinha, Arup Kumar Goswami, and Nidul Sinha. Several variants of kalman filter algorithm for power system harmonic estimation. *International Journal of Electrical Power & Energy Systems*, 78:793–800, 2016.

[101] C. Siva Kumar, A.V.R.S Sarma, and R. Somanatham. Application of active power filter for compensating unbalanced load currents using symmetrical component theory. In *IET-UK International Conference on Information and Communication Technology in Electrical Sciences*, pages 496–502, 2007.

[102] S.A. Soliman and M.E. El-Hawary. Application of kalman filtering for online estimation of symmetrical components for power system protection. *Electric Power Systems Research*, 38(2):113–123, 1996.

[103] R. Strzelecki and G. Benysek. *Power Electronics in Smart Electrical Energy Networks*. Springer, 2008.

[104] W. Tan. Load frequency control: Problems and solutions. In *30th Chinese Control Conference (CCC)*, pages 6281–6286, July 2011.

[105] Xiaobo Tan and Hang Zhang. Novel adaptive iir filter for frequency estimation and tracking. In *3rd IEEE International Conference on Computer Science and Information Technology*, volume 5, pages 259–263, 2009.

[106] A. Timbus, M. Liserre, R. Teodorescu, and F. Blaabjerg. Synchronization methods for three phase distributed power generation systems - an overview and evaluation. In *2005 IEEE 36th Power Electronics Specialists Conference*, pages 2474–2481, June 2005.

[107] Ta-Peng Tsao, Rofig-Ching Wu, and Chia-Ching Ning. The optimization of spectral analysis for signal harmonics. *IEEE Transactions on Power Delivery*, 16(2):149–153, Apr 2001.

[108] Nguyen Duc Tuyen, Goro Fujita, and Mohd Nabil Bin Muhtazaruddin. Notch adaptive filter solution under unbalanced and/or distorted pcc voltage for 3-phase 3-wire shunt active power filter. *Electrical Engineering*, pages 1–12, 2016.

[109] S. Vazquez, J.A. Sanchez, M.R. Reyes, J.I. Leon, and J.M. Carrasco. Adaptive vectorial filter for grid synchronization of power converters under unbalanced and/or distorted grid conditions. *IEEE Transactions on Industrial Electronics*, 61(3):1355–1367, 2014.

[110] A. von Jouanne and B. Banerjee. Assessment of voltage unbalance. *IEEE Transactions on Power Delivery*, 16(4):782–790, Oct 2001.

[111] Baochao Wang. *Intelligent control and power flow optimization of microgrid energy management strategies - energy management strategies.* Thèse de doctorat, Université de Technologie de Compiègne, 2013.

[112] P.J. Werbos. Computational intelligence for the smart grid-history, challenges, and opportunities. *IEEE Computational Intelligence Magazine*, 6(3):14–21, 2011.

[113] Patrice Wira and Thien Minh Nguyen. Adaptive linear learning for on-line harmonic identification: An overview with study cases. In *International Joint Conference on Neural Networks (IJCNN 2013)*, 2013.

[114] Patrice Wira, Djaffar Ould Abdeslam, and Jean Mercklé. *Artificial neural networks to improve current harmonics identification and compensation*, book section 10, pages 256–290. IGI Global, Hershey, PA, USA, 2010.

[115] Patrice Wira, Gerasimos Rigatos, and Pierluigi Siano. Nonlinear modelling and control for renewable energy systems: Applications to power generators and power electronics. In *42nd Annual Conference of IEEE Industrial Electronics Society (IECON 2016)*, October 24-27 2016.

[116] F. Xiong, W. Yue, L. Ming, W. Ke, and L. Wanjun. A novel pll for grid synchronization of power electronic converters in unbalanced and variable-frequency environment. In *The 2nd International Symposium on Power Electronics for Distributed Generation Systems*, pages 466–471, June 2010.

[117] Binying Ye. *Harmonics retrieval for sensorless control of induction machines.* Thèse de doctorat, Université de Technologie de Belfort-Montbeliard, 2015.

[118] A. Zanella, N. Bui, A. Castellani, L. Vangelista, and M. Zorzi. Internet of things for smart cities. *IEEE Internet of Things Journal*, 1(1):22–32, Feb 2014.

[119] Ahmed Faheem Zobaa, Mario Manana Canteli, and Ramesh Bansal. *Power Quality Monitoring, Analysis and Enhancement*. InTech, 2011.